НАЦІОНАЛЬНА АКАДЕМІЯ НАУК УКРАЇНИ
ІНСТИТУТ ЗАГАЛЬНОЇ ТА НЕОРГАНІЧНОЇ ХІМІЇ імені В. І. ВЕРНАДСЬКОГО
КИЇВСЬКИЙ НАЦІОНАЛЬНИЙ УНІВЕРСИТЕТ імені ТАРАСА ШЕВЧЕНКА

УКРАЇНСЬКИЙ ХІМІЧНИЙ ЖУРНАЛ

№ 9
Том 90 / Vol. 90
2024
https://ucj.org.ua

UKRAINIAN CHEMISTRY JOURNAL

Зміст

Contents

UDK 544.363 + 544.4 + 547.815.1 doi: 10.33609/2708-129X.90.9.2024.3-18

MONONITROFLUORESCEINS IN AQUEOUS MEDIA: ACID-BASE EQUILIBRIA, TAUTOMERISM, AND HYDROLYSIS OF DIACETATES

D. V. Kharchenko, S. V. Shekhovtsov, T. A. Cheipesh, N. O. Mchedlov-Petrossyan*

V. N. Karazin Kharkiv National University,
4 Svoboda sq., 61022 Kharkiv, Ukraine
**e-mail: mchedlov@karazin.ua*

This article reports equilibrium and kinetic data for three fluorescein dyes containing the nitro group in the residue of the phthalic acid, 3′-, 4′-, and 5′-nitrofluorescein, in water and 50 mass % aqueous ethanol. These compounds, particularly the recently synthesized 3′-nitrofluorescein, were less considered polyprotic acids than many other fluorescein dyes. The dyes behave as diprotic acids, which can also be protonated: $H_3R^+ \rightleftharpoons H_2R \rightleftharpoons HR^- \rightleftharpoons R^{2-}$. The dissociation constants in water and 50 mass % aqueous ethanol were obtained in buffer solutions of diluted HCl using the spectrophotometric method accompanied by a potentiometric determination of pH at an ionic strength of 0.05 M and 25.0 ± 1 °C. The dye concentrations in the working solutions were, as a rule, within the range of $(5–10)\times10^{-6}$ M. The thermodynamic values of the dissociation constants were calculated using the Debye–Hückel equation, the second approach, for ionic activity coefficients. The absorption spectra in the visible region of the individual molecular and ionic forms were determined for the above-mentioned compounds and the ester of 3′-nitrofluorescein. For the last, the dissociation constants were determined in aqueous ethanol. Whereas in water the fraction of the zwitterionic tautomer of nitrofluoresceins increases as compared with the parent compound, in aqueous ethanol, the colorless lactone predominates. The microscopic dissociation constants were determined and their values are in line with the influence of the electrophilic nitro group. The alkaline hydrolysis of the nitrofluorescein diacetates was investigated in the two aforementioned solvents. The obtained results allowed us to single out the rate constants of the two-step kinetics of the hydrolysis of the diacetyl derivatives of nitrofluoresceins.

Keywords: Nitrofluorescein; acid-base dissociation; water-ethanol binary solvent; absorption spectra; dissociation constants; tautomerism; diacetylfluorescein; two-step alkaline hydrolysis; rate constants.

INTRODUCTION. This paper continues the research of alkaline hydrolysis of diacetylfluorescein [1]. Here, we present the study of diacetates of three nitrofluoresceins with the NO_2 group in the phthalic acid residue in water and 50 mass % aqueous ethanol. To better understand the kinetic data, we examined the acid-base and tautomeric equilibria of these nitrofluoresceins and an ester as model compound in the same solvent.

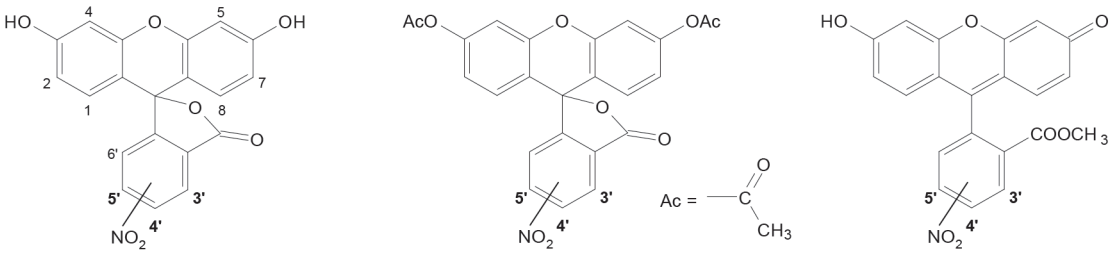

Scheme 1. The molecular structures of nitrofluoresceins, their diacetates, and esters.

The dissociation constants of 3′-, 4′-, and 5′-nitrofluorescein were determined via the spectrophotometric method. The hydrolysis of fluorescein diacetates and similar esters has been numerously studied in the literature [2–4]. Usually, a rate constant of the total hydrolysis was determined without dividing it into two separate constants of stepwise hydrolysis. We have developed an approach based on the knowledge of the spectrum of the single-charged fluorescein anion, which allowed calculating the first and second rate constant [1, 5]. Now, we decided to further this procedure by involving nitrofluoresceins. To the best of our knowledge, the acid-base and tautomeric equilibria of these dyes in aqueous media have not been studied so far. Therefore, a study of their protolytic equilibrium in itself is essential for understanding the behavior of fluorescein dyes in solutions.

The dyes behave as diprotic acids, which can also be protonated, Equations (1–3).

$$H_3R^+ \rightleftharpoons H_2R + H^+, \quad K_{a0} \qquad (1)$$

$$H_2R \rightleftharpoons HR^- + H^+, \quad K_{a1} \qquad (2)$$

$$HR^- \rightleftharpoons R^{2-} + H^+, \quad K_{a2} \qquad (3)$$

EXPERIMENT AND DISCUSSION OF THE RESULTS. The synthesis of the dyes and their diacetates was described in our previous publications [6, 7]. Hydrochloric, acetic, phosphoric, diethylbarbituric acids and analytical grade borax were used to create different pH values. The standard aqueous solution of NaOH was prepared from a saturated solution using CO_2-free water and kept protected from the atmosphere. Besides 96% aqueous ethanol, acetonitrile (Sigma-Aldrich, for HPLC, gradient grade, ⩾ 99.9%) was used to prepare the stock solutions of the dyes. The equilibrium and kinetic experiments were run on a Hitachi U-2000 spectrophotometer at 25.0±1 °C. Because of the limited solubility in water, the stock solutions of the dyes were prepared in acetonitrile, adding 0.013 M diazabicyclo[5.4.0]-undec-7-ene, DBU. The dye concentrations in the working solutions were within the range of $(5–10)\times10^{-6}$ M unless otherwise specified; hereafter, 1 M = 1 mole dm^{-3}. The pH values were determined using a glass electrode in a cell with a liquid junction. The glass electrode was calibrated with standard buffer solutions (pH 1.68, 4.01, 6.86, and 9.18 at 25 °C). When working in 50 mass % ethanol, the instrumental pH values, pH_{instr}, were corrected according to the literature data: $pH = pH_{instr} - 0.20$ [8]. The limiting alkaline forms of the dyes were obtained in diluted NaOH and, in some cases, with DBU (Merck, for synthesis). For each system, the number of solutions with different pH was 25 to 32. The CLINP chemometric program and wavelengths from 430 to 510 nm

with a step of 1 nm were used for calculations [7, 9]. The ionic strength I = 0.05 M was maintained by sodium chloride of analytical grade. In some acidic solutions, e.g., with pH in water below 1.3, the ionic strength in HCl solutions was higher. The hydrolysis kinetics of fluorescein dyes was studied as described previously [1]. The visible spectra were recorded from 400 to 600 nm during either 29 or 40 s for faster and slower reactions, respectively. The time of adding the buffer was considered as the moment of beginning the reaction.

The visible absorption spectra at different pH in water and the dependences of absorbance on pH are exemplified in Figures 1 and 2, respectively.

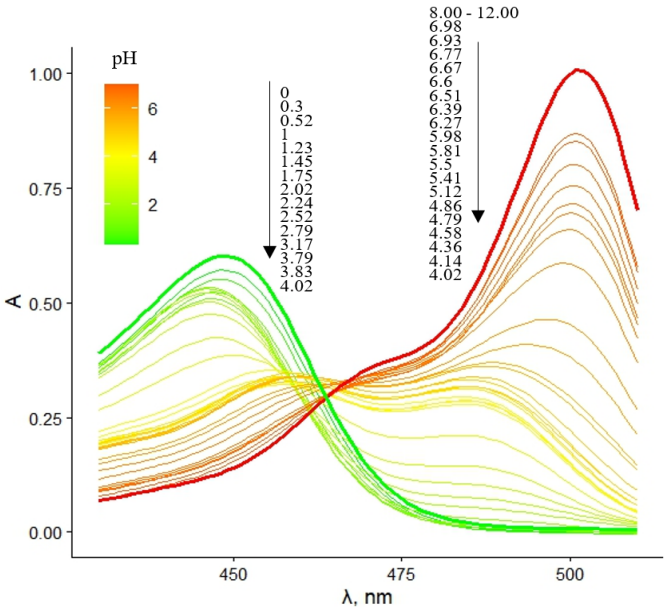

Fig. 1 – The absorption spectra of 3′-nitrofluorescein in aqueous solutions, 25 °C, at different pH values; The dye concentration 1.08×10^{-5} M; I = 0.05 M except forsolutions with pH < 1.3. The pH values are given in the activity scale down to pH 1.3; the concentration scale (–logarithm of HCl concentration) was used below this limit.

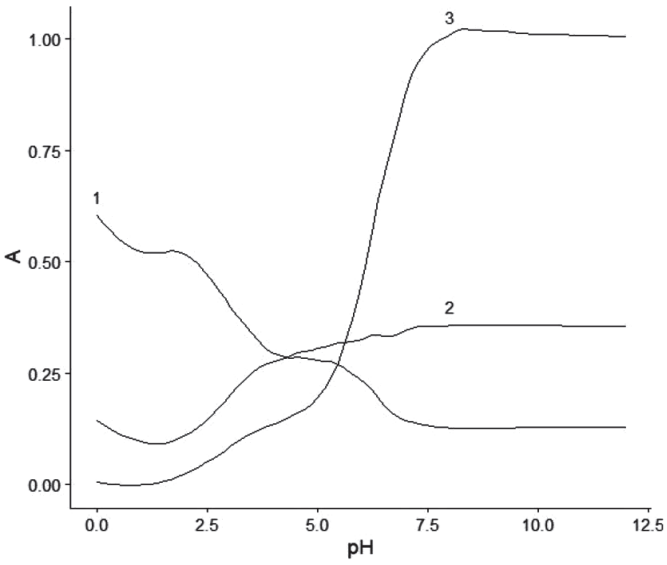

Fig. 2 – The dependence of absorbance of 3′-nitrofluorescein on pH at wavelengths 448 nm (1), 470 nm (2), and 501 nm (3); 25 °C, I = 0.05 M, except the solutions with pH below 1.3.

The results are presented in Table 1. The thermodynamic values of the dissociation constants were calculated using the Debye – Hückel equation, the second approach, for ionic activity coefficients. The values of activity coefficients in water are 0.822 and 0.457 for single and double-charged ions, respectively. The absorption spectra of the individual equilibrium forms of the dyes are presented in Figures 3–5. The spectra of the H_3R^+ and R^{2-} forms were measured directly in 1.0 M HCl and 0.042 M NaOH solutions, respectively, while those of H_2R and HR^- were singled out from the experimental data jointly with calculating the dissociation constants.

Table 1.

The parameters of ionic equilibria of nitrofluoresceins in water, 25 °C, I = 0.05 M[a,b]

Parameter [c]	3′-Nitrofluorescein [d]	4′-Nitrofluorescein	5′-Nitrofluorescein
pK_{a0}	1.06±0.01 (0.98)	1.86±0.01 (1.78)	1.87±0.02 (1.79)
pK_{a1}	2.82±0.01 (2.90)	3.66±0.01 (3.74)	3.68±0.02 (3.76)
pK_{a2}	6.28±0.01 (6.54)	6.36±0.01 (6.62)	6.54± 0.01 (6.80)
λ_{max}/ ε (H_3R^+)×10^{-3}	449 nm /55.72	443 nm /59.73	444 nm /60.29
λ_{max}/ε (H_2R)×10^{-3}	446 nm /43.89	439 nm /23.86	441 nm /26.56
λ_{max}/ε (HR^-)×10^{-3}	459 nm /31.44; 485 nm /29.96	457 nm /34.48 477 nm /33.44	458 nm /35.21 481 nm /33.84
λ_{max}/ε (R^{2-})×10^{-3}	501 nm /93.1	497 nm /85.65	499 nm /94.03
α ($H_2Z^{\pm}$)	≈ 0.8	0.36	0.43
α (H_2Q)	>0.01	0.11	0.07
α (H_2L)	≈ 0.2	0.53	0.50
$pK_{\pm,COOH}$	≈ 1.1	2.22	2.14
$pK_{0,OH}$	—[d]	2.74	2.93
$pK_{1,COOH}$	— [d]	2.78	2.60
$pK_{1,Z}$	≈ 2.7	3.30	3.39

Note. [a] The pK_a values in parenthesis are thermodynamic. [b]The molar absorptivities, ε, are expressed in $M^{-1}cm^{-1}$. [c]For fluorescein, the pK_a values are 2.22, 4.37, and 6.55; the thermodynamic values are 2.14, 4.45, and 6.80 [10]. [d]In this case, the data with pH below 1.3 were not used for calculations.

The spectra of the individual equilibrium forms of the dyes are presented in Figure 3. They were singled out from the total body of spectra by calculating the molar absorptivities of the forms H_2R and HR^- together with the dissociation constants, while those of the ions H_3R^+ and R^{2-} were determined directly at appropriate acidity.

To explain the obtained data, the detailed scheme of the acid-base and tautomeric equilibrium should be considered (Scheme 2) [10, 11].

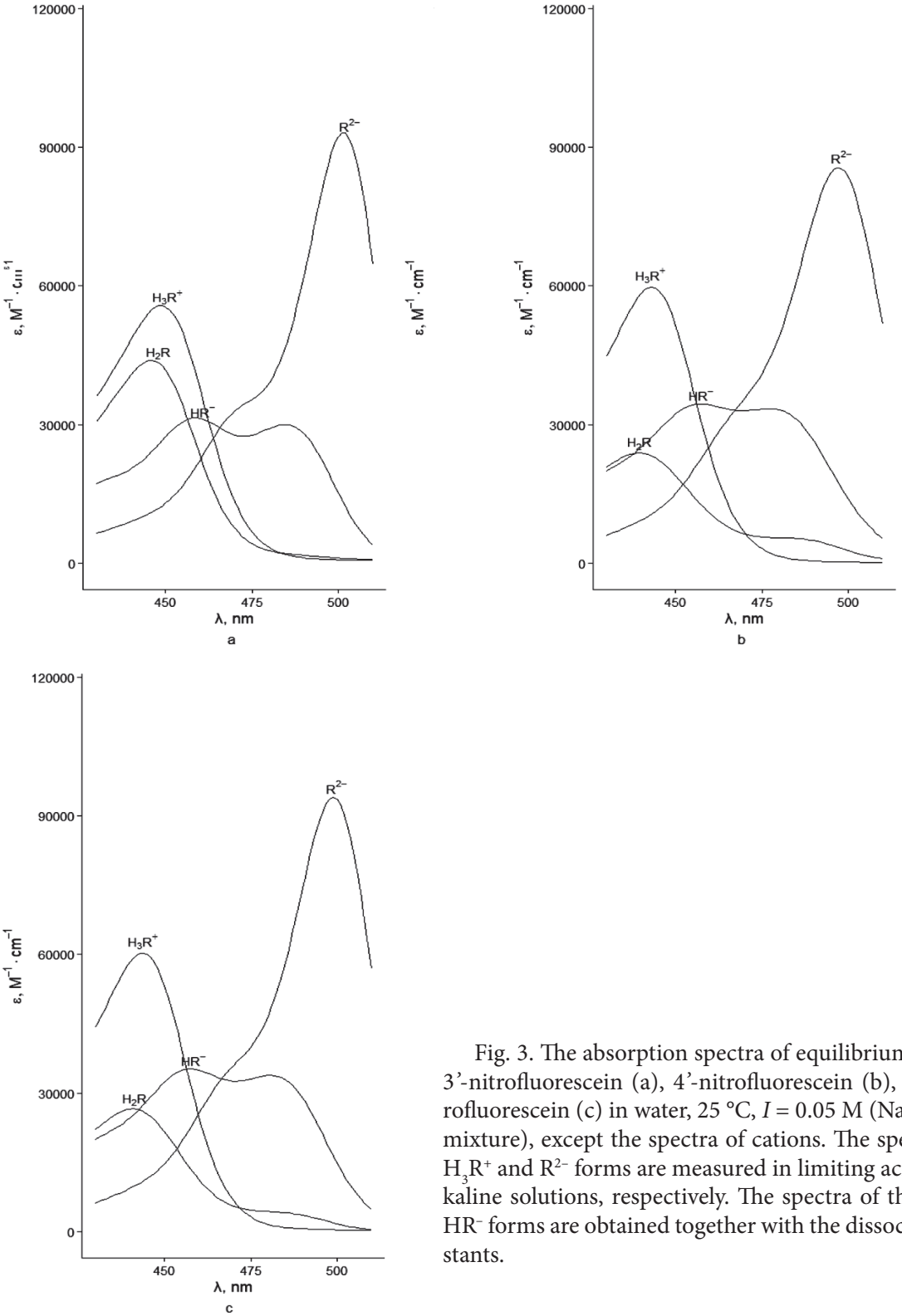

Fig. 3. The absorption spectra of equilibrium species of 3'-nitrofluorescein (a), 4'-nitrofluorescein (b), and 5'-nitrofluorescein (c) in water, 25 °C, I = 0.05 M (NaCl + buffer mixture), except the spectra of cations. The spectra of the H_3R^+ and R^{2-} forms are measured in limiting acidic and alkaline solutions, respectively. The spectra of the H_2R and HR^- forms are obtained together with the dissociation constants.

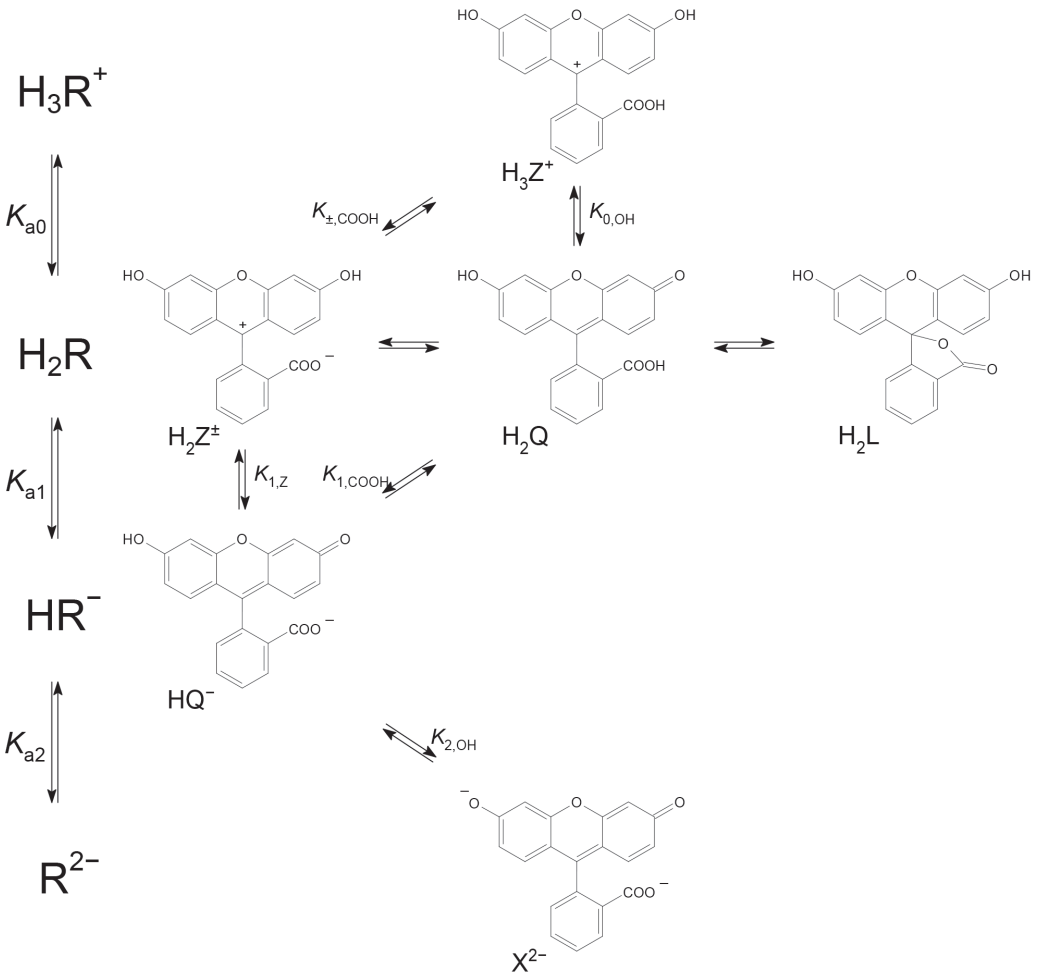

Scheme 2 – Ionic and molecular structures of fluorescein in solution.

It is well known that the absorption spectra of the zwitterionic, $H_2Z^{\pm}$, and quinonoidal, H_2Q, tautomers in the visible are similar to those of the cation, H_3R^+ (structure H_3Z^+ in Scheme 1) and anion HR^- (structure HQ^- in Scheme 1), respectively [10, 11]. The dissociation of the carboxylic group is known to lead only to a slight hypsochromic shift of the band. The lactonic tautomer, H_2L, is colorless due to the sp^3-hybridization of the nodal carbon atom C_9. Using the spectra of the cationic and anionic forms instead of the corresponding tautomers of the H_2R form, respectively, and taking into account the above-mentioned slight shift of the absorption maximum resulting from the dissociation of the COOH group, the fractions α of the latter can be estimated (Table 1). In the case of 3′-nitrofluorescein, the fraction of the tautomer H_2Q is too small to be determined accurately.

Whereas for the unsubstituted fluorescein, α ($H_2Z^{\pm}$) = 0.22; α (H_2Q) = 0.11, and α (H_2L) = 0.67, the stability of the zwitterionic tautomer increases in the case of the nitro derivatives.

The apparent reason is the increase in the acidity strength of the NO_2 group. The 3′, 4′, and 5′ positions correspond to the *ortho*, *meta*, and *para* positions for the COOH group. The *ortho* effect is so pronounced, that the fractions of the quinonoid and lactone tautomers of the 3′-nitrofluorescein cannot be estimated accurately enough. For the other two dyes the fractions of the zwitterionic and quinonoidal tautomers can be assessed more reliably (Table 1). From Scheme 2, Equations (4) and (5) can be derived.

$$pK_{a0} = pK_{\pm,COOH} + \log \alpha(H_2Z^{\pm}) = \\ = pK_{0,OH} + \log \alpha(H_2Q) \quad (4)$$

$$pK_{a1} = pK_{1,COOH} - \log \alpha(H_2Q) = \\ = pK_{1,Z} - \log \alpha(H_2Z^{\pm}) \quad (5)$$

The thermodynamic values of the indices of the so-called microscopic dissociation constants for the unsubstituted fluorescein are as follows: $pK_{\pm,COOH}$ = 2.80; $pK_{0,OH}$ = 3.10; $pK_{1,COOH}$ = 3.49; and $pK_{1,Z}$ = 3.79 [10]. The decrease in the $pK_{1,COOH}$ values for the 4′-, and 5′-nitrofluoresceins as compared to the parent dye is 0.71 and 0.89, respectively, while for the $pK_{\pm,COOH,}$ the values are 0.58 and 0.66 for the same dyes. This corresponds to the *meta* and *para* effects of the nitro group in the benzoic acid and semi-quantitatively agrees with the standard values σ_m = 0.71 and σ_p = 0.78.

The corresponding effects for the $pK_{0,OH}$ values are 0.36 and 0.17, respectively, and for $pK_{1,Z}$, they are 0.49 and 0.40. Thus, despite the absence of conjugation between the benzoic and xanthene parts of the fluorescein molecule, the strong electrophilic properties of the NO_2 group, to some extent, affect the acidity of the OH group. Note that in this case, the influence of the 4′-substitution displays a more substantial effect, obviously because it is in the *para* position for the nodal carbon atom. It aligns with the electron transmittancein the fluorescein molecule, which was earlier studied in DMSO as a solvent [12].

Interestingly, the decrease in the $pK_{1,Z}$ value for the 3′-nitrofluorescein, 1.1, is even more pronounced. Here, the reason may be the steric factor that changes the angle between the two parts of the molecule. Note that the decrease in the pK_{a2} value, which corresponds to $pK_{2,OH}$ in Scheme 2, is 0.26; 0.18; and 0 for the 3′-; 4′-; and 5′-nitrofluorescein, respectively.

The visible absorption spectra at different pH in 50 mass % aqueous ethanol and the dependences of molar absorptivity on pH are shown in Figures 4 and 5, respectively.

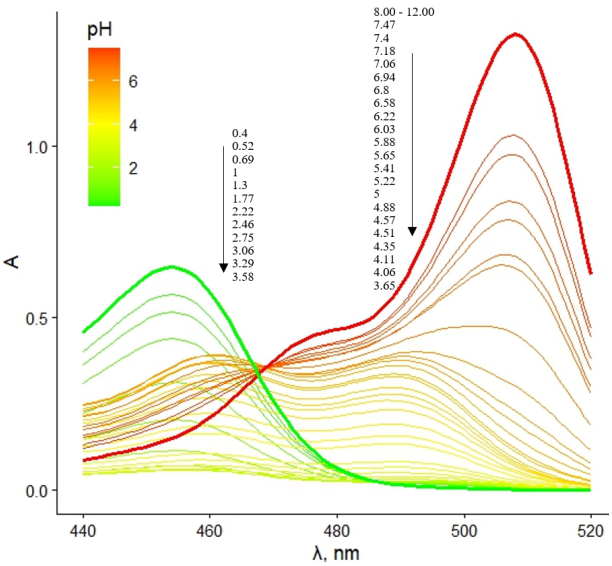

Fig. 4 – The absorption spectra of 3′-nitrofluorescein in 50 mass % aqueous ethanol solutions at different pH, 25°C; The dye concentration 1.31×10^{-5} M; I = 0.05 M except solutions with pH < 1.3. The pH values are given in the activity scale down to pH 1.3; the concentration scale (–logarithm of HCl concentration) was used below this limit.

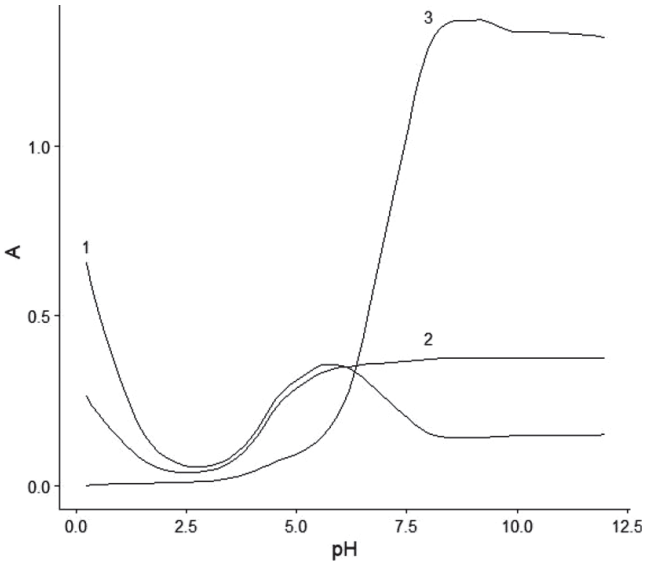

Fig. 5 – The dependence of absorbance of 3′-nitrofluorescein on pH in 50 mass % aqueous ethanol at wavelengths 454 nm (1), 470 (2), and 508 nm (3); 25 °C, I =0.05 M, except the solutions with pH below 1.3.

In Table 2, the results for the equilibria in 50 mass % aqueous ethanol are presented. The relative permittivity of this solvent at 25 °C is 49.0 [11]. The thermodynamic values of the dissociation constants were calculated using the Debye – Hückel equation, the second approach, for ionic activity coefficients. The values of activity coefficients in water are 0.69 and 0.23 for single and double-charged ions, respectively. The spectra of the individual forms of the dyes are presented in Figure 6.

Table 2.

The parameters of ionic equilibria of nitrofluoresceins in 50 mass % ethanol, I = 0.05 M [a,b]

Parameter [c]	3′-Nitrofluorescein	4′-Nitrofluorescein	5′-Nitrofluorescein
pK_{a0}	0.94±0.005 (0.78)	1.12±0.004 (0.96)	0.92±0.008 (0.76)
pK_{a1}	4.33±0.01 (4.49)	5.26±0.01 (5.42)	5.30±0.01 (5.46)
pK_{a2}	6.97±0.01 (7.44)	7.03±0.01 (7.50)	7.12±0.01 (7.59)
$\lambda_{max}/\varepsilon$ (H_3R^+)×10^{-3}	454 nm / 49.39	448 nm / 57.474	449 nm / 58.175
$\lambda_{max}/\varepsilon$ (H_2R)×10^{-3}	444 nm / 2.631 479 nm / 1.645	459 nm / 1.183; 489 nm / 1.108	455 nm / 1.482 481 nm / 1.123
$\lambda_{max}/\varepsilon$ (HR^-)×10^{-3}	448 nm / 31.519 477 nm / 27.880	457 nm / 34.744; 482 nm / 32.195	459 nm / 38.132; 486 nm / 35.741
$\lambda_{max}/\varepsilon$ (R^{2-})×10^{-3}	508 nm / 101.03	503 nm / 90.206	506 nm / 111.796
α ($H_2Z^{\pm}$)	0.018	—	—
α (H_2Q)	0.058	0.034	0.035
α (H_2L)	0.929	0.966	0.965
$pK_{0,OH}$	2.02	2.43	2.22
$pK_{1,COOH}$	3.25	3.95	4.00

Note. [a]The pK_a values in parenthesis are thermodynamic. [b] The molar absorptivities, ε, are expressed in M^{-1}cm^{-1}. [c]For fluorescein, the thermodynamic pK_a values are 0.94, 6.82, and 7.66 [11].

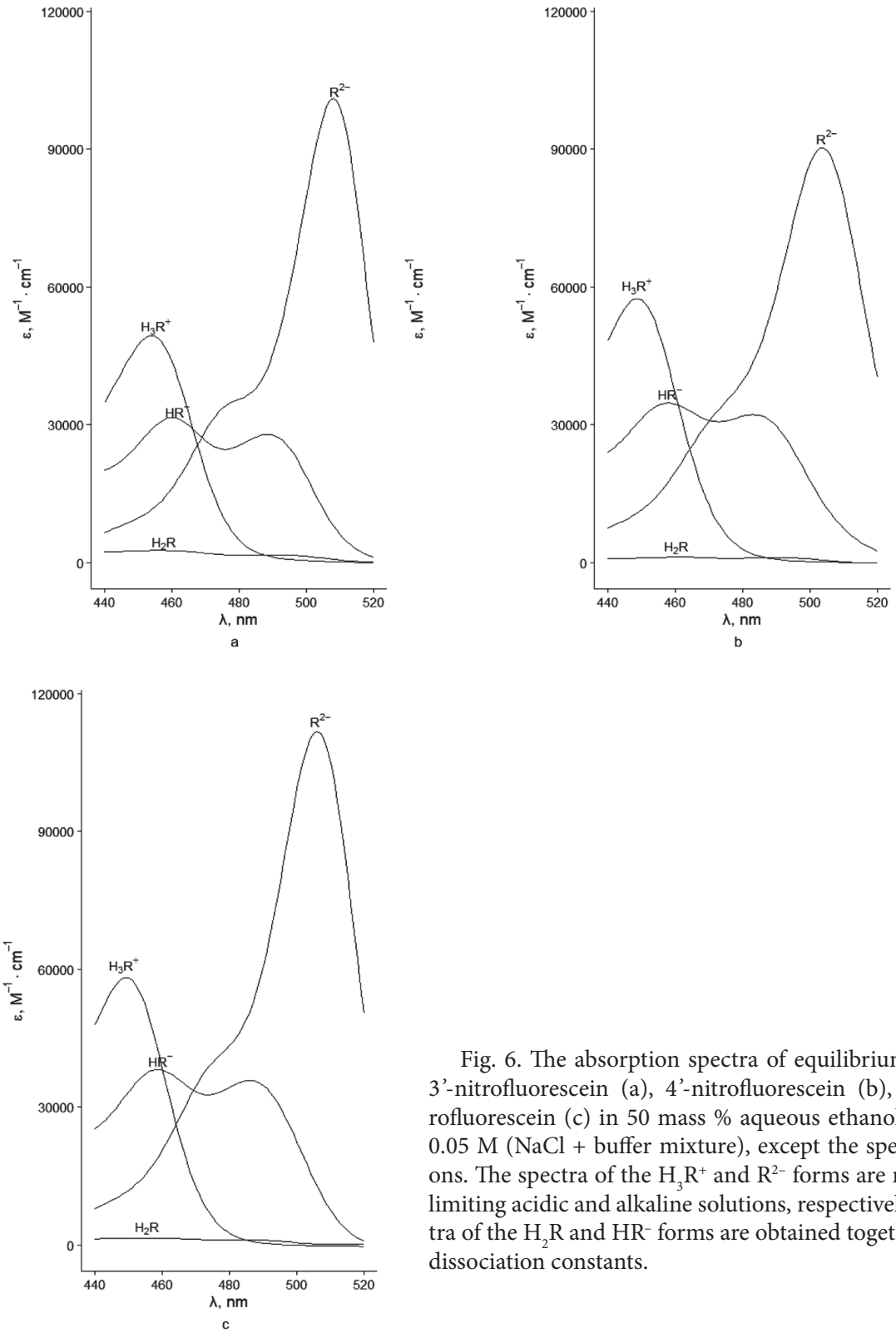

Fig. 6. The absorption spectra of equilibrium species of 3'-nitrofluorescein (a), 4'-nitrofluorescein (b), and 5'-nitrofluorescein (c) in 50 mass % aqueous ethanol; 25 °C, I = 0.05 M (NaCl + buffer mixture), except the spectra of cations. The spectra of the H_3R^+ and R^{2-} forms are measured in limiting acidic and alkaline solutions, respectively. The spectra of the H_2R and HR^- forms are obtained together with the dissociation constants.

The most striking difference when moving from water to this binary solvent is the drop in the molar absorptivity of the neutral form, H_2R. The apparent reason is the substantial shift of the state of the tautomeric equilibrium towards the colorless lactone. Following the above-described approach, the α (H_2Q) value was estimated, while no severe signs of the zwitterion were observed (Table 2). Only in the case of 3′-nitrofluorescein, some signs of the presence of $H_2Z^{\pm}$ were fixed. On the one hand, it reflects the instability of the highly polar tautomer in the organic environment. On the other hand, it proves the marked increase in the acidity of the COOH group in the presence of the NO_2 group in the *ortho* position, which leads to a small yield of $H_2Z^{\pm}$ in 50 mass % aqueous ethanol.

The $pK_{0,OH}$ values for 4′-nitro- and 5′-nitrofluorescein decrease by 0.31 and 0.71 units, respectively, when going from water to the aqueous ethanol, while the $pK_{1,COOH}$ values increase by 1.17 and 1.40 units, respectively. Such medium effects are typical for cationic and neutral acids, respectively. For fluorescein, these changes are –0.69 and +1.89, respectively [11]. Further, the difference between $pK_{1,COOH}$ of fluorescein, and the nitro derivative increases. For 4′-nitro- and 5′-nitrofluorescein,these values are 1.43 and 1.38, respectively. Comparing them with the values for an aqueous solution, 0.71 and 0.89, respectively, one should concludethat Hammett's ρ constant increases in nonaqueous media.

The $pK_{1,COOH}$ values of the nitro derivatives, 3.25, 3.95, and 4.00 (Table 2) are pronouncedly lower than that of fluorescein (5.38) [11]. This should be ascribed to the increase in the Hammett's constant ρ, which is typical for organic solvents [7].

To better understand the equilibrium in aqueous ethanol, we determined the dissociation constants of 3′-nitrofluorescein methyl ester (Scheme 3) synthesized previously [6]. The solubility of the methyl and ethyl esters in water is scarce; therefore the study was performed in aqueous ethanol.

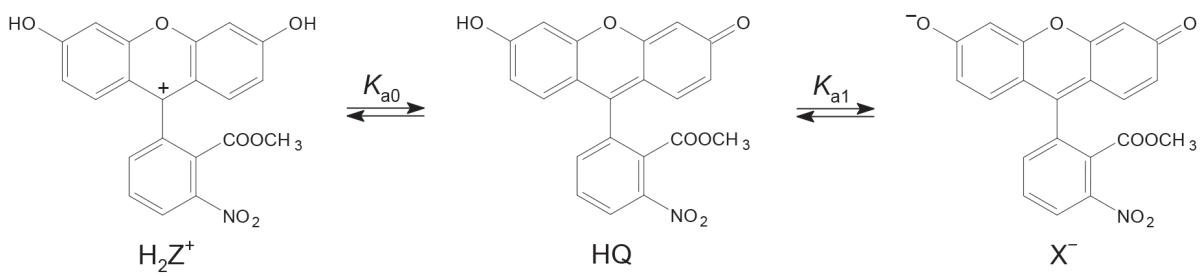

Scheme 3 – Dissociation of methyl ester of 3′-nitrofluorescein in solution.

The absorption spectra at different pHs are shown in Figure 7. The equilibrium parameters are presented in Table 3. The pK_{a0}value of this dye corresponds to the $pK_{0,OH}$ of the parent compound (Table 2); considering the accumulation of errors in assessing the latter, the match can be regarded as satisfactory. This $pK_{0,OH}$ of fluorescein and its ethyl ester in 50 mass % aqueous ethanol are equal to 2.41 and 2.05, respectively [11].

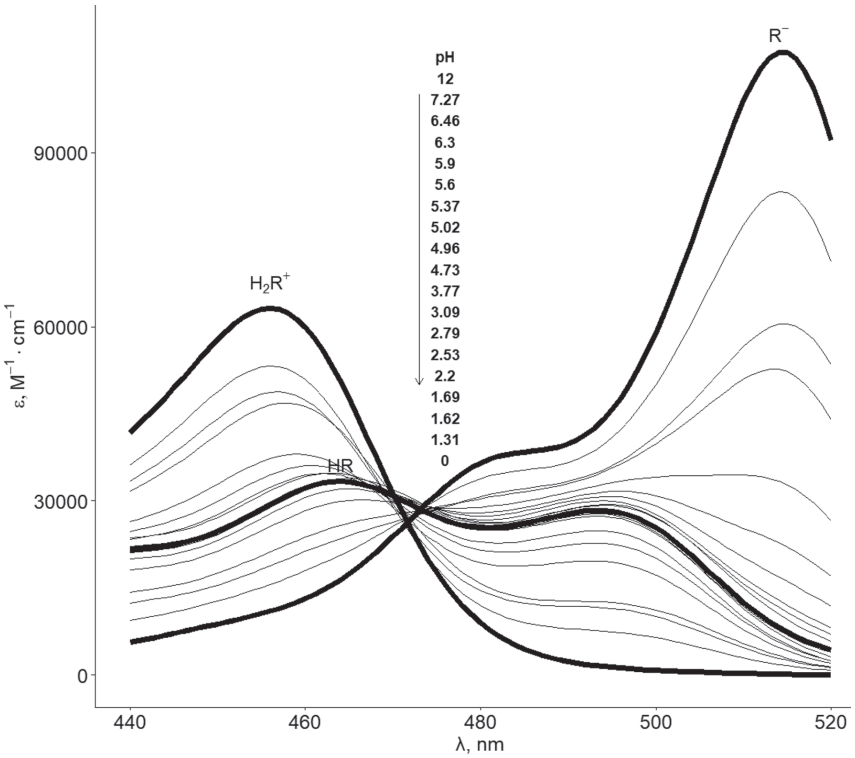

Fig. 7. The absorption spectra of 3'-nitrofluorescein methyl ester in 50 mass % ethanol, 25 °C, at different pH values; I = 0.05 M except for solutions with pH < 1.3. The pH values are given in the activity scale down to pH 1.3; the concentration scale (–logarithm of HCl concentration) was used below this limit. Bold curves represent absorption spectra of equilibrium species.

The difference between the pK_{a1} = 6.59 of the methyl ester and pK_{a2} = 7.44 should be ascribed to the influence of the negative charge of the carboxylate group on the dissociation of the OH group in the resorcinol part, according to the Bjerrum – Kirkwood – Westheimer equation [7, 11]. So, the difference between the $pK_{a2}$of fluorescein and pK_{a1} of its ethyl ester is 0.95 [11].

The final part of this communication is devoted to the kinetics of hydrolysis of the diacetyl derivatives of the three nitrofluoresceins. The two-step hydrolysis (Scheme 4) was described using the pseudo-first-order rate constants, k', at the fixed pH value: $k' = k\, c_{OH^-}$.

Table 3

The parameters of equilibria of 3′-nitrofluorescein methyl ester (Scheme 3) in 50 mass % ethanol [a,b]

pK_{a0}	1.79±0.01 (1.63)
pK_{a1}	6.43±0.02 (6.59)
λ_{max} / ε (H_2R^+)×10^{-3}	456 nm / 63.19
λ_{max} / ε (HR)×10^{-3}	462 nm / 33.34 492 nm / 28.34
λ_{max} / ε (R^-)×10^{-3}	514 nm / 107.29

Note. [a]I = 0.05 M . [b]The molar absorptivities, ε, are expressed in $M^{-1}cm^{-1}$.

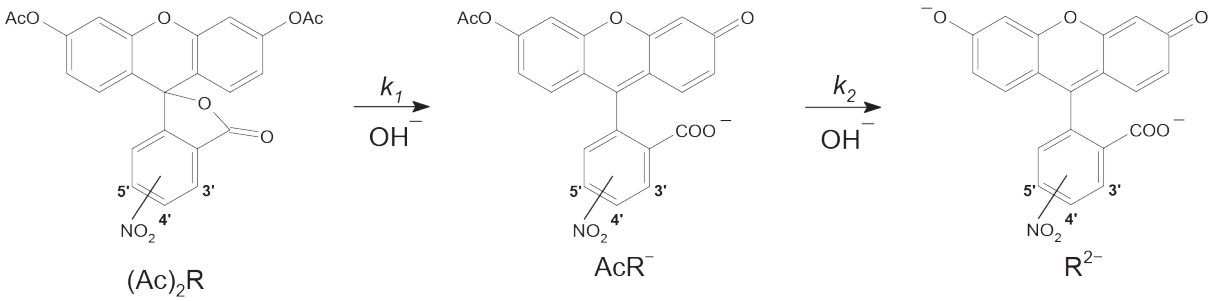

Scheme 4 – Alkaline hydrolysis of the diacetyl derivative of nitrofluoresceins.

The spectral data are typified in Figure 8. The normalized spectra demonstrate two types of colored forms. The main idea is to equating to the absorption spectrum of the AcR^- ion to that of HR^- of the corresponding fluorescein dye [1, 5]. The spectrum of the final product of hydrolysis, R^{2-}, was already determined above. This made it possible to calculate the current concentrations of the AcR^- and R^{2-} forms at each moment. Then, the current concentrations of the colorless $(Ac)_2R$ form can be easily calculated.

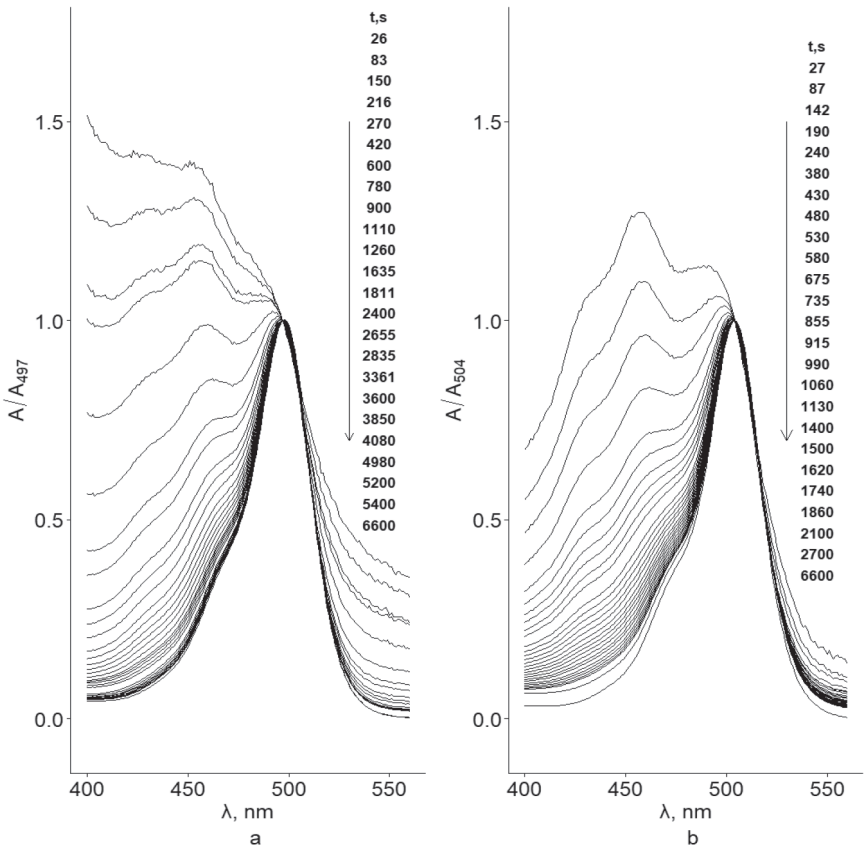

Fig. 8 – Normalized absorption spectra during the hydrolysis of 4′-nitrofluorescein and in water (a) and in 50 mass % aqueous ethanol (b), 25 °C, I = 0.05 M (NaCl + buffer mixture).

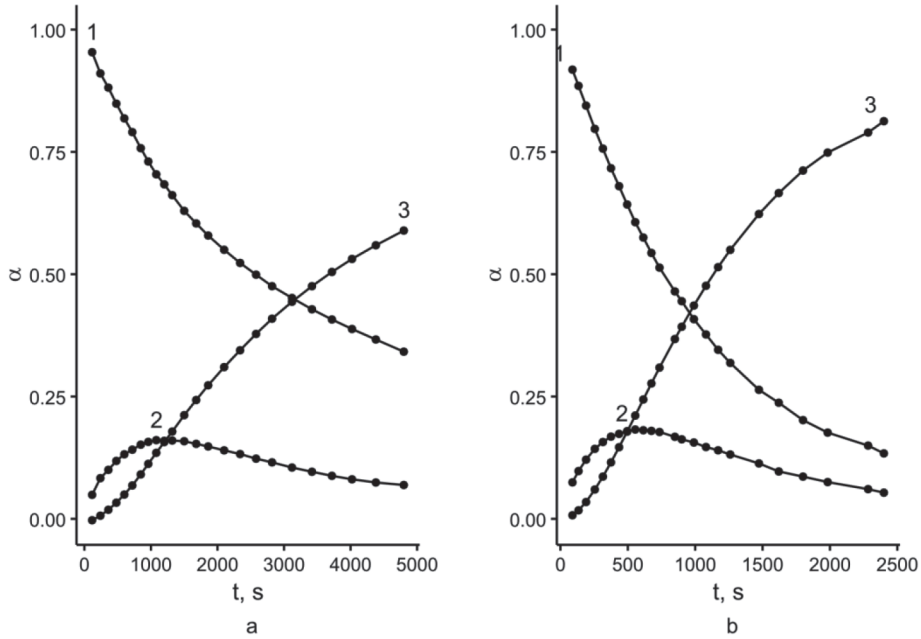

Fig. 9 – Dependences of the molar fractions of $(Ac)_2R$ (1), AcR^- (2), andR^{2-} (3) of 5′-nitrofluorescein in water (a) and in 50 mass % aqueous ethanol (b), 25 °C, I = 0.05 M (NaCl + borate buffer).

Table 4.

The rate constants of hydrolysis of nitrofluoresceins in solution, 25 °C, I = 0.05 M.

Compound	pH	k_1', s^{-1}	k_2', s^{-1}	k_2/k_1
		Water		
Diacetyl fluorescein [1]	9.72	3.5±0.2	4.5±0.3	1.29
Diacetyl 3′-nitrofluorescein	9.67	1.39±0.04	6.72±0.2	4.84
Diacetyl 4′-nitrofluorescein	9.74	4.29±0.13	12.2±0.4	2.85
Diacetyl 5′-nitrofluorescein	9.74	2.44±0.13	9.56±0.5	3.91
		50 mass % aqueous ethanol		
Diacetyl fluorescein [1]	10.50	13.10±0.4	26.00±0.8	1.98
Diacetyl 3′-nitrofluorescein	10.36	7.16±0.08	27.83±0.3	3.89
Diacetyl 4′-nitrofluorescein	10.38	11.28±0.33	24.69±0.25	2.19
Diacetyl 5′-nitrofluorescein	10.28	8.55±0.19	27.71±0.6	3.24

The dependence of the fractions of the three forms on time is demonstrated in Figure 9. The results of the kinetic study are presented in Table 4.

A comparison of the rate constants for a given compound in water and aqueous ethanol demonstrates either no significant changes or deceleration of the hydrolysis in the sec-

ond solvent. For all the nitro derivatives, the k_2/k_1 ratio is higher than that for the parent dye. However, the reasons are not so clear.

The influence of the nitro group on the k_2' value is similar to that of the K_{a2}. Although there is no conjugation between the two parts of the molecule, the electrophilic properties of this substituent result in a slight increase in both K_{a2} and k_2'. In water, the pK_{a2}s for fluorescein, 3′-, 4′-, and 5′-nitrofluorescein are 6.80, 6.54, 6.62, and 6.80, respectively, whereas the k_2' values after re-calculation to pH 9.74 are 4.93, 7.89, 12.2, and 9.56 s^{-1}, respectively. In 50 mass % ethanol, the correspondent pK_{a2} values are equal to 7.66, 7.44, 7.50, and 7.59, while k_2' = 18.8, 27.83, 25.57, and 33.31 s^{-1} (at pH 10.36).

The influence of the nitro group on the first rate constant is less clear, on the one hand, due to the sp^3-hybridization of the nodal carbon atom C_9, and on the other hand, because of the lack of the equilibrium constant that can be compared with the k_1' rate constant. In any case, after reduction to the same pH, the smallest first rate constant is observed for 3′-nitro fluorescein, while the largest one – is for the 4′- derivative. Note that 4′ is the *para* position to the nodal carbon atom.

CONCLUSIONS. The dissociation constants of 3′-, 4′-, and 5′-nitrofluorescein were determined in water and 50 mass % aqueous ethanol. The state of the tautomeric equilibrium of the molecular forms of the nitrofluoresceins substantially differs from that of the parent dye. A feature of the tautomerism of molecular forms of dyes is a sharp increase in the proportion of zwitterion and destabilization of the colorless lactone compared to un-substituted fluorescein. By contrast, the lactone tautomer predominates in aqueous ethanol. The influence of the nitro groups on the rate of hydrolysis is relatively small due to the lack of conjugation between the two parts of the molecule. Nevertheless, for all the nitro derivatives, the k_2/k_1 ratio is higher than that for the parent dye.

This study was partially supported by the Ministry of Education and Science of Ukraine, Ukraine, via grant number 0122U001485 and by the Simons Foundation, USA, via grant number 1030292.

МОНОНІТРОФЛУОРЕСЦЕЇНИ У ВОДНИХ СЕРЕДОВИЩАХ: КИСЛОТНО-ОСНОВНІ РІВНОВАГИ, ТАУТОМЕРИЗМ ТА ГІДРОЛІЗ ДІАЦЕТАТІВ

Д. В. Харченко, С. В. Шеховцов, Т. О. Чейпеш, М. О. Мчедлов-Петросян*

Харківський національний університет імені В. Н. Каразіна,
пл. Свободи, 4, Харків 61022, Україна
**e-mail: mchedlov@karazin.ua*

У статті наведено рівноважні та кінетичні дані для трьох флуоресцеїнових барвників, що містять нітрогрупу в залишку фталевої кислоти, 3′-, 4′- і 5′-нітрофлуоресцеїну, у воді та 50 мас.% водному етанолі. Ці сполуки, зокрема нещодавно синтезований 3′-нітрофлуоресцеїн, вважали менш поліпротонними кислотами, ніж багато інших флуоресцеїнових барвників. Барвники поводяться як дипротонні кислоти, які також можуть бути протонованими: $H_3R^+ \rightleftharpoons H_2R \rightleftharpoons HR^- \rightleftharpoons R^{2-}$. Константи дисоціації у воді та 50 мас.% водному етанолі отримували в буферних розчинах розведеної HCl за до-

помогою спектрофотометричного методу з потенціометричним визначенням pH за іонної сили 0,05 M і 25,0 ±1 °C. Концентрації барвників у робочих розчинах, як правило, були в межах (5–10)×10^{-6} M. Термодинамічні значення констант дисоціації розраховували за допомогою рівняння Дебая – Хюккеля, другий підхід для коефіцієнтів іонної активності. Визначено спектри поглинання у видимій області окремих молекулярних та іонних форм для вищезазначених сполук та складного ефіру 3′-нітрофлюоресцеїну. Для останнього також визначали константи дисоціації у водному етанолі. Якщо у воді частка цвіттер-іонного таутомера нітрофлюоресцеїнів збільшується порівняно з вихідною сполукою, то у водному етанолі переважає безбарвний лактон. Визначено мікроскопічні константи дисоціації, значення яких відповідають впливу електрофільної нітрогрупи. Лужний гідроліз діацетатів нітрофлуоресцеїну досліджували у двох вищезгаданих розчинниках. Отримані результати дозволили виділити константи швидкості двостадійної кінетики гідролізу діацетил-похідних нітрофлуоресцеїнів.

Ключові слова: нітрофлуоресцеїн, кислотно-основна дисоціація, водно-етанольний бінарний розчинник, спектри поглинання, константи дисоціації, таутомерія, двоступінчатий лужний гідроліз, константи швидкості.

REFERENCES

1. Cheipesh T.A., Kharchenko D.V., Taranets Yu.V., Rodik R.V., Mchedlov-Petrossyan N.O., Poberezhnyk M.M., Kalchenko V.I. Reaction rates in aqueous solutions of cationic colloidal surfactants and calixarenes: Acceleration and resolution of two steps of fluorescein diesters hydrolysis. *Colloids Surf. A: Physicochem. Eng. Aspects.* 2020. **606**: 125479. https://doi.org/10.1016/j.colsurfa.2020.125479.
2. Ge F.Y., Chen L.G., Zhou X.L., Pan H.Y., Yan F.Y., Bai G.Y., Yan X.L. Synthesis and study on hydrolytic properties of fluorescein esters. *Dyes Pigm*. 2007. **72**(32): 322–326. https://doi.org/10.1016/j.dyepig.2005.09.012
3. Green V.S., Stott D.E., Diack M. Assay for fluorescein diacetate hydrolytic activity: Optimization for soil samples. *Soil Biol. Biochem.* 2006. **38**: 693–701. https://doi.org/10.1016/j.soilbio.2005.06.020
4. Sánchez-Monedero M. A., Mondini C., Cayuela M. L., Roig A., Contin M., De Nobili M. Fluorescein diacetate hydrolysis, respiration and microbial biomass in freshly amended soils. *Biology and Fertility of Soils*. 2008. **44**(6): 885–890. https://doi.org/10.1007/s00374-007-0263-1
5. Cheipesh T.A., Taranets Yu.V., Mchedlov-Petrossyan N.O. Kinetics of alkaline hydrolysis of dilaurylfluorescein in aqueous ethanol and micellar solution of cetyltrimethylammonium bromide, *Kharkov University Bulletin. Chemical Series*. 2014. **23**: 5–13. https://doi.org/10.26565/2220-637X-2014-23-01
6. Shekhovtsov S.V., Omelchenko I.V., Shishkina S.V., Doroshenko A.O., Vus K.O., Vlasenko H.S., Mchedlov-Petrossyan N.O. 3′-Nitro- and 3′-Aminofluoresceins: Appearance of Previously Missing Dyes.*Colorants*. 2023. **2**: 500–518. https://doi.org/10.3390/colorants2030024
7. Mchedlov-Petrossyan N.O., Cheipesh T.A., Moskaeva E.G., Shekhovtsov S.V., Ostrovskyi K.I. Towards understanding of stepwise acid-base dissociation in systems inclined to tautomerism: Nitro derivatives of fluorescein in dimethyl sulfoxide. *J. Mol. Liquids*. 2023. **386**:122540. https://doi.org/10.1016/j.molliq.2023.122540
8. Kozáková E., Cséfalvayová B., Zajacová J. pH* Values of the standard succinate buffer solution

in the 50 mass % ethanol–water solvent. *Chem. Zvesti.* 1982. **36**(3): 345–351.
9. Konyaev D., Myerniy S., Kholin Y. CLINP Program, http://www-chemo.univer.kharkov.7 ua/kholin/clinp.html
10. Bogdanova L.N., Mchedlov-Petrossyan N.O., Vodolazkaya N.A., Lebed A.V. The influence of *β*–cyclodextrin on acid-base and tautomeric equilibrium of fluorescein dyes in aqueous solution. *Carbohydr. Res.* 2010. **345**(13): 1882–1890.
https://doi.org/10.1016/j.carres.2010.07.002
11. Mchedlov-Petrossyan N.O., Cheipesh T.A., Shekhovtsov S.V., Redko A.N., Rybachenko V.I., Omelchenko I.V., Shishkin O.V. Ionization and Tautomerism of Methyl Fluorescein and Related Dyes. *Spectrochim. Acta A*. 2015. **150**: 151–161.
https://dx.doi.org/10.1016/j.saa.2015.05.037
12. Moskaeva E.G., Ostrovskiy K.I., Shekhovtsov S.V., Mchedlov-Petrossyan N.O. Transmittance of electronic effects in the fluorescein molecule: Nitro and amino groups in the phthalic acid residue. *Kharkiv University Bulletin. Chemical Series*. 2021. **36**: 24–32.
https://doi.org/10.26565/2220-637X-2021-36-05

Стаття надійшла 25.12.2024.

UDC 541.49+546.814 doi: 10.33609/2708-129X.90.9.2024.19-30

STRUCTURE FEATURES AND PHARMACOLOGICAL PROPERTIES OF GERMANIUM(IV) COMPLEXES WITH 1-HYDROXYETHANE-1,1-DIPHOSPHONIC ACID.

Olena Martsynko[1], Inna Seifullina[1], Olena Finik[2], Kyrylo Tsymbaliuk[1,2]

[1]Odesa I. I. Mechnikov National University, Dvoryanska St., 2, Odesa, 65082, Ukraine;
[2]LLC "INSPECTORAT UKRAINE", Udilnyi lane, 1, Odesa, 65009, Ukraine
e-mail: lborn@ukr.net

The review article presents the results of systematic research by the authors of a number of heterometals and mixed-ligand 1-hydroxyethane-1,1-diphosphonatogermanates, their structure, biological and pharmacological properties. It was observed, that hexanuclear cyclic complex anions of the general composition $[Ge_6(\mu\text{-}OH)_{6-n}(\mu\text{-}O)_n(\mu\text{-}hedp)_6]^{(6+n)-}$ were present in the aqueous solutions of investigated compounds. At the same time, the composition and charge of the anion in each compound obtained in the solid state depends on the nature of the cation. They all have a common hexameric structure, with germanium atoms connected in pairs by 1-hydroxyethane-1,1-diphosphonate, hydroxo-, or oxo- and hydroxo-bridges. The coordination polyhedron Ge is a curved octahedron with two six-membered GeO_2P_2C cycles and an eight-membered bimetallic $Ge_2O_4P_2$ closing, and each ligand performs a tetradentate tris(chelate)-μ-bridging function. The ratio of formed oxo- and hydroxo-bridges and, as a result, the charge of the anion varies under the influence of cation parameters and electrostatic interactions. Acute and chronic toxicity studies proved the safety of 1-hydroxyethane-1,1-diphosphonatogermanates. Complexes show a wide spectrum of pharmacological activity: antihypertensive, antiarrhythmic, hepatoprotective, cerebroprotective etc.The pharmacological and biological activities of 1-hydroxyethane-1,1-diphosphonatogermanates(IV) are ensured by the combined action of all biologically active components, which do not compete but show synergistic action. It was concluded that the preparation of new complexes of germanium(IV) with etidronic acid by chemical modification of their composition is a promising area of research in the field of creating coordination compounds with a wide range of pharmacological effects.

Keywords: germanium(IV), 1-hydroxyethane-1,1-diphosphonic (etidronic) acid, nitrogen heterocycles, coordination compounds, biological activity.

INTRODUCTION. As a result of years of systematic research providedat the Odesa I.I. Mechnikov National University, the authors have synthesized a wide range of coordination compounds of germanium(IV) and implemented a new approach to developing biocoordination chemistry of germanium(IV) as an independent scientific field. The complexes demonstrated significant advantages compared to organic compounds of germanium such as low toxicity, solubility in water and environmentally friendly synthetic route.

The authors have synthesized germanium(IV) coordination compounds with O, P, N-containing chelating organic ligands with physiological activity [1, 2]. It was shown that the synergism of germanium and bioligands provides their pharmacological properties.

The uniqueness of germanium as a complexing agent and biogenic element is most clearly demonstrated by the example of 1-hydroxyethane-1,1-diphosphonic (etidronic) acid (H_4hedp), a well-known multifunctional phosphonic complex with various valuable properties used in pharmacy and cosmetology.

Etidronic acid, due to its specific stereochemistry and mutual interaction of phosphonic fragments, is capable of forming both monomeric complexes with s-, p-, d-, and f-element ions and coordination di-, oligo-, and polymers. Compared to other phosphonic complexing agents, a considerable number of coordination compounds of etidronic acid with various metals have been synthesized and structurally characterized using different methods [3–9].

The uniqueness of germanium as a complexing agent and biogenic element is most clearly demonstrated by the example of 1-hydroxyethane-1,1-diphosphonic (etidronic) acid (H_4hedp), a well-known multifunctional phosphonic complex with various valuable properties used in pharmacy and cosmetology. H_4hedp belongs to the class of moderately toxic substances and does not possess sensitizing or cumulative properties, which makes it suitable for use as a pharmaceutical agent [10–14]. The high efficacy of metal coordination compounds with H_4hedp has been demonstrated in applications for pain relief in cases of bone metastases (^{186}Re) and the diagnosis (^{188}Re) of bone cancer [15].

The aim of this work is analysis of the array of experimental data on the structure, biological and pharmacological properties of homo- and heterometallic, mixed-ligand 1-hydroxyethane-1,1-diphosphonatogermanates(IV) and identify promising areas of their application.

Structural insights into 1-hydroxyethane-1,1-diphosphonatogermanates. Previously spectrophotometric measurements have proved that an acidic complex with a molar ratio Ge : ligand = 1:1 exists in solution in the GeO_2 - H_4hedp - H_2O system at pH = 2 [16]. Subsequently, methods were developed for the isolation of germanium(IV) coordination compounds with ethidronic acid. It was shown that the interaction of germanium dioxide and germanium tetrachloride with H_4hedp in water produces the same X-ray amorphous glassy compound. As a result of complexation, hydrolysis of germanium tetrachloride is inhibited. Detailed methods for the synthesis of various types of 1-hydroxyethane-1,1-diphosphonatogermanates(IV) are given in [1, 16–18].

The idea of introducing an outer-sphere (exo-) ligand into the reaction medium, for example, an organic molecule capable of protonation, such as nicotinic acid, nicotinamide, piracetam, etc., was proposed to obtain crystals [1]. Also, alkali and alkaline earth metals were introduced and bimetallic complexes were obtained.

X-ray crystallographic data of complexes with nicotinic acid
$(HNic)_6[Ge_6(\mu\text{-}OH)_6(\mu\text{-}hedp)_6]\cdot 12H_2O$,
magnesium
$[Mg(H_2O)_6]_2H_2[Ge_6(\mu\text{-}OH)_6(\mu\text{-}hedp)_6]\cdot 28H_2O$
and barium
$Ba_3[Ge_6(\mu\text{-}OH)_6(\mu\text{-}hedp)_6]\cdot 25H_2O$
were received.

It was found that the crystals of the compounds were based on identical hexanuclear

cyclic complex anions $[Ge_6(\mu\text{-}OH)_6(\mu\text{-}hedp)_6]^{6-}$ (рис. 1) in which six germanium atoms are interconnected by six bridging ligand molecules (phosphonium groups are completely deprotonated, each of them is connected to different germanium atoms), as well as six bridging hydroxo-groups. The coordination polyhedron is a curved octahedron typical of tetravalent germanium. The cations are cations of $NicH^+$ protonated on the nitrogen atom of the nicotinic acid heterocycle and hexaquacations of s-metals.

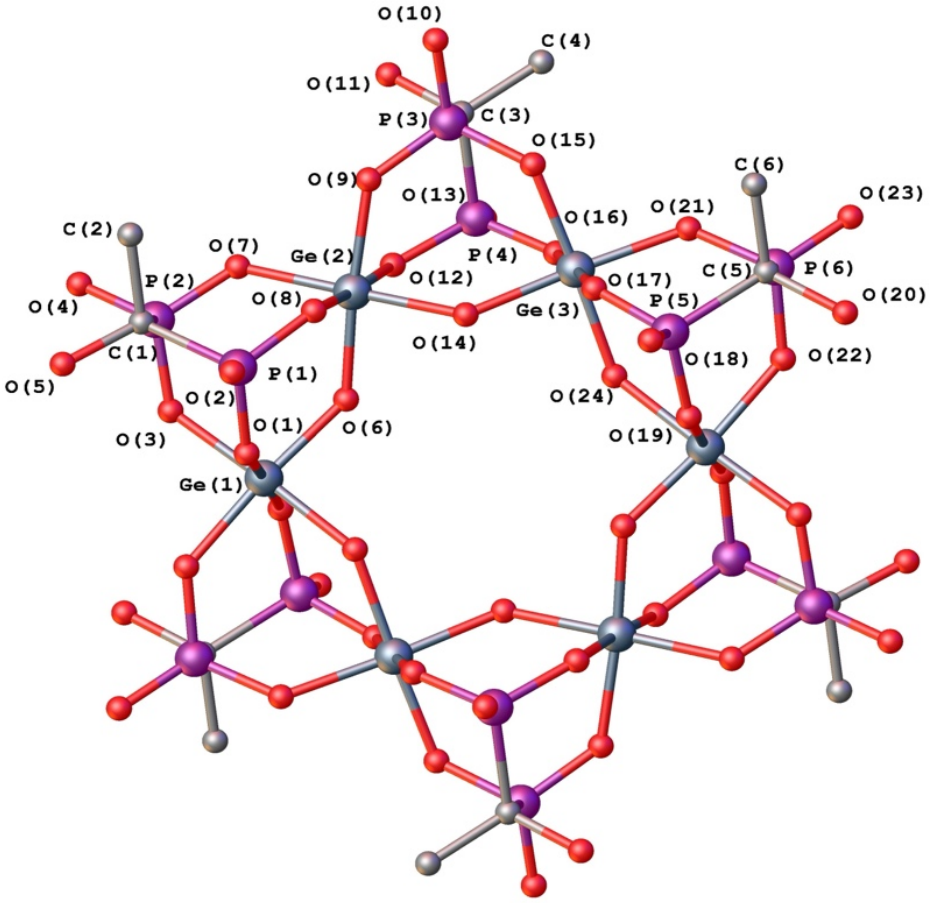

Fig. 1. Crystal structure of the anion $[Ge_6(\mu\text{-}OH)_6(\mu\text{-}hedp)_6]^{6-}$ [1].

In the structure $Ba_3[Ge_6(\mu\text{-}OH)_6(\mu\text{-}hedp)_6]\cdot 25H_2O$ the barium atoms are coordinated exclusively by the oxygen atoms of water molecules. However, the significant disorder of all Ba^{2+} cations and some water molecules prevented the precise determination of the crystal structure, coordination number and coordination polyhedron of barium atoms, and the way the structural units are packed in the crystal.

The structure of 1-hydroxyethane-1,1-diphosphonatogermanates(IV) of metals of other electronic units was investigated. After obtain-

ing the structural data of the bimetallic complex with zinc, $Zn_4[Ge_6(\mu\text{-}OH)_4(\mu\text{-}O)_2(\mu\text{-}hedp)_6]\cdot 38H_2O$, it was found that there is a change in the structure of the hexanuclear anion (2 hydroxo-bridges out of 6 are converted to oxo-bridges). This structure also contains octahedral complex zinc cations with different ligand environments: hexaquacations and cations in which two of the six adjacent (cis) vertices of the zinc octahedron are occupied by the terminal ligand atoms of the two hexanuclear anions, and the remaining four vertices contain oxygen atoms of water molecules (Fig. 2). That is, the molecular formula of these compound can be written as $[Zn_4(H_2O)_{18}][Ge_6(\mu\text{-}OH)_4(\mu\text{-}O)_2(\mu\text{-}Oedph)_6]\cdot 20H_2O$.

The complex cations and hexanuclear anions are connected by an extensive network of hydrogen bonds through coordinated and crystallising water molecules. A single independent hydrogen bond is also implemented, which directly connects each hexanuclear anion with four neighbouring ones, thus forming a polymeric anionic layer.

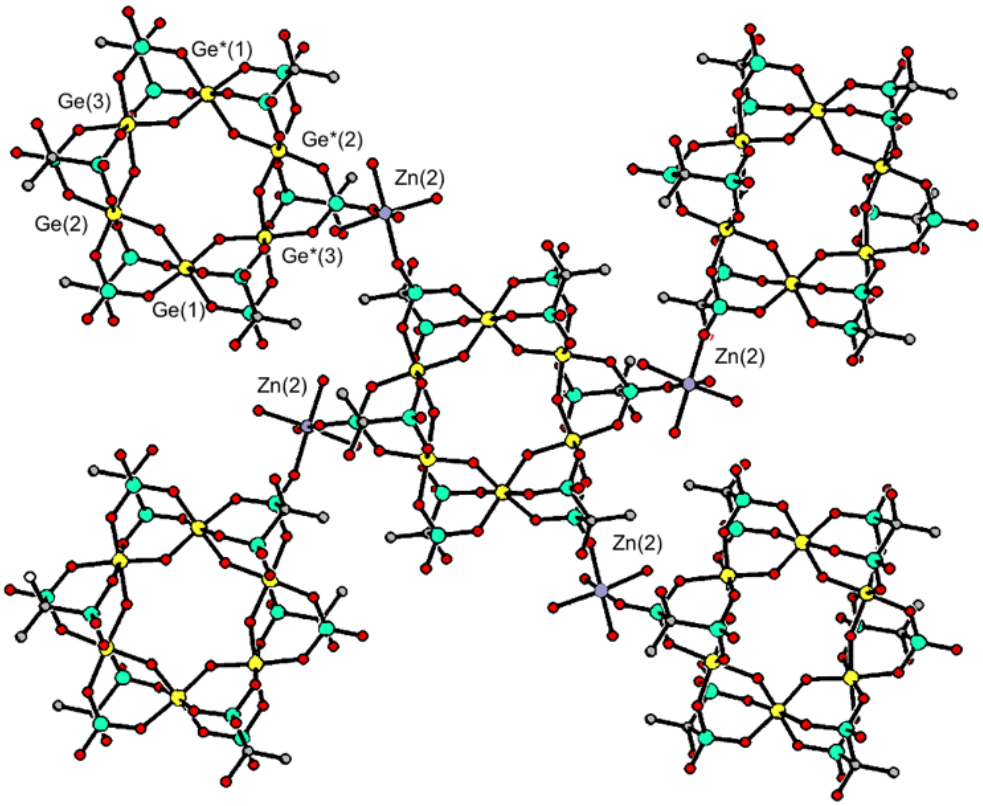

Fig. 2. Fragment of the domain layer $[Zn(2)\{Ge_6(\mu\text{-}OH)_4(\mu\text{-}O)_2(\mu\text{-}hedp)_6\}]_n$ in the crystal structure of $[Zn_4(H_2O)_{18}][Ge_6(\mu\text{-}OH)_4(\mu\text{-}O)_2(\mu\text{-}Oedph)_6]\cdot 20H_2O$.

Coordination compounds with lanthanides are coordination polymers. The X-ray diffraction study of three heterometallic coordination polymers of general formula $\{Ln_2[LnGe_6(\mu\text{-}hedp)_6(\mu\text{-}O)_3(\mu\text{-}OH)_3(H_2O)_4]\cdot xH_2O\}_n$ (Ln = Nd, x ~ 26; Er, x ~ 24; Tm, x ~ 20) is perfor-

med. The basis element of structures is a hexanuclear complex anion $[Ge_6(\mu\text{-hedp})_6(\mu\text{-O})_3(\mu\text{-OH})_3]^{9-}$, in which bridging hydroxo- and oxo-ligands are statistically disordered with equal probability. Hexameric units are connected by $Ln1(H_2O)_4$ fragments into a framework (fig. 3). In structures are channels accommodating disordered lanthanide atoms and water molecules. The complete disordering of lanthanide atoms in the channels and the almost complete disordering of water molecules coordinating them do not allow us to determine the actualhydrate composition of complexes.

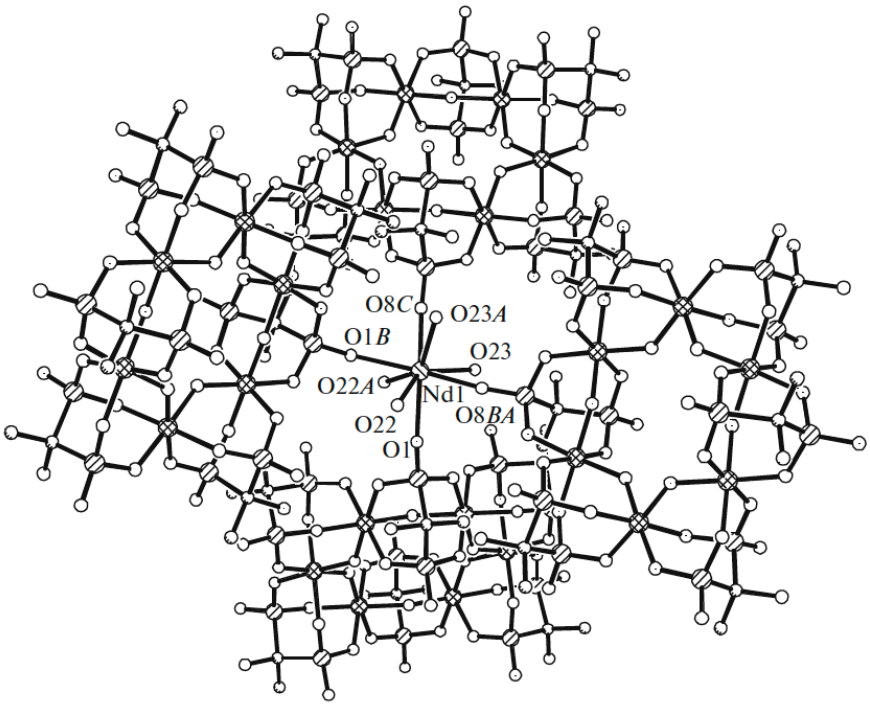

Fig. 3. Fragment of thestructure of $\{Nd_2[NdGe_6(\mu\text{-hedp})_6(\mu\text{-O})_3(\mu\text{-OH})_3(H_2O)_4]\cdot 26H_2O\}_n$

The next step was the introduction of additional ligands (1,10-phenanthroline, phen; 2,2'-bipyridine, bipy) and the preparation of different-ligand and heterometal complexes with 3d metals. The result demonstrated the presence of the hexanuclear anion $[Ge_6(\mu\text{-OH})_6(\mu\text{-hedp})_6]^{6-}$ (fig. 1) in the obtained compounds. However, there is a diversity in the structure of cations depending on the d-metal.

Complexes with structure $[\{Co(phen)_3\}_2\{Co(phen)(H_2O)_4\}_2][\{Ge(\mu\text{-OH})(\mu\text{-hedp})\}_6Cl_2]$, $[\{Cu(phen)_2(H_2O)\}_2(Hphen)_2][Ge(\mu\text{-OH})(\mu\text{-hedp})]_6\cdot 20H_2O$ were synthesized byusing the initial chlorides of 3d metals. According to X-ray diffraction data, these compoundsare cation–anion type complexes in which the anions are represented by $[Ge_6(\mu\text{-OH})_6(\mu\text{-hedp})_6]^{6-}$ (in the case of Co-complex two additional Cl^- ions too), while the cations are $[Co(phen)_3]^{2+}$,$[Co(phen)(H_2O)_4]^{2+}$in Co-complex (fig. 4) and $[Cu(phen)_2(H_2O)]^{2+}$, $Hphen^+$ in Cu-complex (fig. 5).

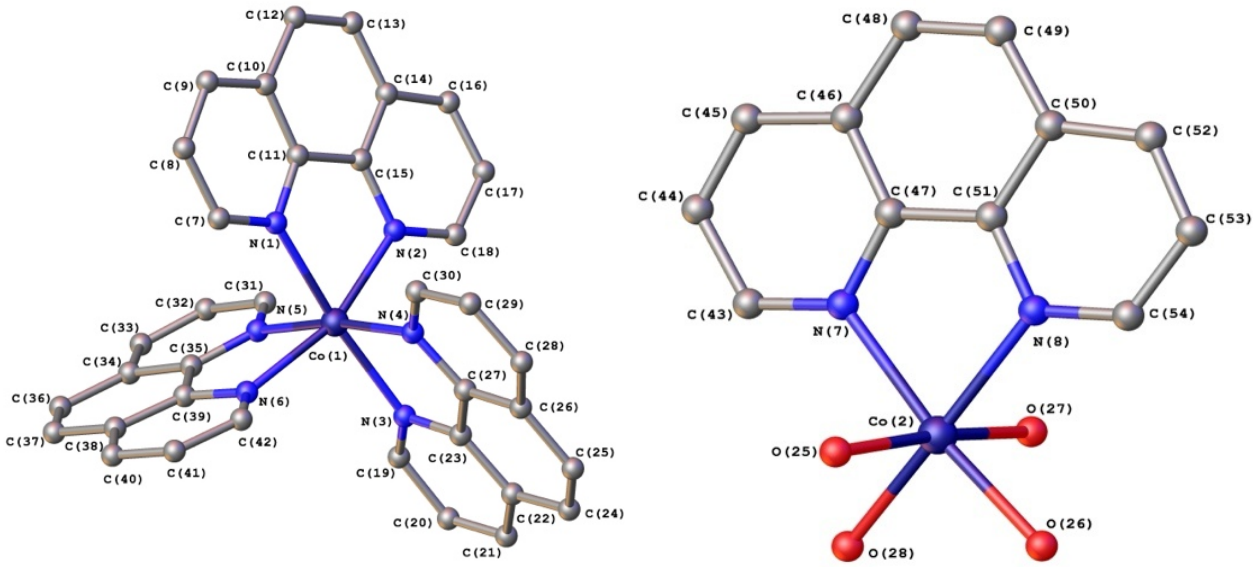

(a) (b)

Fig. 4. Molecular structure of cations $[Co(phen)_3]^{2+}$ (a) and $[Co(phen)(H_2O)_4]^{2+}$ (b).

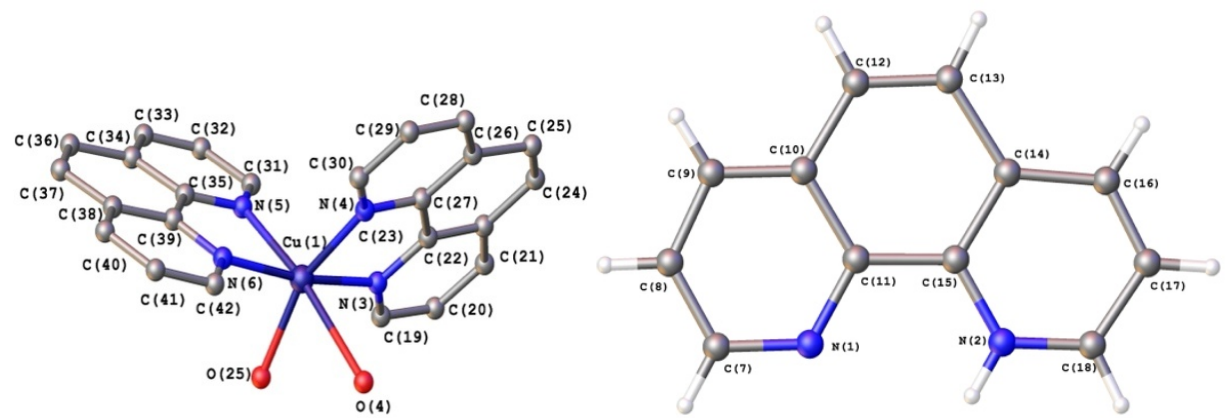

(a) (b)

Fig. 5. Molecular structure of cations $[Cu(phen)_2(H_2O)]^{2+}$ (a) and $Hphen^+$ (b).

In the crystals of compounds the cations, anions, andwater molecules are combined by numerous intermolecular hydrogen bonds, giving rise to a 3D network (fig. 6).

A distinction of these coordination compounds from the previously studied 1-hydroxyethane-1,1-diphosphonatogermanates(IV) [1] is the formation of supramolecular assemblies based on simple and complex cations and anions, which mutually counterbalance their charges. This is caused by both the replacement of Co^{2+} by Cu^{2+} and the incorporation of 1,10-phenanthroline, which can function simultaneously as a bidentate chelating ligand and an outer-sphere cation in the Hp hen$^+$ monoprotonated form.

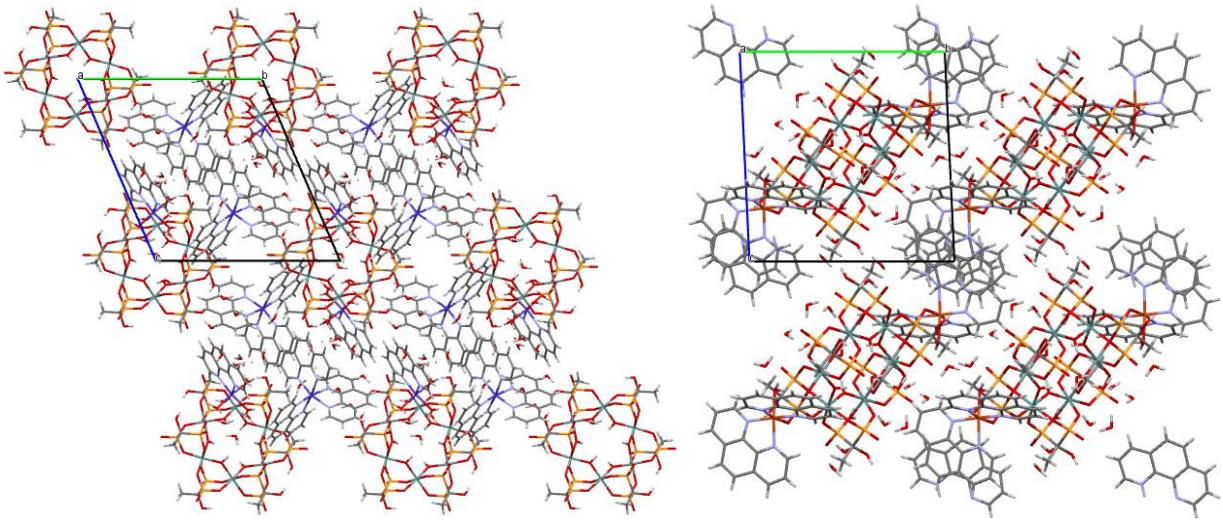

(a) (b)

Fig. 6. Crystal structure of compounds $[\{Co(phen)_3\}_2\{Co(phen)(H_2O)_4\}_2][\{Ge(\mu\text{-}OH)(\mu\text{-}hedp)\}_6Cl_2]$ (a) and $[\{Cu(phen)_2(H_2O)\}_2(Hphen)_2][Ge(\mu\text{-}OH)(\mu\text{-}hedp)]_6\cdot 20H_2O$ (b).

The developed synthesis methods allowed us to obtain Ge(IV)-3d-metals coordination compounds with 1-hydroxyethane-1,1-diphosphonic acid and 2,2'-bipyridine. Complexes are characterized by the methods of elemental analysis, IR-spectroscopy, thermogravimetric analysis. It was established that the obtained compounds to the cation-anion type. They consist of the hexanuclear cyclic anions $[Ge6(\mu\text{-}OH)_4(\mu\text{-}O)_2(\mu\text{-}hedp)_6]^{8-}$, complex cations $[M(bipy)_3]^{2+}$ (M = Co, Ni), $[Cu(H_2O)(bipy)_2]^{2+}$ (Fig. 7) and crystallization water molecules. In the cation of complexes with Co(II) and Ni(II) the octahedral coordination polyhedron of the 3d-metals formed by the six nitrogen atoms of three 2,2´-bipyridine. The coordination number of Cu atoms is five, and the polyhedron is formed by the four nitrogen atoms of two molecules of 2,2´-bipyridine and the oxygen atom of the water molecule. The synthesized complexes correspond to the formulas $[M(bipy)_3]_4[Ge_6(\mu\text{-}OH)_4(\mu\text{-}O)_2(\mu\text{-}hedp)_6]\cdot nH_2O$ (M = Co, n = 20; Ni, n = 12), $[Cu(H_2O)(bipy)_2]_4[Ge_6(\mu\text{-}OH)_4(\mu\text{-}O)_2(\mu\text{-}hedp)_6]\cdot 14H_2O$ [18].

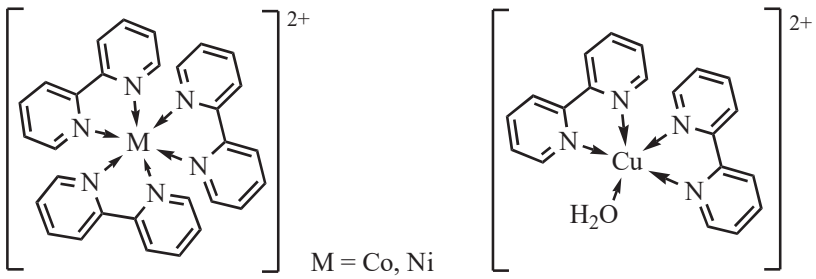

Fig. 7. Scheme of structures of cations $[M(bipy)_3]^{2+}$, $[Cu(H_2O)(bipy)_2]^{2+}$.

Pharmacological and biological activity of 1-hydroxyethane-1,1-diphosphonatogermanates(IV).

The pharmacological activity of a number of 1-hydroxyethane-1,1-diphosphonatogermanates(IV), which according to the results of acute toxicity testing are classified as low-toxic, was investigated [19–22].

The specific effect of complexes with nicotinic acid and magnesium on the cardiovascular system was established on the model of arrhythmia caused by intraperitoneal administration of aconitine alkaloid to rats. The antiarrhythmic effect was found, and it was more pronounced in the complex with magnesium [23–25].

In acute cerebral ischemia caused by carotid artery occlusion, 1-hydroxyethane-1,1-diphosphonatogermanates(IV) with piracetam has a pronounced anti-ischemic effect and is also characterised by high absorption and elimination rate constants in the body [26].

A high hepatoprotective effect of the complex with nicotinic acid was also determined; it prevents changes in total cholesterol, phospholipids and maintains the qualitative and quantitative composition of phospholipid fractions at the level of control values in erythrocyte membranes and in the liver [27].

Studies of the in vitro interferonogenic activity of these compounds on a fibroblast cell culture line showed that the complex with nicotinic acid induces interferon, and at a concentration of 25 to 100 μg/ml leads to a 100% delay in the cytopathic effect of vesicular stomatitis virus in cell culture, which is superior to the comparison drugs.

In the model of endotoxemia of post-traumatic genesis (which can occur, for example, in peritonitis), the detoxifying effect of the complex with magnesium was shown, which is expressed in a decrease in the level of medium-weight molecules in the blood serum – a universal marker of endogenous intoxication and lipid peroxidation products in the liver homogenate, i.e. the degree of damage to cellular and subcellular membranes [28].

The screening for hepatoprotective activity among compounds with 3d-metals revealed that the administration of the complex with copper resulted in a significantly lower increase in the activity of cytolysis and cholestasis enzymes than in untreated animals with hepatitis. The compound also reduced bilirubin levels in blood serum and liver tissue. Importantly, it has low toxicity with different types of administration: oral, intraperitoneal and subcutaneous [29–30].

It was studied the effect of mixed-ligand complexes of Ge(IV) – Co(II) (Ni(II), Cu(II)) with 1-hydroxyethane-1,1-diphosphonic acid and 2,2′-bipyridine on the activity of elastase and fibrinogenase isolated from Bacillus sp. IMV B-7883. It has shown that complexes Co(II) and Ni(II) inhibited the activity of elastase by 54 and 71% respectively, while complex Cu(II) enhanced it by 30%. All three complexes have a stimulating effect on fibrinogenase activity in more than 50% [18].

CONCLUSION. As a result of systematic studies of the structure of a number of mixed-ligand 1-hydroxyethane-1,1-diphosphonatogermanates(IV) with different metals, it was observed, that hexanuclear cyclic complex anions of the general composition $[Ge_6(\mu\text{-}OH)_{6-n}(\mu\text{-}O)_n(\mu\text{-}hedp)_6]^{(6+n)-}$ were present in the aqueous solutions of investigated compounds.

At the same time, the composition and charge of the anion in each compound obtained in the solid state depends on the nature of the cation (fig. 8).

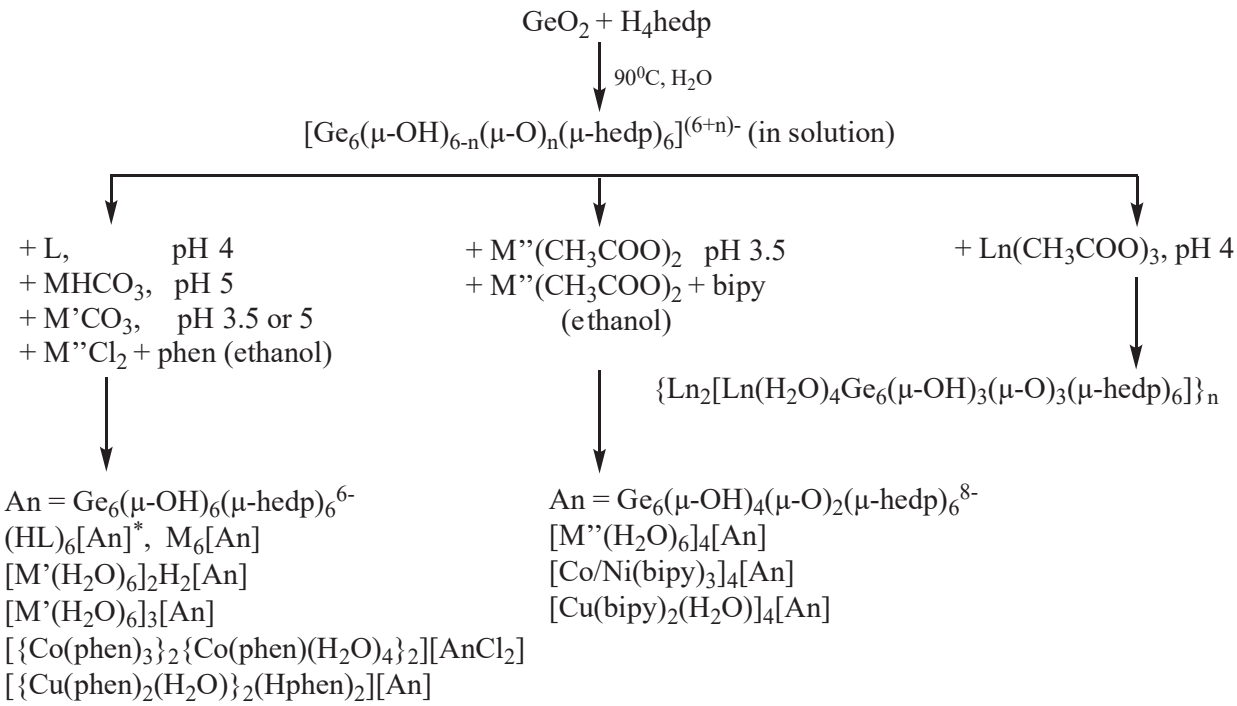

L= nicotinic acid, niacinamide, isoniazid, imidazole, piracetam;
M = Na, K; M' = Mg, Ca, Sr, Ba; M'' = Co(II), Ni(II), Cu(II), Zn; Ln = Nd(III), Er(III), Tm(III);
bipy – 2,2'-bipyridine; phen – 1,10-phenanthroline; *all compounds are hydrates

Fig. 8. Synthetic route and structures of different types of 1-hydroxyethane-1,1-diphosphonatogermanates.

They all have a common hexameric structure, with germanium atoms connected in pairs by 1-hydroxyethane-1,1-diphosphonate, hydroxo-, or oxo- and hydroxo-bridges. The coordination polyhedron Ge is a curved octahedron with two six-membered GeO_2P_2C cycles and an eight-membered bimetallic $Ge_2O_4P_2$ closing, and each ligand performs a tetradentate tris(chelate)-μ-bridging function. The ratio of formed oxo- and hydroxo-bridges and, as a result, the charge of the anion varies under the influence of cation parameters and electrostatic interactions. However, the structure of complex anions is quite stable and is not destroyed even by interactions with complex cations.

Most obtained compounds refer to the cation-anion type with various cations (protonated organic molecules, hexaaqua-, bipyridine-, and phenanthroline metal cations). In the structure of lanthanide compounds complex hexanuclear anions $[Ge_6(\mu\text{-}OH)_3(\mu\text{-}O)_3(\mu\text{-}hedp)_6]^{9-}$ and $Ln(H_2O)_4$ fragments are combined into a 3D-framework.

The pharmacological and biological activities of 1-hydroxyethane-1,1-diphosphonatogermanates(IV) are ensured by the combined action of all biologically active components,

which do not compete but show synergistic action.

In view of the above, it can be concluded that the preparation of new complexes of germanium(IV) with etidronicacid by chemical modification of their composition is a promising area of research in the field of creating coordination compounds with a wide range of pharmacological effects.

This work was done according to the theme "Chemical construction of organo-inorganic ensembles of coordinating, supramolecular, polymeric nature for use as new materials and pharmaceuticals", No state registration: 0122U201403, 2022-2026.

ОСОБЛИВОСТІ БУДОВИ ТА ФАРМАКОЛОГІЧНІ ВЛАСТИВОСТІ КОМПЛЕКСІВ ГЕРМАНІЮ(IV) З 1-ГІДРОКСИЕТАН-1,1-ДИФОСФОНОВОЮ КИСЛОТОЮ

О. Марцинко[1], І. Сейфулліна[1], О. Фінік[2], К. Цимбалюк[1,2]

[1]Одеський національний університет імені І. І. Мечникова, вул. Дворянська, 2, Одеса 65082, Україна;
[2]ТОВ «ІНСПЕКТОРАТ УКРАЇНА», провулок Удільний, 1, м. Одеса 65009, Україна
e-mail: lborn@ukr.net

В оглядовій статті представлено результати систематичних досліджень авторів низки гетерометалів і різнолігандних 1-гідроксиетан-1,1-дифосфонатогерманатів, їхньої структури, біологічних і фармакологічних властивостей. Встановлено, що у водних розчинах досліджуваних сполук присутні шестиядерні циклічні комплексні аніони загального складу $[Ge_6(\mu\text{-}OH)_{6-n}(\mu\text{-}O)_n(\mu\text{-}hedp)_6]^{(6+n)-}$. При цьому склад і заряд аніона в кожній сполуці, отриманій в твердому стані, залежить від природи катіона. Усі вони мають спільну гексамерну структуру аніона, в якій атомами германію попарно з'єднані 1-гідроксиетан-1,1-дифосфонатними, гідроксо- або оксо- та гідроксомістками. Координаційний поліедр Ge є викривленим октаедром з двома шестичленними циклами GeO_2P_2C та восьмичленним біметалічним циклом $Ge_2O_4P_2$, кожен ліганд виконує тетрадентатнутрис(хелатну)-μ-місткову функцію. Співвідношення утворених оксо- і гідроксомістків і, як наслідок, заряд аніона змінюється під впливом параметрів катіонів і електростатичних взаємодій. Дослідження гострої та хронічної токсичності довели безпечність 1-гідроксиетан-1,1-дифосфонатогерманатів. Комплекси виявляють широкий спектр фармакологічної дії: антигіпертензивну, антиаритмічну, гепатопротекторну, церебропротекторну та ін. Фармакологічна та біологічна активність 1-гідроксиетан-1,1-дифосфонатогерманатів(IV) забезпечується спільною дією всіх біологічно активних компонентів, які не конкурують, а виявляють синергічний ефект. Зроблено висновок, що отримання нових комплексів германію(IV) з етидроновою кислотою шляхом хімічної модифікації їхнього складу є перспективним напрямком досліджень у галузі створення координаційних сполук із широким спектром фармакологічної дії.

Ключові слова: германій(IV), 1-гідроксиетан-1,1-дифосфонова (етидронова) кислота, нітрогенвмісні гетероцикли, координаційні сполуки, біологічна активність.

REFERENCES

1. Martsinko E.E., Seifullina I.I. Design and synthesis of molecular complexes and complexonates of germanium(IV) with a wide spectrum of pharmacological action. 2018. Odesa. ONU. (*in Ukranian*).
2. SeifullinaI.I., Martsinko E.E., Afanasenko E.V. Design and synthesis of new homo- and heterometal coordination compounds of germanium(IV) for preparation of low toxic drugs with a wide the rapeuticaction. *Visn. Odes. nac. univ., Him*. 2015. **20**(4): 6–17. https://doi.org/10.18524/2304-0947.2015.4(56).56690
3. Bouhsina S., Buglyó P., AbiAad E., Aboukais A., Kiss T. Formation of oligonuclear complexes between copper(II) and 1-hydroxyethane-1,1-diphosphonic acid. *Inorganica Chim Acta*. 2004. **357**(1): 305–310. doi:10.1016/s0020-1693(03)00445-6
4. Reed W.A., Rao L., Zanonato P., Garnov A.Y., Powell B.A., Nash K.L. Complexation of UVI with 1-Hydroxyethane-1,1-diphosphonic Acidin Acidicto Basic Solutions. *Inorg. Chem*. 2007. **46**(7): 2870–2876. doi:10.1021/ic0621401
5. Wang W.N., Sun Z.G., Zhu Y.Y., Dong D.P. et al. Hydrothermal synthesis, structures, and luminescent properties of four new zinc(II) diphosphonate hybrids with mixed ligands. *Cryst Eng. Comm*. 2011. **13**(20): 6099–6106. doi: 10.1039/C1CE05291H.
6. Liu B., Ding T., Hua W.J., Liu X.M., Hu H.M., Li S.H., Zheng L.M. Diruthenium(III, III) diphosphonate with a spinground state *S* = 2. *Dalton Trans*. 2013. **42**(10): 3429–3433. doi: 10.1039/C2DT32306K
7. Sun S.H., Sun Z.G., Zhu Y.Y., Dong D.P., Jiao C.Q., Zhu J., Li J., Chu W., Tian H., Zheng M.J., Shao W.Y., Lu Y.F. Four Novel Oxomolybdenum-Organodiphosphonate Hybrids in the Presence of Cu(II)–Organonitrogen Building Blocks: Synthesis, Crystal Structures, and Surface Photovoltage Properties. *Cryst. Growth. Des.* 2013. **13**(11): 226–238. doi: 10.1021/cg301392p
8. Liao Z., Ling J., Reinke L., Szymanowski J. Sigmon G., Burns G. Cage clusters built from uranyl ions bridged through peroxo and 1-hydroxyethane-1,1-diphosphonic acid ligands. *Dalton Trans*. 2013. **42**(19): 6793–6799. doi: 10.1039/c3dt33025g.
9. Jiao C.Q., Zhao Z., Ma C., Sun Z.G., Dong D.P., Zhu Y.Y., Li J. Chiral and Achiral Copper(II) Carboxyphosphonates Supramolecular Structures: Synthesis, Structures, Surface Photovoltage, and Magnetic Properties. *Cryst. Growth. Des*. 2016. **16**(10): 5624–5635. doi: 10.1021/acs.cgd.6b00197.
10. Ma K.R., Yin J.Z., Hu H., Kan Y.H. Syntheses, Structures and Fluorescent Properties of TwoZn(II)-Diphosphonate Coordination Polymers. *J Clust. Sci.* 2021. **32**: 875–886. doi: 10.1007/s10876-020-01854-z.
11. Saji H., Ogawa K., Kitamura Y., Kubota-Akizawa M., Kawashima H. Chemical Control of Biological Activity and Biodistribution of Metal Compounds: Drug Design of Metal Complexes with Biological Activity and Target-Specific Biodistribution. *Biomed. Res. Trace. Elem*. 2007. **18**(3): 255–263. doi: 10.11299/brte.18.255
12. Campello A., Rodrigues R., Alves F., Miranda K., Brum S., Mdala I., Siqueira J., Rôças I. Enhancing the Intracanal Antibacterial Effects of Sodium Hypochlorite with Etidronic Acidor Citric Acid. *J Endodontics*. 2022. **48**(9): 1161–1168. doi:10.1016/j.joen.2022.06.006.
13. Bajpe S., Shetty C., Shetty A., Kaur G., Saji S.A., Prabha C. Scanning electronmicroscopy evaluation of smear layer removal using ethylenediaminetetraacetic acid, etidronic acid, and chitosan nanoparticle solution as root canal irrigants. *Endodontology*. 2023. **35**(1): 48–53. doi:10.4103/endo.endo_126_22.
14. Supraja A., Arali V., Rapala H., Vemagiri C., Kallakuri M., Kumar G. Evaluation of Antimicrobial Efficacy of Etidronic Acid against Enterococcus faecalis in Primary Teeth: An In Vivo Study. *Intern J Clinical Pediatric Dentistry*. 2024. **17**(4): 433–436. doi: 10.5005/jp-journals-10005-2834.

15. Petriev V.M. Influence of reactant concentrations and solution acidity on the complexation of ^{188}Re with 1-hydroxyethane-1,1-diphosphonic acid. *Radiochemistry*. 2008. **50**: 203–206. doi: 10.1134/S1066362208020227.
16. Martsinko E.E. Synthesis, structure and prospects of application of homo- and heterometallic 1-hydroxyethylidenediphosphonategermanates. *Ukr. Chem. J.* 2014. **80**(8): 88–95. (in Ukrainian).
17. Martsynko O.E., Seifullina I.I. Double Ge(IV)-Co(II) complexes with 1-hydroxyethylidenedi phosphonic acid and 2,2′-bipyridine. *Visn. Odes. Nac. Univ. Him*. 2022. **27**(1): 31–38. doi:10.18524/2304-0947.2022.1(81).255828. (in Ukrainian).
18. Gudzenko O., Varbanets L., Seifullina I., Martsynko O., Tsymbalyuk K. Mixed-ligand complexes of germanium – 3d-metal with 1-hydroxyethane-1,1-diphosphonic acidand 2,2′-bipyridine as modulators of Bacillussp. IMV B-7883 elastase and fibrinogenase activity. *Ukr. Biochem. J*. 2024. **96**(1): 96–102. doi:10.15407/ubj96.01.096.
19. Kresyun V., Seifullina I., Vidavska G., Shemonaeva K. Prospects for the creation of new drugs based on oxyethylidene diphosphonic acid. *Medical chemistry*. 2004. **6**(3): 133–138. (in Ukrainian).
20. Godovan V.V., Kresyun V.Y., Seifullina I.I. Comparative pharmacological activity of new biologically active substances – derivatives of diphosphonicacids. *Integrative anthropology*. 2007. **2**(10): 13–17. (in Ukrainian).
21. Kresyun V., Godovan V.,Seifullina I. Influence of oxyethylidene diphosphonate germanate derivatives on the phospholipid composition of membranes in toxic liver damage. *J. Academy Med. Sci. Ukraine*. 2008. **14**(1): 63–71. (in Ukrainian).
22. Lukianchuk V., Seifullina I., Litvinenko D., Martsynko O. Pharmacological properties of organic and coordination germanium compounds – modern concepts. *Pharmacology and Drug Toxicology*. 2016. **1**(47): 3–13. (in Ukrainian).
23. Godovan V.V., Kresyun V.Y., Seifullina I.I. Tissue respiration and oxidative phosphorylationin heart mitochondriain experimental myocardial dystrophyandits drug correction. *Odes'kij medični jžurnal.* 2006. **3**(95): 13–17. (in Ukrainian).
24. Godovan V.V., Kresyun V.Y., Seifullina I.I. Biologically active antiarrhythmic substance germacord (UA Patent No. 20658). Ukraine. 2007. (in Ukrainian).
25. Godovan V.V., Kresyun V.Y., Seifullina I.I. Magnesium oxyethylidene diphosphonato-germanate characterised by vasodilatoraction (UA Patent No. 19965). Ukraine. 2007. (in Ukrainian).
26. Lukianchuk V.D., Krylova O.E., Seifullina I.I., Martsynko O.E., Tkachenko V.M. 2-Oxo-1-pyrrolidinyl acetamide hydroxyethylidene diphosphonate germanate(IV) with cerebroprotective activity (UA Patent No. 45070). Ukraine. 2009. (in Ukrainian).
27. Godovan V.V., Kresyun V.Y., Seifullina I.I. Nicogerm - a biologically active hepatoprotective substance (UA Patent No.51482). Ukraine. 2010. (in Ukrainian).
28. Lukianchuk V.D., Seifullina I.I., Rysukhina N.V., Martsynko O.E. Method of detoxification of the body in case of endotoxicosis of post-traumatic origin by a complex compound based on germanium, magnesium and oxyethylidenediphosphonic acid (UA Patent No. 36684). Ukraine. 2008. (in Ukrainian).
29. Tymchyshyn O.L., Godovan V.V., Seifullina I.I. A cute toxicity of medgerm – a new derivative of germanium salt of diphosphonic acid with copper. *Odes'kij medični jžurnal.* 2010. **2**(118): 23–26. (in Ukrainian).
30. Tymchyshyn O.L., Godovan V.V., Kresyun V..Y, Seifullina I.I., Martsynko O.E. Medgerm – a biologically active hepatoprotective substance (UAPatent No. 66392). Ukraine. 2011. (in Ukrainian).

Стаття надійшла 10.06.2024.

UDC 546.26-162 doi: 10.33609/2708-129X.90.9.2024.31-56

NEW DRUGS ON THE PHARMACEUTICAL MARKET CONTAINING FLUORINE AND RESIDUES OF TAILOR-MADE AMINO ACIDS.

Jianlin Han[1*], Alicja Wzorek[2], Gagan Dhawan[3,4*], Wei Zhang[5*], Alexander E. Sorochinsky[6*], Daniel Baecker[7*], Taizo Ono[8], Karel D. Klika[9], Vadim A. Soloshonok[10,11*]

[1]Jiangsu Co-Innovation Center of Efficient Processing and Utilization of Forest Resources, College of Chemical Engineering, Nanjing Forestry University, 210037 Nanjing, China;
[2]Institute of Chemistry, Jan Kochanowski University in Kielce, 7 Uniwersytecka, 25–406 Kielce, Poland;
[3]School of Allied Medical Sciences, Delhi Skill and Entrepreneurship University, Dwarka, 110077 New Delhi, India;
[4] Department of Biomedical Science, Acharya Narendra Dev College, University of Delhi, Kalkaji, 110019 New Delhi, India;
[5] Department of Chemistry, University of Massachusetts Boston, 02125 Boston MA, Unites States;
[6]V.P. Kukhar Institute of Bioorganic Chemistry and Petrochemistry, the National Academy of Sciences of Ukraine, 02094 Kyiv, Ukraine
[7] Department of Pharmaceutical and Medicinal Chemistry, Institute of Pharmacy, Freie Universität Berlin, 2+4 Königin-Luise-Straße, 14195 Berlin, Germany;
[8]National Institute of Advanced Industrial Science and Technology (AIST), 2266–98, Anagahora, Shimoshidami, Moriyama-ku, 463–8560 Nagoya, Japan;
[9]Molecular Structure Analysis, German Cancer Research Center (DKFZ), 280 Im Neuenheimer Feld, 69120 Heidelberg, Germany;
[10] Department of Organic Chemistry I, Faculty of Chemistry, University of the Basque Country UPV/EHU, 3 Paseo Manuel Lardizábal, 20018 San Sebastián, Spain;
[11]IKERBASQUE, Basque Foundation for Science, 3 María Díaz de Haro, Plaza Bizkaia, 48013 Bilbao, Spain
**email: vadimsoloshonok@gmail.com*

This article profiles five newly drugs containing fluorine along with fragments of amino acids or their derivatives approved by the FDA in 2024. These pharmaceuticals include Voydeya® (danicopan), Ojemda® (tovorafenib), Itovebi® (inavolisib), Scemblix® (asciminib), and Revuforj® (revumenib). For each drug, we discuss the discovery, therapeutic areas of application, and detailed chemical synthesis.

Key words: Fluorine, Tailor-made amino acids, Pharmaceutical drugs, Drug design, Synthesis, Bioactivity.

INTRODUCTION. Amino acids are fundamental to the development of life as they are the building blocks of proteins, which perform a vast array of functions within living organisms [1]. Proteins are involved in virtually every cellular process, including enzymatic catalysis, structural support, transport, communication, and immune response. Without amino acids, the complex molecules necessary for life as we know it would notexist [2–18]. They play a crucial role in maintaining the structure and function of cells, tissues, and organs, making them essential for growth, repair, and overall health [19–32].

In the modern pharmaceutical industry, amino acids are invaluable due to their versatility and their influence on drug design and development. Tailor-made amino acids (AAs) [33] can be incorporated into drugs to enhance their efficacy, stability, and specificity. By manipulating the structure of amino acids, pharmaceutical researchers can design drugs that precisely target specific biological pathways, reduce side effects, and improve patient outcomes [34–41]. Additionally, amino acids are used in the synthesis of peptide-based drugs, which are increasingly important in treating a range of conditions from cancer to metabolic disorders [42–48]. Their role in the pharmaceutical industry underscores the profound impact of amino acids not only on life itself but also on the advancement of medical science and therapeutics [49–51].

Another trend in the design of modern pharmaceuticals is a selective incorporation of fluorine atoms or/and fluorine-containing groups [52–63]. Thus, fluorine plays a crucial role in modern drug design due to its unique chemical properties, such as high electronegativity, small atomic size, and ability to form stable bonds. These properties allow fluorine to enhance the potency, selectivity, metabolic stability, and pharmacokinetics of drugs. Incorporating fluorine into drug molecules can improve their efficacy and reduce side effects, making them more effective therapeutic agents [64–69].

Fluorine-containing amino acids are particularly valuable in drug design because they combine the benefits of fluorine with the structural versatility of amino acids [70–74]. These tailor-made amino acids can be used to fine-tune the activity and pharmacokinetics of drug candidates, leading to more targeted and efficient treatments. The synthesis of tailor-made fluorinated α- [75–100] and β-amino acids [101–121] has been one of the areas of intense research activity in the last 20+ years [122–143]. The selective introduction of fluorine into bioactive compounds has become a mature strategy in drug development, resulting in numerous FDA-approved fluorinated drugs [64, 66–69].

Overall, the incorporation of fluorine and amino acids into pharmaceuticals represents a significant advancement in the field of medicinal chemistry, offering new opportunities for the development of more effective and safer drugs. In the present article, we profile five newly FDA-approved (2024) small-molecule pharmaceuticals (Figure 1) that contain fluorine and a residue of an amino acid or its derivative. These include: Voydeya® (danicopan) **1**, Ojemda® (tovorafenib) **2**, Itovebi®(inavolisib) **3**, Scemblix® (asciminib) **4**, and Revuforj® (revumenib) **5**. For each drug, we discuss the discovery, therapeutic areas of application, and detailed chemical synthesis.

ISSN 2708-129X. Укр. хім. журн., 2024

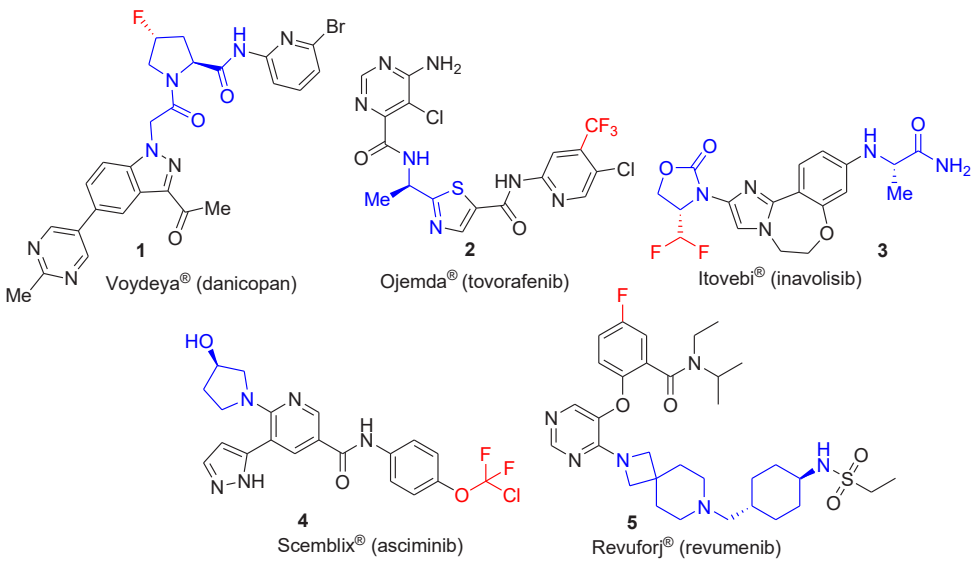

Fig. 1. Chemical structures of new pharmaceutical drugs **1**-**5** containing fluorine (marked in red) and a residue of an amino acid or its derivative (marked in blue).

Voydeya® (Danicopan) (1)

Danicopan, marketed under the name Voydeya®, is a drug derived from γ-fluorine-substituted proline. The FDA approved this compound on March 29, 2024. Developed by Alexion Pharmaceuticals, a subsidiary of AstraZeneca, this drug targets rare diseases, with Alexion being renowned for their expertise in orphan drugs [144]. Cyclic amino acids, such as those used in this compound, are particularly important in drug design because they are more sterically constrained than their linear counterparts [145, 146]. Adding fluorine [147] or CF_3 groups [148–150] on five-membered rings further restricts the range of accessible conformations, enabling the fine-tuning of biological properties. The introduction of a fluorine atom into the pyrrolidine-2-carboxamide framework, as compared to non-fluorinated analogs like compounds **6** and **7** (Figure 2), significantly boosts activity, achieving an IC_{50} of 0.027 μM. This modification demonstrates exceptional potency and underscores the compound's potential to surpass other molecules in its class [151, 152].

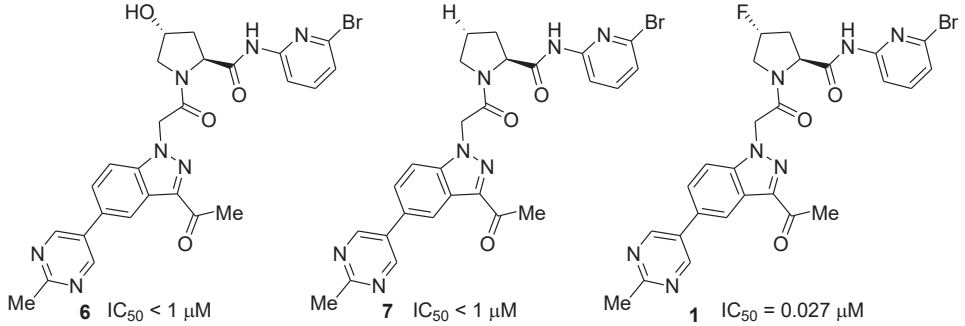

Fig. 2. Structures of Voydeya® (Danicopan) **1** and its fluorine-free analogs **6** and **7**.

Voydeya, an oral complement factor D inhibitor, serves as an add-on therapy to the complement C5 inhibitors Ravulizumab and Eculizumab for treating extravascular hemolysis (EVH) in adults with paroxysmal nocturnal hemoglobinuria (PNH) [153,154]. PNH is a rare condition where the immune system's complement attacks red and white blood cells and platelets, leading to intravascular hemolysis and a heightened risk of thrombosis and organ damage. Although C5 inhibitors are the primary treatment, some patients still experience residual extravascular hemolysis and anemia [155]. Danicopan received its initial approval in Japan on January 18, 2024, for treating adults with PNH in combination with C5 inhibitors [156]. On February 23, 2024, the European Medicines Agency also recommended its market authorization for patients with residual hemolytic anemia despite C5 inhibition therapy [157].

The synthesis of Voydeya® (Danicopan) was developed by Alexion Pharmaceuticals [158–160]. This process starts with the creation of several key intermediates. As outlined in Scheme 1, 5-bromo-1*H*-indazole-3-carbonitrile **8** reacts with methyl magnesium bromide forming an imine magnesium salt intermediate. This intermediate is then hydrolyzed with acid treatment at pH 5 to produce ketone **9**. Following this, a Michael addition is carried out, yielding the ester **10** with an 81% yield.

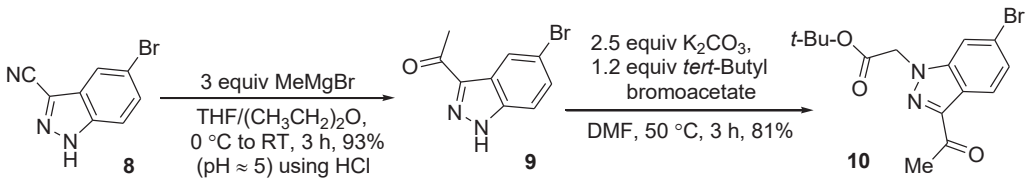

Scheme 1. Synthesis of key intermediate **10**.

The synthesis of another important compound **13**, is detailed in Scheme 2. Boc-protected fluoropyrrolidine **11** undergoes amide alkylation using Ghosez reagent and diisopropylethylamine (DIPEA) [161]. This is followed by deprotection of the amino group, resulting in the precursor **13**.

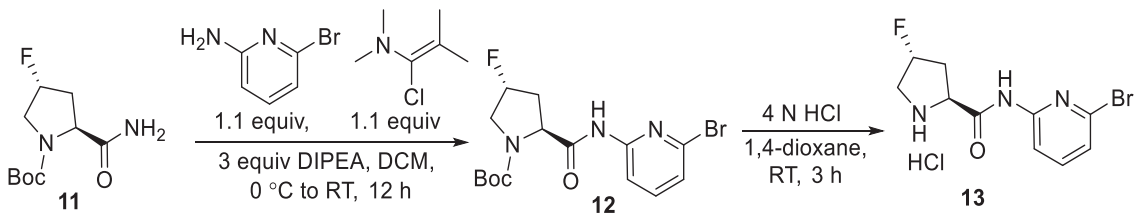

Scheme 2. Synthesis of key intermediate **13**.

ISSN 2708-129X. Укр. хім. журн., 2024

The assembly of Danicopan's structure using key compounds **10** and **13** is detailed in Scheme 3. Initially, bromide **10** reacts with **14**, forming intermediate **15**. This is followed by a Suzuki – Miyaura coupling reaction with compound **16** in the presence of a palladium catalyst and a base, resulting in ester **17**. Ester hydrolysis with trifluoroacetic acid (TFA) then produces carboxylic acid **18** in quantitative yield. Finally, a coupling reaction with fluoro-proline derivative **13** leads to the synthesis of Voydeya® (Danicopan) (**1**).

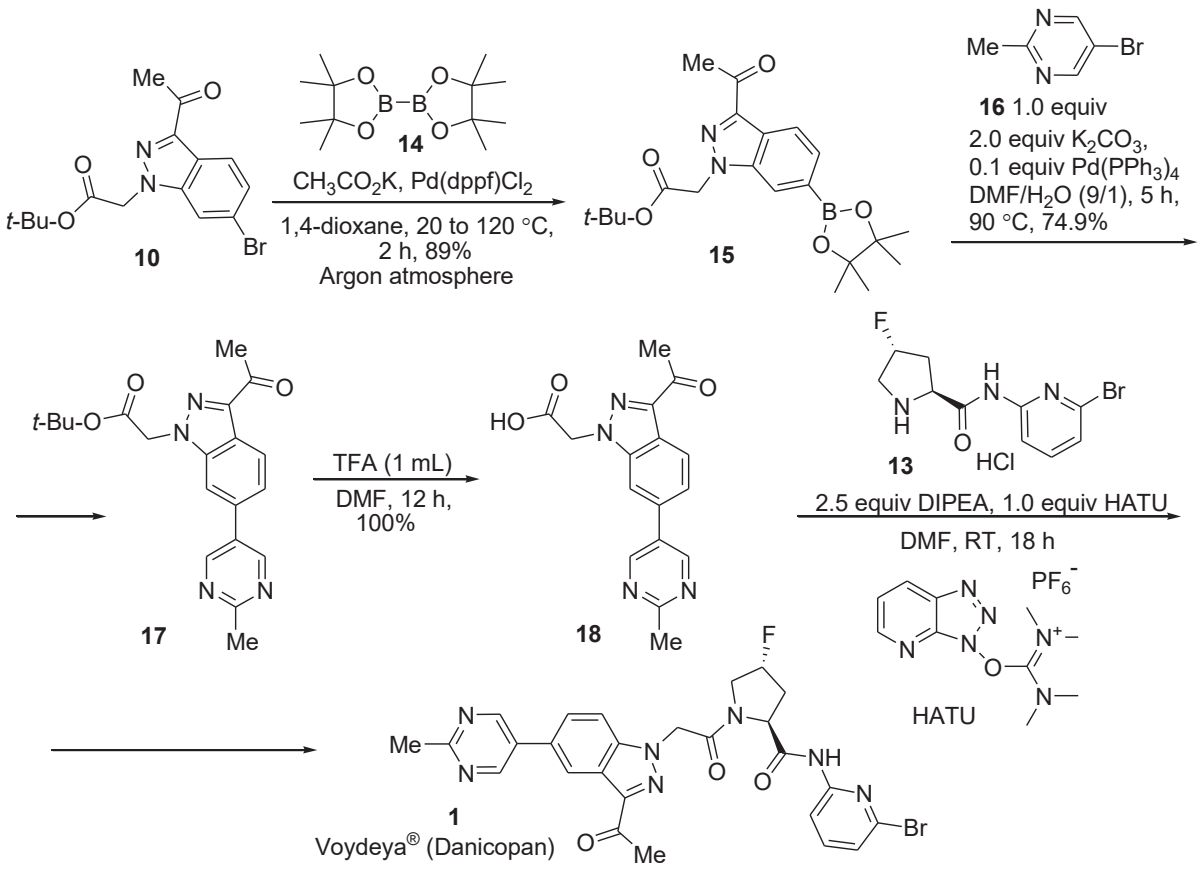

Scheme 3. Synthesis of Danicopan**1**.

Ojemda® (Tovorafenib) (2)

Tovorafenib, branded as Ojemda® (**2**), is an aromatic trifluoromethyl-containing complex structure developed by Day One Biopharmaceuticals Inc (California, USA) under a license agreement with Takeda Oncology (Massachusetts, USA). This drug, also known as DAY101, is a targeted therapy for cancers with RAF alterations, including pediatric low-grade glioma [162–164]. Tovorafenib**2** has shown the most effective inhibitory activity against RAF kinases like BRAF and CRAF when compared

to non-fluorinated analogs, such as **19** (Figure 3) [165, 166]. It received FDA approval on April 23, 2024. Ojemda is an oral kinase inhibitor that targets mutant BRAF V600E, wild-type BRAF, and wild-type CRAF kinases. It is intended for patients aged 6 months and older with relapsed or refractory pediatric low-grade glioma (pLGG) harboring BRAF fusions, rearrangements, or V600 mutations [167, 168]. This accelerated approval was granted based on clinical responses and the duration of response observed in the phase 2 FIREFLY-1 trial (NCT04775485; PNOC026) [169]. The recommended dose is 380 mg/m² taken orally once weekly (maximum 600 mg) until disease progression or unacceptable toxicity [170].

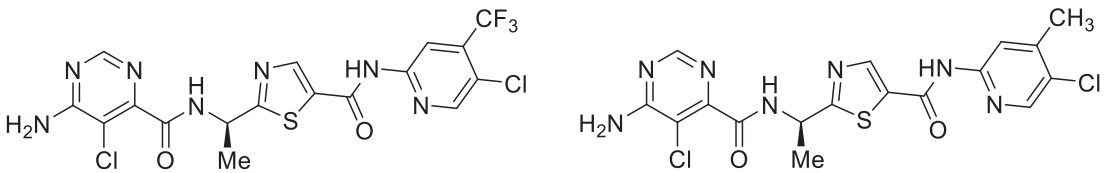

Fig. 3. Structures of Tovorafenib**2** and its non-fluorinated analog **19**.

Scheme 4 outlines the synthesis of Ojemda® (Tovorafenib) [171]. The process begins with the reaction of thiazole **20** with compound **21** using oxalyl chloride as the activating reagent, yielding target amide **22** with a 96% yield. Compound **22** is then mixed with ethanol, 1.1 equivalents of diphenylmethanamine **23**, and acetic acid in a flask equipped with a Dean–Stark trap, and the mixture is refluxed for 6.5 hours. After cooling and stirring for 1 hour, Schiff base **24** is obtained with an 87% yield. Next, compound **24** is dissolved in dichloromethane and combined with [Ir (cod)$_2$] BArF and (*S*)-Monophos, then placed in an autoclave. Hydrogen is introduced, and the mixture is heated to 50°C and stirred for 24 hours, resulting in compound **25**. Acetonitrile and water are added, followed by 1.1 equivalents of *N*-bromosuccinimide, and the reaction proceeds at room temperature for 18 hours to generate the corresponding free amino compound in situ. Optical resolution [172] is performed using (*S*)-mandelic acid, yielding crystallized product **26** with a 75% yield. Subsequent purification involving 2.0 equivalents of sodium bicarbonate and activated carbon in a water–acetonitrile mixture produces compound **27**. Finally, intermediate **27** is coupled with 6-amino-5-chloropyrimidine-4-carboxylic acid **28** under EDC/*t*-BuOH conditions, resulting in Ojemda® (Tovorafenib) **2** with an 88% yield [171].

Itovebi® (inavolisib)(3)

Inavolisib, marketed under the brand name Itovebi®, has been approved by the FDA for treating locally advanced or metastatic breast cancer [173]. It functions as an inhibitor of the phosphatidylinositol-4,5-bisphosphate 3-kinase (PI3K) pathway, representing a new generation of inhibitors with an improved toxicity profile compared to the previously approved inhibitor alpelisib [174, 175].

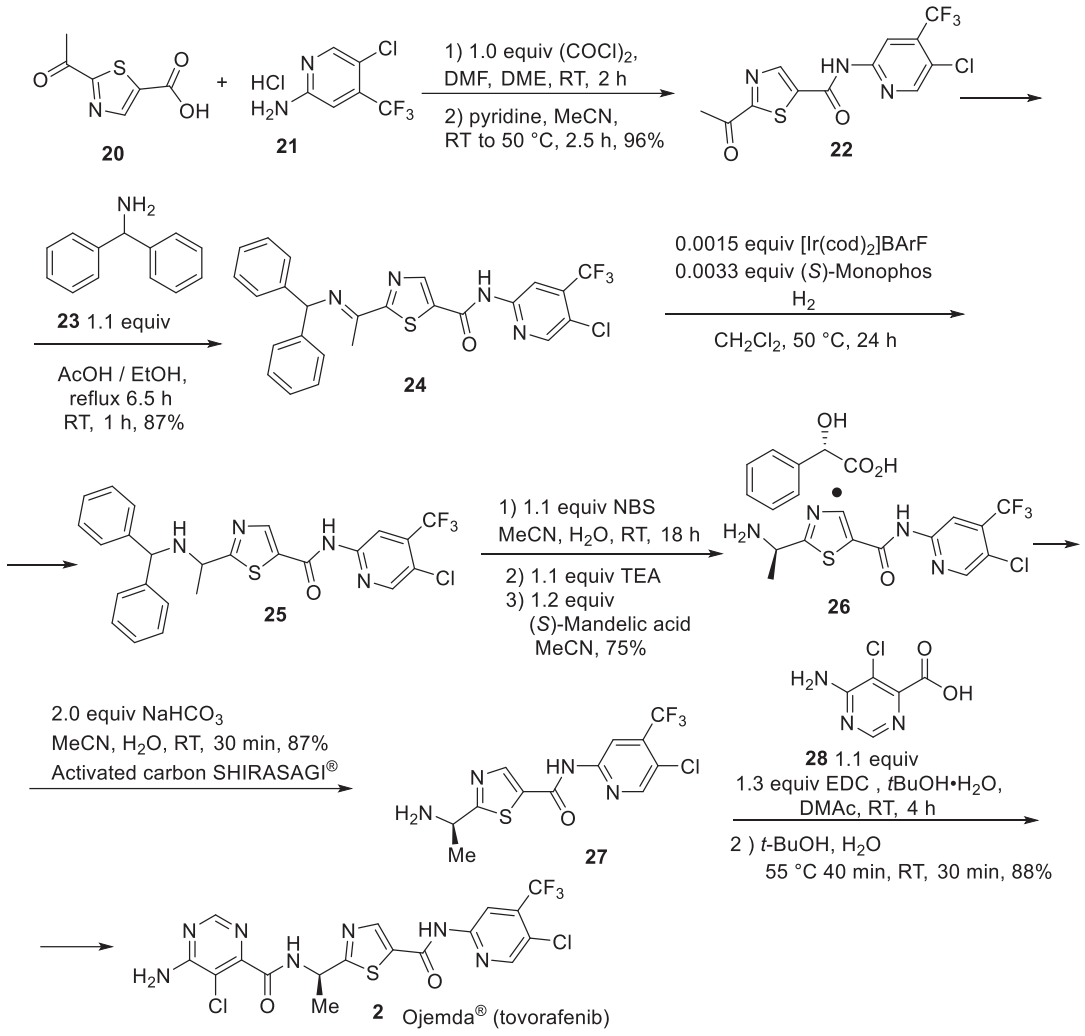

Scheme 4. Synthesis of Ojemda® (Tovorafenib) **2**.

PI3K enzymes play a crucial role in cell growth and differentiation, consisting of regulatory and catalytic subunits [176]. There are four isoforms: PI3Kα, PI3Kβ, PI3Kγ, and PI3Kδ. PI3Kα is most closely linked to tumorigenesis due to mutations and amplifications in the PIK3CA gene encoding the p110α unit [177, 178]. Approximately one-third of breast cancer cases exhibit such pathway disorders [179], which are considered poor prognostic factors [173].Therefore, selective inhibitors of PI3Kα, which do not induce side effects by blocking other PI3K isoforms, are highly desirable [180]. Inavolisib demonstrates an enzyme inhibitory concentration (IC_{50}) of 0.034 nM for PI3Kα, 100 nM for PI3Kβ, 18 nM for PI3Kγ, and 12 nM for PI3Kδ, indicating a more than 350-fold selectivity for PI3Kα [181]. Additionally, inavolisib promotes the degradation of the mutated p110α subunit [182].

It is note worthy that the introduction of a trifluoromethyl group in compound **29** (Figure 4), which has a PI3Kα IC_{50} of 0.095 nM and a PI3Kδ/PI3Kα ratio of 171, resulted in less selectivity towards the α isoform compared to the difluoromethyl group in compound **3** (PI3Kα IC50 of 0.034 nM and a PI3Kδ/PI3Kα ratio of 361) [183].

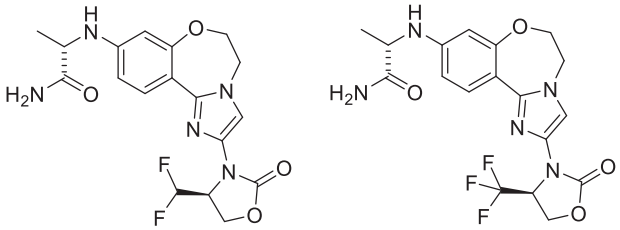

Fig. 4. Structures of Itovebi® (inavolisib)**3** and its CF_3-containing analog **29**.

Chemically, inavolisib features a benzoxazepine oxazolidinone core, an alanine amide moiety, and an amino alcohol derived from difluoroalanine. This difluoroalanine derivative is particularly favored by PI3Kα, enhancing the selectivity for this isoform. The precise interactions of inavolisib with its target are facilitated by hydrogen bonds from the amide and amino groups of the alanine fragment. Additionally, the difluoromethyl group of inavolisib interacts with the hydroxyl group of Ser774 within the p110α pocket [181]. Thus, fluorination plays a crucial role in the unique effectiveness of this next-generation PI3Kα inhibitor.

The synthetic route to prepare inavolisib (Scheme 5) starts with 1,2:5,6-bis-*O*-(1-methylethylidene)-D-mannitol **30**, which serves as a source for the desired stereochemical configuration [183]. Sodium periodate ($NaIO_4$) in hot water is added to silica, forming a powder. This mixture is then combined with compound **30** dissolved indichloromethane (DCM) and stirred at room temperature for 1 hour, producing carbaldehyde **31**. To the cooled carbaldehyde **31** solution in DCM, diethylaminosulfur trifluoride (DAST) is added dropwise and stirred at room temperature for 3 hours, yielding (*R*)-4-difluoromethyl-2,2-dimethyl [1,3] dioxolane **32**. This intermediate is dissolved in methanol (MeOH), and hydrochloric acid (HCl) in dioxane is added, stirring at room temperature for 30 minutes. The acetal is cleaved to form the respective diol. After work-up, the residue is dissolved in DCM, followed by the addition of *tert*-butyldimethylsilyl chloride(TBDMS), Et_3N, and catalytic amounts of 4-Dimethylaminopyridine(DMAP). Compound **33** was obtained after stirring for 1 hour at room temperature. Following this, trifluoromethanesulfonic anhydride (Tf_2O) was added dropwise to a solution of **33** and pyridine in DCM. The temperature was maintained at -20 °C for 20 minutes, then brought to 0 °C for 1 hour while stirring. After extraction and work-up, the residue was dissolved in DMF, and sodium azide (NaN_3) was added, stirring for 2 hours at room temperature to produce intermediate **34**. The azide was then reduced using

palladium hydroxide on carbon (Pd-OH/C) under hydrogen (H_2) by stirring for 16 hours in ethyl acetate (EtOAc) and MeOH, yielding primary amine **35**. This product was dissolved in MeOH and stirred in a solution of HCl (in dioxane) for 2 hours at room temperature to remove the protective group. After work-up, the crude product was dissolved in toluene and aqueous potassium hydroxide (KOH) at 0°C. Phosgene ($COCl_2$) was added gradually, followed by stirring for 1 hour to obtain (*S*)-4-difluoromethyloxazolidin-2-one **36**. This was combined with 9-bromo-2-iodo-5,6-dihydrobenzo[*f*]imidazo[1,2-*d*][1,4]-oxazepane **37**, copper acetate monohydrate ($Cu(OAc)_2{\cdot}H_2O$), 3,4,7,8-tetram ethyl-1,10-phenanthroline (TMPhen), and cesium carbonate (Cs_2CO_3) in dioxane. The mixture was heated to 100 °C for 18 hours under an argon (Ar) atmosphere, resulting in compound **38**. The reagent **37** can be obtained as described in the literature [184]. Compound **38** was then suspended in dimethyl sulfoxide (DMSO) with L-alanine, cuprous iodide (CuI), and potassium phosphate tribasic (K_3PO_4), and heated at 100 °C for 2 hours. After cooling to room temperature, DMSO, ammonium chloride (NH_4Cl), and Et_3N were added. To this suspension, 1-[bis(dimethylamino)methylene]-1*H*-1,2,3-triazolo[4,5-*b*]-pyridinium 3-oxide hexafluorophosphate (HATU) was added dropwise and stirred at room temperature for 1 hour. Finally, inavolisib**3** was obtained [183].

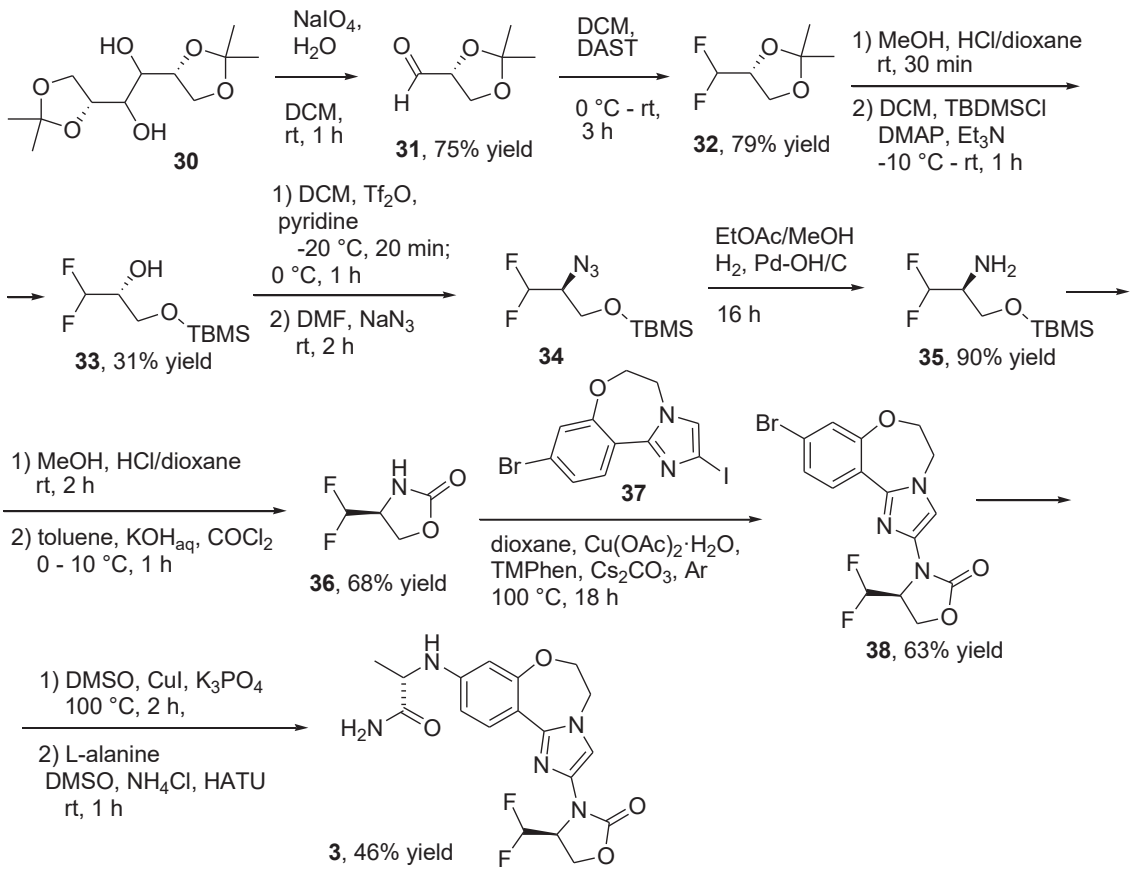

Scheme 5. Synthesis of Itovebi® (inavolisib) **3**.

Scemblix® (asciminib)(4)

Asciminib is an efficacious, small-molecule, orally bioavailable, and a selective allosteric inhibitor discovered and developed by Novartis for the treatment of hematologic malignancies, including Philadelphia chromosome-positive (Ph+) chronic myeloid leukemia (CML) [185,186]. In October 2021, the U.S. FDA approved Scemblix® for two distinct indications in CML [185]. In vitro anticancer activity tests against MV411 (ATCC) and K562 (ATCC) leukemia cells demonstrated that asciminib exhibited potent inhibitory activity, with cellular IC_{50} values of 8.65 μmol/L for K562 and 0.32 μmol/L for MY411. However, its structurally similar analog, compound **39** (Figure 5), showed moderate activity against the leukemia cell lines (K562 IC_{50} > 30 μmol/L and MY411 IC_{50} > 30 μmol/L).

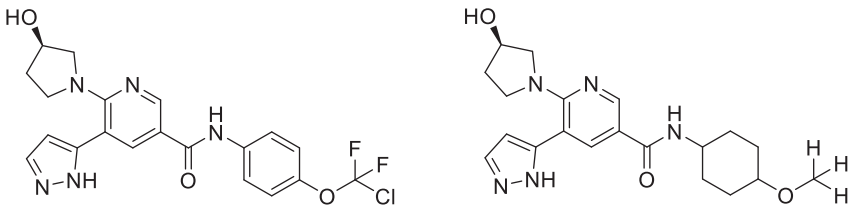

Fig. 5. Structures of Scemblix® (asciminib) **4** and its fluorine-free analog **39**.

This study indicated that the CF_2Cl group in the asciminib structure is crucial for inducing inactive conformations. Additionally, the pyrazole ring in its structure reduces hERG toxicity [186, 187]. As an allosteric inhibitor targeting ABL1, asciminib binds to the myristoyl pocket of ABL1 to inhibit BCR-ABL1 activity, differing from competitive inhibitors that target the ATP-binding site, such as imatinib, dasatinib, and nilotinib, which are associated with risks of resistance and site mutations [188–191]. Due to its unique allosteric regulatory mechanism, asciminib not only inhibits wild-type ABL1 kinase but also exhibits high activity against the T315I-mutated ABL1, significantly reducing the potential off-target effects of ATP-binding site inhibitors. In October 2024, the U.S. FDA granted accelerated approval to asciminib for the treatment of newly diagnosed adult patients with Philadelphia chromosome-positive chronic myeloid leukemia in chronic phase (Ph+ CML-CP) [192].

The synthesis of asciminib **4** has been documented by several groups [186, 193, 194]. One efficient method, illustrated in Scheme 6, begins with 5-bromo-6-chloronicotinic acid **40** as the starting material [186]. Chlorination of 5-bromo-6-chloronicotinic acid **40** using thionyl chloride in the presence of DMF in toluene at 80 °C produces acid chloride **41**. This intermediate then undergoes insitu condensation with 4-(chlorodifluoromethoxy)aniline **42** in the presence of DIPEA in THF at room temperature, forming amide **43** with a 77% yield. Next, compound **43** is reacted with (*R*)-pyrrolidin-3-ol **44** in the presence of DIPEA and isopropanol at 140 °C for 1 hour, producing derivative **45** with a 92% yield. Compound **45** is then

subjected to a standard Suzuki – Miyaura coupling reaction with the protected (1-(tetrahydro-2*H*-pyran-2-yl)-1*H*-pyrazol-5-yl)boronic acid pinacol ester **46**, resulting in compound **47**. Finally, the protecting group is removed at 10 °C in the presence of trifluoroacetic acid in DCM, yielding the target product, asciminib **4**, with a 77% yield.

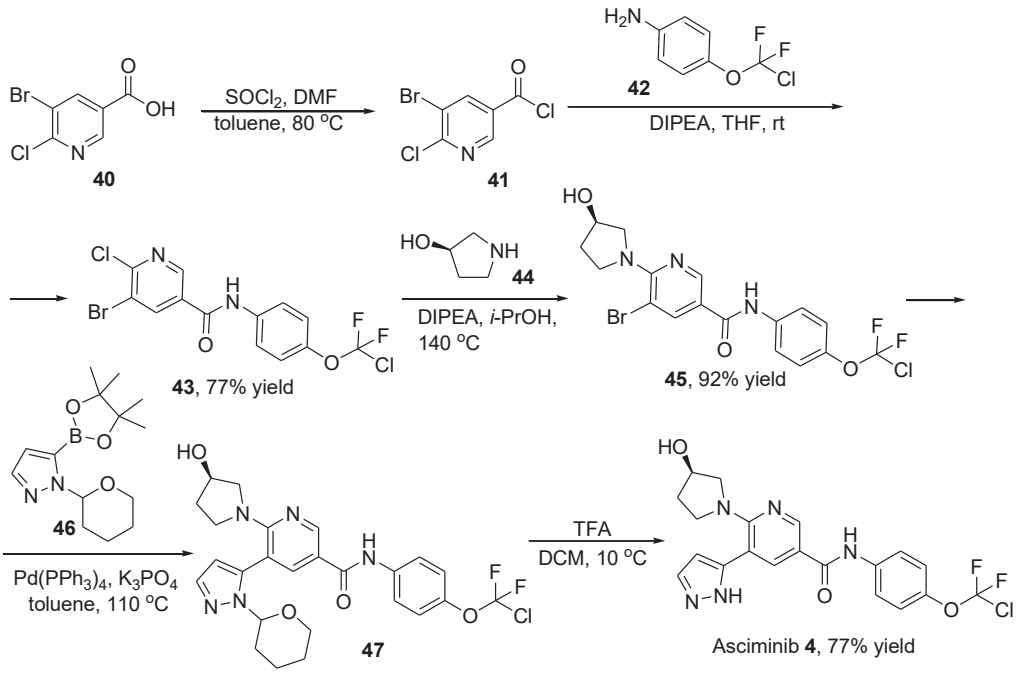

Scheme 6. Synthesis of Scemblix® (asciminib) **4**.

Revuforj® (revumenib)(5)

Revumenib, an orally administered and first-in-class menin inhibitor developed by Syndax Pharmaceuticals, received FDA approval in November 2024 for the treatment of patients with relapsed or refractory (R/R) acute leukemia harboring lysine methyltransferase 2A (KMT2A) gene translocations [195, 196]. Before this approval, revumenib was granted orphan drug designation by the FDA for the treatment of acute myeloid leukemia (AML), acute lymphoblastic leukemia (ALL), and acute undifferentiated leukemia (ALAL), as well as by the European Commission for the treatment of AML [197].

This novel drug disrupts the interaction between menin and KMT2A fusion proteins, which are key drivers of leukemogenesis [195,198]. By inhibiting this interaction, revumenib helps restore normal gene expression, effectively halting cancer cell proliferation and promoting cell differentiation.

In cellular experiments, revumenib demonstrated an IC_{50} of 10–20 nmol/L for inhibiting Menin-MLL, whereas its structurally similar compounds **48** and **49** (Figure 6) showed poorer inhibitory activity with IC_{50} values for Menin-MLL exceeding 20 nmol/L. The superior inhibitory activity of revumenib **5** against Menin-MLL may be attributed to the fluorine atom in its structure [199].

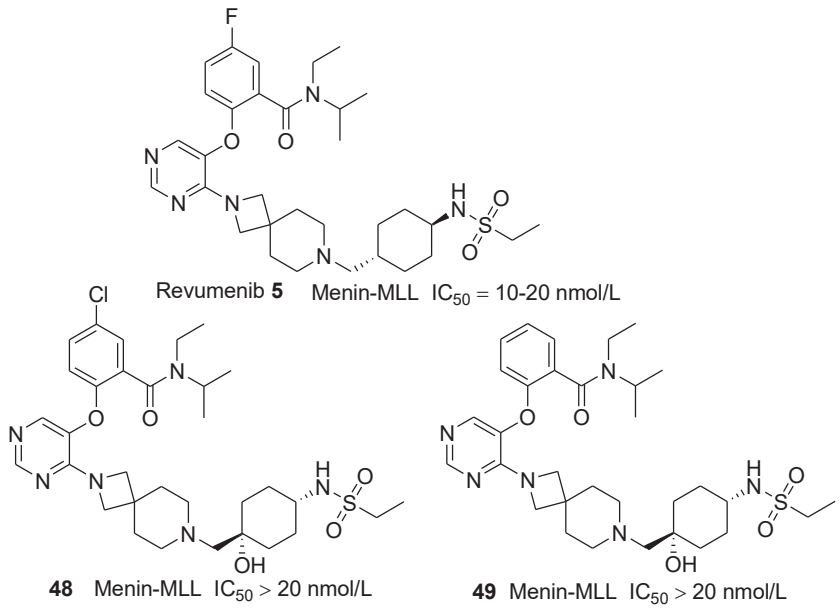

Fig. 6. Structures of Revuforj® (revumenib) **5** and its fluorine-free analogs **48** and **49**.

Clinical trials have shown promising results. When used as monotherapy for relapsed or refractory AML, revumenib **5** demonstrated significant efficacy, particularly in cases with nucleophosmin 1 (NPM1) mutations. This approval marks a significant advancement in the field of leukemia treatment, offering new hope for patients with limited therapeutic options [200, 201].

The synthetic route for the preparation of revumenib (**5**) is outlined in Scheme 7, starting with 2-bromo-4-fluorophenol **50** as the initial material [202]. Compound **50** underwent a substitution reaction with ethyl 2-bromoacetate in the presence of K_2CO_3, yielding compound **51** with an 86% yield. Compound **51** was first reacted in anhydrous THF, using ethyl formate and NaH as reagents. It then underwent a cyclization condensation reaction with thiourea at 90°C, resulting in the pyrimidinone compound **52** with a 54% yield.

Subsequently, compound **52** was subjected to a desulfurization reduction reaction in the presence of Raney Ni, yielding compound **53** with a 99% yield. Compound **53** was then reacted with CO and methanol under the catalysis of $Pd(dppf)Cl_2$, affording compound **54** with a 45% yield. In the presence of $SOCl_2$, compound **54** underwent a substitution reaction, resulting in derivative**55** with a 57% yield. Ester **55** was then reacted with bicyclic properly protected diamine **56** in the presence of TEA, using isopropanol as the solvent, to yield compound **57** with a 77% yield. Precursor **57** first underwent a hydrolysis reaction in the presence of LiOH, followed by an amidation reaction with amine **58** in the presence of BOP, yielding product **59** with a 70% yield. Derivative **59** was first deprotected of its Boc-protecting group in the presence of TEA and DCM as solvents. It subsequently reacted with activated cyclic amino alcohol **60** in the presence of K_2CO_3, KI, and NMP, giving rise torevumenib **5** with a 37% yield [202].

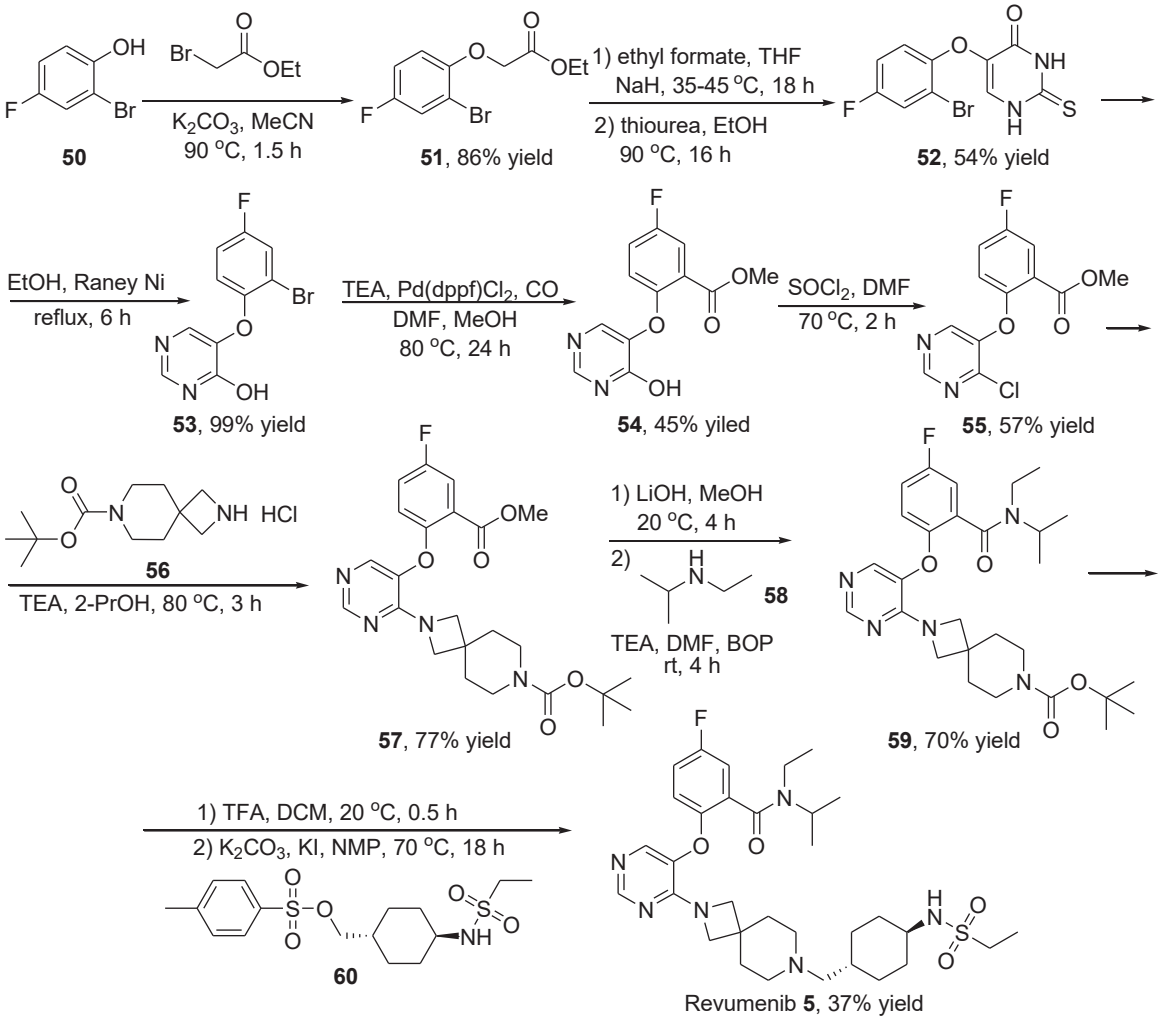

Scheme 7. Synthesis of Revuforj® (revumenib) **5**.

CONCLUSIONS. This year's crop of FDA-approved small-molecule drugs containing fluorine and amino acid residues consists of five pharmaceuticals: Voydeya® (danicopan) **1**, Ojemda® (tovorafenib) **2**, Itovebi® (inavolisib) **3**, Scemblix® (asciminib) **4**, and Revuforj® (revumenib) **5**. Four of these drugs (**2**-**5**) were developed to fight various types of cancer, while danicopan (**1**) was approved for the treatment of a rare form of blood disease.

The tailor-made amino acidsinclude 3-substituted proline (**1**), alanine (**2**, **3**), and amino acid-derived cyclic amino alcohols (**3**, **4**) and diamines (**5**). The types of fluorination are represented by cyclic CHF (**1**), hetero-aromatic CF_3 (**2**), aliphatic CHF_2 group (**3**), aromatic $CClF_2$-O group (**4**), and aromatic fluorine (**5**).

An important trend observed in new small-molecule pharmaceuticals, and this group of drugs in particular, is that all five compounds

under discussion are chiral, possessing one (**2**, **3**) or two (**1**, **3**, **4**) stereogenic carbons. Considering the FDA requirements for chiral drugs, continuous advances in the asymmetric synthesis and characterization of chiral fluorine-containing compounds are of great importance. In this regard, particular attention should be given to the phenomenon of the self-disproportionation of enantiomers (SDE), a non-linear behavior of enantiomerically enriched compounds [203–205]. The SDE properties of chiral drugs, especially those containing fluorine [206–208] and/or AA residues [209–211], are a critical public safety issue, requiring additional scrutiny in evaluating their enantiomeric purity [212–215].

We gratefully acknowledge the financial support from the National Natural Science Foundation of China (No. 21761132021), the Qing-Lan Project of Jiangsu Province (for Han) and IKERBASQUE, Basque Foundation for Science (for Soloshonok).

НОВІ ПРЕПАРАТИ НА ФАРМАЦЕВТИЧНОМУ РИНКУ, ЩО МІСТЯТЬ ФТОР І ЗАЛИШКИ СПЕЦІАЛЬНО СТВОРЕНИХ АМІНОКИСЛОТ

Ц. Хань[1*], А. Взорек[2], Г. Дхаван[3,4*], В. Зханг[5*], О. Є. Сорочинський[6*], Д. Бекер[7*], Т. Оно[8], К. Д. Клика[9], В. А. Солошонок[10,11*]

[1]Спільний інноваційний центр Цзянсу з ефективного оброблення та використання лісових ресурсів, Коледж хімічної інженерії, Нанкінський лісотехнічний університет, 210037 Нанкін, Китай;
[2]Інститут хімії, Університет імені Яна Кохановського в Кельцях, Кельці, Польща;
[3] Школа медичних наук, Університет підприємництва, Делі, 110077 Нью-Делі, Індія
[4]Коледж Ачаріа Нарендра Дев, Університет Делі, 110019 Нью-Делі, Індія;
[5]Департамент хімії, Массачусетський університет, Бостон, 02125 Массачусетс, США;
[6]Інститут біоорганічної хімії та нафтохімії ім. В. П. Кухаря НАН України, Київ, Україна;
[7]Департамент фармацевтичної та медичної хімії, Інститут фармації, Вільний університет Берліна, 14195 Berlin, Germany;
[8]Національний інститут передових промислових наук і технологій, 463–8560 Нагоя, Японія
[9]Німецький центр дослідження раку (DKFZ), 69120 Гейдельберг, Німеччина;
[10]Хімічний факультет, Університет Країни Басків, 20018 Сан-Себастьян, Іспанія;
[11]ІКЕРБАСК, Баскський фонд науки, 48013 Більбао, Іспанія
**email: vadimsoloshonok@gmail.com*

У статті розглянуто п'ять нових препаратів, схвалених FDA, що містять фтор і фрагменти амінокислот або їхніх похідних. До цих лікарських засобів належать: Voydeya® (danicopan), Ojemda® (tovorafenib), Itovebi® (inavolisib), Scemblix® (asciminib) та Revuforj® (revumenib). Описано відкриття кожного препарату, терапевтичне застосування та детальний хімічний синтез.

Ключові слова: фтор, спеціально створені амінокислоти, фармацевтичні препарати, дизайн ліків, синтез, біоактивність.

REFERENCES

1. Vickery H.B., Schmidt C.L.A. The history of the discovery of the amino acids. *Chem. Rev*. 1931. **9**(2): 169–318. doi: 10.1021/cr60033a001.
2. Luisi P.L. *The Emergence of Life: From Chemical Origins to Synthetic Biology*. Cambridge University Press. 2006. doi: 10.1017/CBO9780511817540
3. Anfinsen C.B., Edsall J.T., Richards F.M. *Advances in Protein Chemistry*. New York: Academic Press. 1972.
4. Michal G., Schomburg D., eds. *Biochemical Pathways: An Atlas of Biochemistry and Molecular Biology.* 2nd Ed. Oxford: Wiley-Blackwell. 2012.
5. Genchi G. An overview on D-amino acids. *Amino Acids*. 2017. **49**(9): 1521–1533. doi: 10.1007/s00726-017-2459-5.
6. Wong J. T.-F. A Co-Evolution Theory of the Genetic Code. *Proc. Nat. Acad. Sci. USA*. 1975. **72**(5): 1909–1912. doi: 10.1073/pnas.72.5.1909.
7. Trifonov E.N. Consensus temporal order of amino acids and evolution of the triplet code. *Gene*. 2000. **261**(1): 139–151. doi: 10.1016/s0378-1119(00)00476-5.
8. Higgs P.G., Pudritz R.E. A thermodynamic basis for prebiotic amino acid synthesis and the nature of the first genetic code. *Astrobiology*. 2009. **9** (5): 483–90. doi: 10.1089/ast.2008.0280.
9. Meierhenrich U. *Amino acids and the asymmetry of life*. Berlin: Springer. 2008. doi: 10.1007/978-3-540-76886-9.
10. Hanessian S. Reflections on the total synthesis of natural products: Art, craft, logic, and the chiron approach. *Pure Appl. Chem*.1993. **65**(6): 1189–1204. doi: 10.1351/pac199365061189.
11. Blaser H.U. The chiral pool as a source of enantioselective catalysts and auxiliaries. *Chem. Rev*. 1992. **92**(5): 935–952. doi: 10.1021/cr00013a009.
12. Kitadai N., Maruyama S. Origins of building blocks of life: A review. *Geosci. Front*. 2018. **9**(4): 1117–1153. doi: 10.1016/j.gsf.2017.07.007.
13. Danchin A. From chemical metabolism to life: the origin of the genetic coding process. *Beilstein J. Org. Chem*. 2017. **13**(1): 1119–1135. doi: 10.3762/bjoc.13.111.
14. Frenkel-Pinter M., Samanta M., Ashkenasy G., Leman L.J. Prebiotic Peptides: Molecular Hubs in the Origin of Life. *Chem. Rev*. 2020. **120**(11): 4707–4765. doi: 10.1021/acs.chemrev.9b00664.
15. Milner-White E.J. Protein three-dimensional structures at the origin of life. *Interface Focus*. 2019. **9**(6): 20190057. doi: 10.1098/rsfs.2019.0057.
16. Chatterjee S., Yadav S. The Coevolution of Biomolecules and Prebiotic Information Systems in the Origin of Life: A Visualization Model for Assembling the First Gene. *Life*. 2022. **12**(6): 834. doi: 10.3390/life12060834.
17. Kirschning A. The coenzyme/protein pair and the molecular evolution of life. *Nat. Prod. Rep*. 2021. **38**(5): 993–1010. doi: 10.1039/D0NP00037J.
18. Gutteridge A., Thornton J.M. Understanding nature's catalytic toolkit. *Trends in Biochem. Sci*. 2005. **30**(11): 622–629. doi: 10.1016/j.tibs.2005.09.006.
19. McCoy R.H., Meyer C.E., Rose W.C. Feeding experiments with mixtures of highly purified amino acids. VIII. Isolation and identification of a new essential amino acid.*J. Biol. Chem*. 1935. **112**: 283–302.
20. Steinhardt J., Reynolds J. A. *Multiple equilibria in proteins*. New York: Academic Press. 1969.
21. Xie J., Schultz P.G. Adding amino acids to the genetic repertoire. *Curr. Opin. Chem. Biol*. 2005. **9**(6): 548–554. doi: 10.1016/j.cbpa.2005.10.011.
22. Park M.H. The post-translational synthesis of a polyamine-derived amino acid, hypusine, in the eukaryoti c translation initiation factor 5A (eIF5A). *J. Biochem*. 2006. **139**(2): 161–169. doi: 10.1093/jb/mvj034.
23. Curis E., Nicolis I., Moinard C. et al. Almost all about citrulline in mammals. *Amino Acids*. 2005. **29**(3): 177–205.

doi: 10.1007/s00726-005-0235-4.
24. Sakami W., Harrington H. Amino acid metabolism. *Annu. Rev. Biochem.* 1963. **32**(1): 355–398.
doi: 10.1146/annurev.bi.32.070163.002035.
25. Wang X., Li J., Dong G., Yue J. The endogenous substrates of brain CYP_2D. *Eur. J. Pharmacol.* 2014. **724**: 211–218.
doi: 10.1016/j.ejphar.2013.12.025.
26. Petroff O.A. GABA and glutamate in the human brain. *Neurosci.* 2002. **8**(6): 562–573.
doi: 10.1177/1073858402238515.
27. Turner E.H., Loftis J.M., Blackwell A.D. Serotonin a la carte: supplementation with the serotonin precursor 5-hydroxytryptophan. *Pharmacol. Ther*. 2006. **109**(3): 325–338.
doi: 10.1016/j.pharmthera.2005.06.004.
28. Kostrzewa R.M., Nowak P., Kostrzewa J.P. *et al*. Peculiarities of L-DOPA treatment of Parkinson's disease. *Amino Acids*. 2005. **28**(2): 157–164.
doi: 10.1007/s00726-005-0162-4.
29. Leuchtenberger W., Huthmacher K., Drauz K. Biotechnological production of amino acids and derivatives: current status and prospects. *Appl. Microbiol. Biotechnol*. 2005. **69**(1): 1–8.
doi: 10.1007/s00253-005-0155-y.
30. Sanda F., Endo T. Syntheses and functions of polymers based on amino acids. *Macromol. Chem. Phys*. 1999. **200**(12): 2651–2661.
doi: 10.1002/(SICI)1521-3935.
31. Lengyel P., Söll D. Mechanism of protein biosynthesis. *Bacteriol. Rev*. 1969. **33**(2): 264–301.
doi: 10.1128/br.33.2.264-301.1969.
32. Marasco D., Perretta G., Sabatella M., Ruvo M. Past and future perspectives of synthetic peptide libraries. *Curr. Protein Pept. Sci*. 2008. **9**(5): 447–467.
doi: 10.2174/138920308785915209.
33. Soloshonok V.A., Cai C., Hruby V.J., Meervelt L.V. Asymmetric synthesis of novel highly sterically constrained (2*S*,3*S*)-3-methyl-3-trifluoromethyl- and (2*S*,3*S*,4*R*)-3-trifluoromethyl-4-methylpyroglutamic acids. *Tetrahedron*. 1999. **55**(41): 12045–12058.
doi: 10.1016/S0040-4020(99)00711-5.
34. Blaskovich M.A.T. Unusual amino acids in medicinal chemistry. *J Med Chem*. 2016. ***59*** (24): 10807–10836.
doi: 10.1021/acs.jmedchem.6b00319.
35. Han J., Konno H., Sato T. *et al*.Tailor-made amino acids in the design of small-molecule blockbuster drugs. *Eur. J. Med. Chem*. 2021. **220**: 113448.
doi: 10.1016/j.ejmech.2021.113448.
36. Liu J., Han J., Izawa K. *et al*. Cyclic tailor-made amino acids in the design of modern pharmaceuticals. *Eur. J. Med. Chem*. 2020. **208**: 112736.
doi: 10.1016/j.ejmech.2020.112736.
37. Stevenazzi A., Marchini M., Sandrone G., Vergani B., Lattanzio M. Amino acidic scaffolds bearing unnatural side chains: An old idea generates new and versatile tools for the life sciences. *Bioorg. Med. Chem. Lett*. 2014. **24**(23): 5349–5356.
doi: 10.1016/j.bmcl.2014.10.016.
38. Ma J.S. Unnatural amino acids in drug discovery. *Chim. Oggi-Chem. Today*. 2003. **21**(6): 65–68.
39. Liu A., Han J., Nakano A., *et al*. New pharmaceuticals approved by FDA in 2020: Small-molecule drugs derived from amino acids and related compounds. *Chirality*. 2022. **34**(1): 86–103.
doi: 10.1002/chir.23376.
40. Han J., Lyutenko N.V., Sorochinsky A.E., *et al*. Tailor-Made Amino Acids in Pharmaceutical Industry: Synthetic Approaches to Aza-Tryptophan Derivatives. *Chem. Eur. J*. 2021. **27**(70): 17510–17528.
doi: 10.1002/chem.202102485.
41. Yin Z., Hu W., Zhang W. *et al*. Tailor-made amino acid-derived pharmaceuticals approved by the FDA in 2019. *Amino Acids*. 2020. **52**(9): 1227–1261.
doi: 10.1007/s00726-020-02887-4.
42. Hodgson D.R.W., Sanderson J.M. The synthesis of peptides and proteins containing non-natural amino acids. *Chem. Soc. Rev*. 2004. **33**(7): 422–430.
doi: 10.1039/B312953P.
43. Henninot A., Collins J.C., Nuss J.M. The current state of peptide drug discovery: Back to the

future? *J. Med. Chem*. 2018. **61**(4): 1382–1414. doi: 10.1021/acs.jmedchem.7b00318.
44. Han, J., Konno H., Sato T., *et al*. Peptidomimetics and Peptide-Based Blockbuster Drugs. *Curr. Org. Chem*. 2021. **25**(14):1627–1658. doi: 10.2174/1385272825666210610155047.
45. Qiu W., Gu X., Soloshonok, V.A. et al. Stereoselective synthesis of conformationally constrained reverse turn dipeptide mimetics. *Tetrahedron Lett*. 2001. **42**(2): 145–148. doi: 10.1016/S0040-4039(00)01864-5.
46. Fosgerau K., Hoffmann T. Peptide therapeutics: current status and future directions. *Drug Discov. Today*. 2015. **20**(1): 122–128. doi: 10.1016/j.drudis.2014.10.003.
47. Cai M., Cai C., Mayorov A.V. *et al*. Biological and conformational study of β-substituted prolines in MT-II template: steric effects leading to human MC5 receptor selectivity. *J. Pept. Res*. 2004. **63**(2): 116–131. doi: 10.1111/j.1399-3011.2003.00105.x.
48. Craik D.J., Fairlie D.P., Liras S., Price D. The future of peptide-based drugs. *Chem. Biol. Drug Des*. 2013. **81**(1): 136–147. doi: 10.1111/cbdd.12055.
49. Hamley I.W. *Introduction to Peptide Science.* Wiley: Weinheim, Germany. 2020. ISBN: 978-1-119-69817-3.
50. Saladin K. *Anatomy and Physiology: The Unity of Form and Function.* 6th Ed. McGraw-Hill Science/Engineering/Math. 2011.
51. Soloshonok V.A., Izawa K. Eds. *Asymmetric Synthesis and Application of α-Amino Acids. ACS Symposium Series 1009*. Washington, District of Columbia: American Chemical Society, 2009.
52. Wang J., Sánchez-Roselló M., Aceña J.L. *et al*. Fluorine in pharmaceutical industry: Fluorine-containing drugs introduce ed to the market in the last decade (2001–2011). *Chem. Rev*. 2014. **114**(4): 2432–2506. doi: 10.1021/cr4002879.
53. Zhou Y., Wang J., Gu Z. *et al*. Next Generation of Fluorine-Containing Pharmaceuticals, Compounds Currently in Phase II–III Clinical Trials of Major Pharmaceutical Companies: New Structural Trends and Therapeutic Areas. *Chem. Rev*. 2016. **116**(2): 422–518. doi: 10.1021/acs.chemrev.5b00392.
54. Zhu Y., Han J.L., Wang J.*et al*. Modern Approaches for Asymmetric Construction of Carbon–Fluorine Quaternary Stereogenic Centers: Synthetic Challenges and Pharmaceutical Needs. *Chem. Rev*. 2018. **118**(7): 3887–3964. doi: 10.1021/acs.chemrev.7b00778.
55. Zhu W., Wang J., Wang S.*et al*.Recent advances in the trifluoromethylation methodology and new CF_3-containing drugs. *J. Fluorine Chem*. 2014. **167**: 37–54. doi: 10.1016/j.jfluchem.2014.06.026.
56. Gillis E.P., Eastman K.J., Hill M.D. *et al*. Applications of Fluorine in Medicinal Chemistry. *J. Med. Chem*. 2015. **58**(21): 8315–8359. doi: 10.1021/acs.jmedchem.5b00258.
57. Meanwell N.A. Fluorine and Fluorinated Motifs in Design and Application of Bioisosteres for Drug Design. *J. Med. Chem*. 2018. **61**(14): 5822–5880. doi: 10.1021/acs.jmedchem.7b01788.
58. Johnson B.M., Shu Y-Z., Zhuo X., Meanwell N.A. Metabolic and Pharmaceutical Aspects of Fluorinated Compounds. *J. Med. Chem*. 2020. **63**(12): 6315–86. doi: 10.1021/acs.jmedchem.9b01877.
59. Han J., Kiss L., Mei H. *et al*. Chemical aspects of human and environmental overload with fluorine. *Chem. Rev*. 2021. **121**(8): 4678–4742. doi: 10.1021/acs.chemrev.0c01263.
60. Pan Y. The Dark Side of Fluorine. *ACS Med. Chem. Lett*. 2019. **10**(7): 1016–1019. doi: 10.1021/acsmedchemlett.9b00235.
61. Khan M.F., Murphy C.D. Bacterial degradation of the anti-depressant drug produces trifluoroacetic acid and fluoride ion. *Appl. Microbiol. Biotechnol*. 2021. **105**(24): 9359–9369. doi: 10.1007/s00253-021-11675-3.
62. Sun M., Cui J.N., Guo J. *et al*. Fluorochemicals biodegradation as a potential source of trifluoroacetic acid (TFA) to the environment. *Chemosphere*. 2020. **254**: 126894. doi: 10.1016/j.chemosphere.2020.126894.
63. Garnett K., Van Calster G. The Concept of Essential Use: A Novel Approach to Regulating

Chemicals in the European Union. *Transnatl. Environ. Law*. 2021. **10**(1): 159–187. doi: 10.1017/S2047102521000042.
64. Mei H., Han J., Fustero S. Fluorine-Containing Drugs Approved by the FDA in 2018. *Chem. Eur. J.* 2019. **25**(51): 11797–11819. doi: 10.1002/chem.201901840.
65. Han J., Remete A.M., Dobson L.S. *et al*. Next generation organofluorine containing blockbuster drugs. *J. Fluor. Chem*. 2020. **239**: 109639. doi: 10.1016/j.jfluchem.2020.109639.
66. Mei H., Remete A.M., Zou Y. *et al*. Fluorine-containing drugs approved by the FDA in 2019. *Chin. Chem. Lett*. 2020. **31**(9): 2401–2413. doi: 10.1016/j.cclet.2020.03.050.
67. He J., Li Z., Dhawan G. *et al*. Fluorine-containing drugs approved by the FDA in 2021. *Chin. Chem. Lett*. 2023. **34**(1): 107578. doi: 10.1016/j.cclet.2022.06.001.
68. Yu Y., Liu A., Dhawan G. *et al*. Fluorine-containing pharmaceuticals approved by the FDA in 2020: Synthesis and biological activity. *Chin. Chem. Lett.* 2021. **32**(11): 3342–3354. doi: 10.1016/j.cclet.2021.05.042.
69. Wang Q., Bian Y., Dhawan G. *et al*. FDA approved fluorine-containing drugs in 2023. *Chin. Chem. Lett*. 2024. **35**(11): 109780. doi: 10.1016/j.cclet.2024.109780.
70. Han J., Wzorek A., Dhawan G. *et al*. New drugs appearing on the market in 2023: molecules containing fluorine and fragments of tailor-made amino acids. *Ukr. Bioorg. Acta*. 2024. **19**(1): 3–20. Doi: 10.15407/bioorganica2024.01.003.
71. Wang N., Mei H., Dhawan G. *et al*. New Approved Drugs Appearing in the Pharmaceutical Market in 2022, Featuring Fragments of Tailor-Made Amino Acids and Fluorine. *Molecules.* 2023. **28**(9): 3651. doi: 10.3390/molecules28093651.
72. Li J., Zhou S., Wang J. *et al*.Asymmetric synthesis of aromatic and heteroaromatic α-amino acids using recyclable axially chiral ligand. *Eur. J. Org. Chem*. 2016. **2016**(5): 999–1006. doi: 10.1002/ejoc.201501442.
73. Mei H., Han J., White S. *et al*. Tailor-made amino acids and fluorinated motifs as prominent traits in modern pharmaceuticals. *Chem. Eur. J.* 2020. **26**(50): 11349–11390. doi: 10.1002/chem.202000617.
74. Mei H., Han J., Klika K.D. *et al*. Applications of fluorine-containing amino acids for drug design. *Eur. J. Med. Chem*. 2020. **186**: 111826. doi: 10.1016/j.ejmech.2019.111826.
75. Osipov S.N., Artyushin O.I., Kolomiets A.F. *et al*. Synthesis of fluorine-containing cyclic α-amino acid and α-amino phosphonate derivatives by alkene metathesis. *Eur. J. Org. Chem*. 2001. **2001**(20): 3891–3897. doi:10.1002/1099-0690(200110)2001:20<3891::AID-EJO C3891>3.0.CO;2-R.
76. Remete A.M., Nonn M., Fustero S. *et al*. Synthesis of fluorinated amino acid derivatives through late-stage deoxyfluorinations. *Tetrahedron*. 2018. **74**(44): 6367–6418. doi: 10.1016/j.tet.2018.09.021.
77. Konno T., Kanda M., Ishihara T., Yamanaka H. A novel synthesis of fluorine-containing quaternary amino acid derivatives via palladium-catalyzed allylation reaction. *J. Fluorine Chem.*2005. **126**(11–12): 1517–1523. doi: 10.1016/j.jfluchem.2005.08.013.
78. Krause H.W., Kreuzfeld H.J., Döbler C. Unusual amino acids: II. Asymmetric synthesis of fluorine containing phenylalanines. *Tetrahedron: Asymmetry*. 1992. **3**(4): 555–566. doi: 10.1016/S0957-4166(00)80262-1.
79. Tsushima T., Kawada K., Nishikawa J. *et al*. Fluorine-containing amino acids and their derivatives. 3. Stereoselective synthesis and unusual conformational features of threo- and erythro-3-fluorophenylalanine. *J. Org. Chem*. 1984. **49**(7): 1163–1169. doi: 10.1021/jo00181a003.
80. Vine W.H., Hsieh K.H., Marshall G.R. Synthesis of fluorine-containing peptides. Analogs of angiotensin II containing hexafluorovaline. *J. Med. Chem.*1981. **24**(9): 1043–1047. doi: 10.1021/jm00141a005.
81. Sorochinsky A.E., Ueki H., Aceña J.L. *et al*. Chemical deracemization and (*S*) to (*R*) interconversion of some fluorine-containing α-amino acids. *J. Fluorine Chem*. 2013. **152**: 114–118.

doi: 10.1016/j.jfluchem.2013.02.022.
82. Smits R., Cadicamo C.D., Burger K., Koksch B. Synthetic strategies to α-trifluoromethyl and α-difluoromethyl substituted α-amino acids. *Chem. Soc. Rev.* 2008. **37**(8): 1727–1739. doi: 10.1039/B800310F.
83. Gutiérrez-Bonet Á., Liu W. Synthesis of alkyl fluorides and fluorinated unnatural amino acids via photochemical decarboxylation of α-fluorinated carboxylic acids. *Org. Lett*. 2023. **25**(3): 483–487. doi: 10.1021/acs.orglett.2c04144.
84. Soloshonok V. A., Cai C., Hruby V. J. *et al*. Stereochemically defined C-substituted glutamic acids and their derivatives. 1. An efficient asymmetric synthesis of (2*S*, 3*S*)-3-methyl- and -3-trifluoromethylpyroglutamic acids. *Tetrahedron*. 1999. **55**(41): 12031–12044. doi: 10.1016/S0040-4020(99)00711-5.
85. Soloshonok V.A., Avilov D.V., Kukhar V.P. Highly diastereoselective asymmetric aldol reactions of chiral Ni(II)-complex of glycine with alkyl trifluoromethyl ketones. Tetrahedron: Asymmetry. 1996. **7**(6): 1547–1550. doi: 10.1016/0957-4166(96)00177-2.
86. Soloshonok V.A., Kacharov A.D., Hayashi T. Gold(I)-catalyzed asymmetric aldol reactions of isocyanoacetic acid derivatives with fluoroaryl aldehydes. *Tetrahedron*. 1996. **52**(1). 245–254. doi: 10.1016/0040-4020(95)00893-D.
87. Soloshonok V.A., Kukhar V.P. Biomimetic base-catalyzed [1,3]-proton shift reaction. A practical synthesis of β-fluoroalkyl-β-amino acids. *Tetrahedron*. 1996. **52**(20): 6953–6964. doi: 10.1016/0040-4020(96)00300-6.
88. Soloshonok V.A., Hayashi T., Ishikawa K., Nagashima N. Highly diastereoselective aldol reaction of fluoroalkyl aryl ketones with methyl isocyanoacetate catalyzed by silver(I)/triethylamine. *Tetrahedron Letters*. 1994. **35**(7): 1055–1058. doi: 10.1016/S0040-4039(00)79964-3.
89. Soloshonok V.A., Avilov D.V., Kukhar V.P. *et al*. An efficient asymmetric synthesis of (2*S*, 3*S*)-3-trifluoromethylpyroglutamic acid. *Tetrahedron Lett*. 1997. **38**(27): 4903–4904. doi: 10.1016/S0040-4039(97)01054-X.
90. Soloshonok V.A., Kacharov A.D., Avilov D.V. *et al*. Transition metal/base-catalyzed aldol reactions of isocyanoacetic acid with prochiral ketones, a straightforward approach to stereochemically defined β,β-disubstituted-β-hydroxy-α-amino acids. Scope and limitations. *J. Org. Chem.* 1997. **62**(11): 3470–3479. doi: 10.1021/jo9623402.
91. Bravo P., Guidetti M., Viani F. *et al*. Chiral sulfoxide controlled asymmetric additions to C N double bond. An efficient approach to stereochemically defined α-fluoroalkyl amino compounds. *Tetrahedron.*1998. **54**(42): 12789–12806. doi: 10.1016/S0040-4020(98)00779-0.
92. Bravo P., Capelli S., Meille S.V. *et al*. Synthesis of optically pure (*R*)- and (*S*)-α-trifluoromethyl-alanine. *Tetrahedron*: *Asymmetry*. 1994. **5**(10): 2009–2018. doi: 10.1016/S0957-4166(00)86276-X.
93. Soloshonok V.A., Hayashi T. Gold(I)-catalyzed asymmetric aldol reaction of methyl isocyanoacetate with fluorinated benzaldehydes. *Tetrahedron Lett*. 1994. **35**(17): 2713–2716. doi: 10.1016/S0040-4039(00)77013-4.
94. Takeda R., Kawamura A., Kawashima A. *et al*. Chemical dynamic kinetic resolution and *S*/*R* interconversion of unprotected α-amino acids. *Angew. Chem. Int. Ed.* 2014. **53**(3): 12214–12217. doi: 10.1002/anie.201407944.
95. Bravo P., Farina A., Kukhar V. P. *et al*. Stereoselective additions of α-lithiated alkyl-*p*-tolylsulfoxides to *N*-PMP fluoroalkyl aldimines. An efficient approach to enantiomerically pure fluoro amino compounds. *J. Org. Chem*. 1997. **62**(11): 3424–3425. doi: 10.1021/jo970004v.
96. Soloshonok V.A., Hayashi T. Gold(I)-catalyzed asymmetric aldol reaction of fluorinated benzaldehydes with α-isocyanoacetamide *Tetrahedron*: *Asymmetry.* 1994. **5**(6): 1091–1094. doi: 10.1016/0957-4166(94)80059-6.
97. Nian Y., Wang J., Zhou S. *et al*. Recyclable ligands for the non-enzymatic dynamic kinetic resolution of challenging α-amino acids. *Angew.*

Chem. Int. Ed. 2015. **54**(44): 12918–12922. doi: 10.1002/anie.201507273.
98. Soloshonok V.A., Avilov D.V., Kukhar V.P. Asymmetric aldol reactions of trifluoromethyl ketones with a chiral Ni(II) complex of glycine: Stereocontrolling effect of the trifluoromethyl group. *Tetrahedron.*1996. **52**(38): 12433–12442. doi: 10.1016/0040-4020(96)00741-7.
99. Turcheniuk K.V., Poliashko K.O., Kukhar V.P. *et al*. Efficient asymmetric synthesis of trifluoromethylated β-aminophosphonates and their incorporation into dipeptides. *Chem. Commun*. 2012. **48**(94): 11519–11521. doi: 10.1039/C2CC36702E.
100. Röschenthaler G.-V., Kukhar V.P., Kulik I.B. *et al*. Asymmetric synthesis of phosphonotrifluoroalanine and its derivatives using *N-tert*-butanesulfinyl imine derived from fluoral. *Tetrahedron Lett*. 2012. **53**(5): 539–542. doi: 10.1016/j.tetlet.2011.11.096.
101. Brittain W.D., Lloyd C.M., Cobb S.L. Synthesis of complex unnatural fluorine-containing amino acids. *J. Fluorine Chem*. 2020. **239**: 109630. doi: 10.1016/j.jfluchem.2020.109630.
102. Acena J.L., Simon-Fuentes A., Fustero S. Recent developments in the synthesis of fluorinated β-amino acids. *Curr. Org. Chem*. 2010. **14**(9): 928–949. doi: 10.2174/138527210791111777.
103. Ouchakour L., Ábrahámi R.A., Forró E. *et al*. Stereocontrolled synthesis of fluorine-containing piperidine γ-amino acid derivatives. *Eur. J. Org. Chem*. 2019. **2019**(12): 2202–2211. doi: 10.1002/ejoc.201801540.
104. Zhang X.-X., Gao Y., Hu X.-S. *et al*. Recent advances in catalytic enantioselective synthesis of fluorinated α-and β-amino acids. *Adv. Synth. Catal*. 2020. **362**(22): 4763–4793. doi: 10.1002/adsc.202000966.
105. Tolman V. Syntheses of fluorinated amino acids: from the classical to the modern concept. *Amino Acids*. 1996. **11**(1): 15–36. doi: 10.1007/BF00805718.
106. Lin D., Wang J., Liu H. Recent developments in the synthesis of fluorine-containing β-amino acids and β-lactams. *Chin. J. Org. Chem*. 2013. **33**(10): 2098–2107. doi: 10.6023/cjoc201303020.
107. Albler C., Schmid W. Synthetic routes towards fluorine-containing amino sugars: synthesis of fluorinated analogues of tomosamine and 4-amino-4-deoxyarabinose. *Eur. J. Org. Chem*. 2014. **2014**(12): 2451–2459. doi: 10.1002/ejoc.201301614.
108. Vera-Ayoso Y., Borrachero P., Cabrera-Escribano F. *et al*. Towards cyclic, conformationally constrained, fluorine-containing β-amino acid derivatives from D-glucose. *Tetrahedron: Asymmetry*. 2001. **12**(14): 2031–2041. doi: 10.1016/S0957-4166(01)00354-8.
109. Soloshonok V.A., Kirilenko A.G., Fokina N.A. *et al*. Biocatalytic resolution of β-fluoroalkyl-β-amino acids. *Tetrahedron*: *Asymmetry.* 1994. **5**(6): 1119–1126. doi: 10.1016/0957-4166(94)80063-4.
110. Yamada T., Okada T., Sakaguchi K. *et al*. Efficient asymmetric synthesis of novel 4-substituted and configurationally stable analogues of thalidomide. *Org. Lett.* 2006, **8**(24): 5625–5628. doi: 10.1021/ol0623668.
111. Shibata N., Nishimine T., Shibata N. *et al*. Organic base-catalyzed stereodivergent synthesis of (*R*)- and (*S*)-3-amino-4,4,4-trifluorobutanoic acids. *Chem. Commun*. 2012. **48**(34): 4124–4126. doi: 10.1039/C2CC30627A.
112. Soloshonok V.A., Kirilenko A.G., Kukhar V.P., Resnati G. Transamination of fluorinated β-keto carboxylic esters. A biomimetic approach to β-polyfluoroalkyl-β-amino acids. *Tetrahedron Lett*. 1993. **34**(22): 3621–3624. doi: 10.1016/S0040-4039(00)73652-5.
113. Soloshonok V.A., Kirilenko A.G., Fokina N.A. *et al*. Chemo-enzymatic approach to the synthesis of each of the four isomers of α-alkyl-β-fluoroalkyl-substituted β-amino acids. *Tetrahedron: Asymmetry*.1994. **5**(7): 1225–1228. doi: 10.1016/0957-4166(94)80163-0.
114. Soloshonok V.A., Kirilenko A.G., Galushko S.V., Kukhar V.P. Catalytic asymmetric synthesis of β-fluoroalkyl-β-amino acids via biomimetic [1,3]-proton shift reaction. *Tetrahedron-*

Lett. 1994. **35**(28): 5063–5064.
doi: 10.1016/S0040-4039(00)73320-X.
115. Soloshonok V.A., Ono T. The effect of substituents on the feasibility of azomethine-azomethine isomerization: New synthetic opportunities for biomimetic transamination. *Tetrahedron.*1996. **52**(47): 14701–14712.
doi: 10.1016/0040-4020(96)00920-9.
116. Soloshonok V.A., Kukhar V.P. Biomimetic transamination of α-keto perfluorocarboxylic esters. An efficient preparative synthesis of β,β,β-trifluoroalanine. *Tetrahedron.* 1997. **53**(25): 8307–8314.
doi: 10.1016/S0040-4020(97)00517-6.
117. Soloshonok V.A., Ono T., Soloshonok I. V. Enantioselective biomimetic transamination of β-keto carboxylic acid derivatives. An efficient asymmetric synthesis of β-fluoroalkyl β-amino acids. *J. Org. Chem*. 1997. **62**(22): 7538–7539.
doi: 10.1021/jo9710238.
118. Soloshonok V.A., Ohkura H., Yasumoto M. Operationally convenient asymmetric synthesis of (*S*)- and (*R*)-3-amino-4,4,4-trifluorobutanoic acid: Part II. Enantioselective biomimetic transamination of 4,4,4-trifluoro-3-oxo-*N*-[(*R*)-1-phenylethyl)butanamide. *J. Fluorine Chem*. 2006. **127**(7): 930–935.
doi: 10.1016/j.jfluchem.2006.04.004.
119. Soloshonok V.A., Soloshonok I.V., Kukhar V.P., Svedas V.K. Biomimetic transamination of α-alkyl β-keto carboxylic esters. Chemoenzymatic approach to the stereochemically defined α-Alkyl β-Fluoroalkyl β-Amino Acids. *J. Org. Chem*. 1998. **63**(6): 1878–1884.
doi: 10.1021/jo971777m.
120. Sorochinsky A., Voloshin N., Markovsky A. *et al*. Convenient asymmetric synthesis of β-substituted α,α-difluoro-β-amino acids via Reformatsky reaction between Davis'*N*-sulfinylimines and ethyl bromodifluoroacetate. *J. Org. Chem*. 2003. **68**(19): 7448–7454.
doi: 10.1021/jo030082k.
121. Soloshonok V.A., Ohkura H., Sorochinsky A. *et al*. Convenient, large-scale asymmetric synthesis of β-aryl-substituted α,α-difluoro-β-amino acids. *Tetrahedron Lett*. 2002. **43**(31): 5445–5448. doi: 10.1016/S0040-4039(02)01103-6.
122. Kukhar VP. Fluorine-containing amino acids. *J. Fluorine Chem*. 1994. **69**(3): 199–205.
doi: 10.1016/0022-1139(94)03131-2.
123. Qiu X.-L., Qing F.-L. Recent advances in the synthesis of fluorinated amino acids. *Eur. J. Org. Chem*. 2011. **2011**(18): 3261–3278.
doi: 10.1002/ejoc.201100032.
124. Qiu X.-L, Meng W.-D, Qing F.-L. Synthesis of fluorinated amino acids. *Tetrahedron*. 2004. **60**(32): 6711–6745.
doi: 10.1016/j.tet.2004.05.051.
125. Sutherland A., Willis C.L. Synthesis of fluorinated amino acids. *Nat. Prod. Rep*. 2000. **17**(6): 621–631.
doi: 10.1039/A707503K.
126. Kiss L., Fülöp F. Selective synthesis of fluorine-containing cyclic β-amino acid scaffolds. *Chem. Rec.* 2018. **18**(3): 266–281.
doi: 10.1002/tcr.201700038.
127. Zhou M., Feng Z., Zhang X. Recent advances in the synthesis of fluorinated amino acids and peptides. *Chem. Commun*. 2023. **59**(11): 1434–1448.
doi: 10.1039/D2CC06787K.
128. Moschner J., Stulberg V., Fernandes R.*et al*. Approaches to obtaining fluorinated α-amino acids. *Chem. Rev*. 2019. **119**(18): 10718–10801.
doi: 10.1021/acs.chemrev.9b00024.
129. Mykhailiuk P.K. Fluorine-containing prolines: Synthetic strategies, applications, and opportunities. *J. Org. Chem*. 2022. **87**(11): 6961–7005.
doi: 10.1021/acs.joc.1c02956.
130. Otaka A., Mitsuyama E., Watanabe J. *et al*. Synthesis of fluorine-containing bioisosteres corresponding to phosphoamino acids and dipeptide units. *Pept. Sci.* 2004. **76**(2): 140–149.
doi:10.1002/bip.10570.
131. Tarui A., Sato K., Omote M. *et al*. Stereoselective synthesis of α-fluorinated amino acid derivatives. *Adv. Synth. Catal*. 2010. **352**(16): 2733–2744.
doi: 10.1002/adsc.201000506.
132. Wang Y., Song X., Wang J. *et al*. Recent approaches for asymmetric synthesis of α-amino acids via homologation of Ni(II) complexes. *Amino Acids*. 2017. **49**(9): 1487–1520.

doi: 10.1007/s00726-017-2458-6.
133. Soloshonok V.A. Highly diastereoselective Michael addition reactions between nucleophilic glycine equivalents and β-substituted-α,β-unsaturated carboxylic acid derivatives; a general approach to the stereochemically defined and sterically χ-constrained α-amino acids. *Curr. Org. Chem.* 2002. **6**(4): 341–364. doi: 10.2174/1385272024605014.
134. Han J., Sorochinsky A.E., Ono T., Soloshonok V.A. Biomimetic transamination - a metal-free alternative to the reductive amination. Application for generalized preparation of fluorine containing amines and amino acids. *Curr. Org. Synth*. 2011. **8**(2): 281–294. doi: 10.2174/157017911794697277.
135. Soloshonok V.A., Sorochinsky A.E. Practical methods for the synthesis of symmetrically α,α-disubstituted α-amino acids. *Synthesis*. 2010. **2010**(14): 2319–2344. doi: 10.1055/s-0029-1220013.
136. Mikami K., Fustero S., Sánchez-Roselló M. *et al.* Synthesis of fluorinated β-amino acids. *Synthesis*. 2011. **2011**(19): 3045–3079. doi: 10.1055/s-0030-1260173.
137. Sorochinsky A.E., Soloshonok V.A. Asymmetric synthesis of fluorine-containing amines, amino alcohols, α- and β-amino acids mediated by chiral sulfinyl group. *J. Fluorine Chem*. 2010. **131**(2): 127–139. doi: 10.1016/j.jfluchem.2009.09.015.
138. Sorochinsky A.E., Aceña J.L., H. Moriwaki H. *et al*. Asymmetric synthesis of α-amino acids via homologation of Ni(II) complexes of glycine Schiff bases; Part 1: alkyl halide alkylations. *Amino Acids.* 2013. **45**(4): 691–718. doi: 10.1007/s00726-013-1539-4.
139. Aceña J.L., Sorochinsky A.E., Soloshonok V.A. Recent advances in asymmetric synthesis of α-(trifluoromethyl)-containing α-amino acids. *Synthesis*. 2012. **44**(11): 1591–1602. doi: 10.1055/s-0031-1289756.
140. Sorochinsky A.E., Aceña J.L., Moriwaki H. *et al*. Asymmetric synthesis of α-amino acids via homologation of Ni(II) complexes of glycine Schiff bases. Part 2: Aldol, Mannich addition reactions, deracemization and (*S*) to (*R*) interconversion of α-amino acids. *Amino Acids*. 2013. **45**(5): 1017–1033. doi:10.1007/s00726-013-1580-3.
141. Aceña J.L., Sorochinsky A.E., Moriwaki H. *et al*. Synthesis of fluorine-containing α-amino acids in enantiomerically pure form via homologation of Ni(II) complexes of glycine and alanine Schiff bases. *J. Fluorine Chem*. 2013. **155**: 21–38. doi:10.1016/j.jfluchem.2013.06.004.
142. Aceña J.L., Sorochinsky A.E., Soloshonok V. Asymmetric synthesis of α-amino acids via homologation of Ni(II) complexes of glycine Schiff bases. Part 3: Michael addition reactions and miscellaneous transformations. *Amino Acids.* 2014. **46**(9): 2047–2073. doi: 10.1007/s00726-014-1764-5.
143. Kukhar V.P., Sorochinsky A.E., Soloshonok V.A. Practical synthesis of fluorine-containing α- and β-amino acids: recipes from Kiev, Ukraine. *Future Med. Chem.* 2009. **1**(5): 793–819. doi: 10.4155/fmc.09.70.
144. Drug Trials Snapshots: VOYDEYA. Available at https://www.fda.gov/drugs/drug-approvals-and-databases/drug-trials-snapshots-voydeya (accessed, December, 2024).
145. Hao J., Milcent T., Retailleau P. *et al*. Asymmetric synthesis of cyclic fluorinated amino acids. *Eur. J. Org. Chem*. 2018. **2018**(27–28): 3688–3692. doi: 10.1002/ejoc.201800255.
146. Sato T., Izaw K., Aceña J.L. *et al*. Tailor-made α-amino acids in pharmaceutical industry: synthetic approaches to (1*R*,2*S*)-1-amino-2-vinylcyclopropane-1-carboxylic acid (vinyl-ACCA). *Eur. J. Org. Chem*. 2016. **2016**(16): 2757–2774. doi: 10.1002/ejoc.201600112.
147. Yamada T., Okada T., Sakaguchi K. *et al*. Efficient asymmetric synthesis of novel 4-substituted and configurationally stable analogues of thalidomide. *Org. Lett*. 2006. **8**(24): 5625–5628. doi:10.1021/ol0623668.
148. Cai C., Soloshonok V.A., Hruby V.J. Michael addition reactions between chiral Ni(II) complex of glycine and 3-(*trans*-Enoyl)oxazolidin-2-ones. A case of electron donor–acceptor

attractive interaction-controlled face diastereoselectivity. *J. Org. Chem*. 2001. **66**(4): 1339–1350.
doi: 10.1021/jo0014865.

149. Soloshonok V.A., Ueki H., Tiwari R. *et al*. Virtually complete control of simple and face diastereoselectivity in the Michael addition reactions between achiral equivalents of a nucleophilic glycine and (*S*)- or (*R*)-3-(*E*-enoyl)-4-phenyl-1,3-oxazolidin-2-ones: practical method for preparation of β-substituted pyroglutamic acids and prolines.*J. Org. Chem*. 2004. **69**(15): 4984–4990.
doi: 10.1021/jo0495438.
150. Soloshonok V.A., Ueki H., Ellis T.K. *et al*. Application of modular nucleophilic glycine equivalents for truly practical asymmetric synthesis of β-substituted pyroglutamic acids. *Tetrahedron Lett*. 2005. **46**(7): 1107–1110.
doi: 10.1016/j.tetlet.2004.12.093.
151. Wiles J.A., Phadke A.S., Deshpande M., Agarwal A., Chen D., Gadhachanda V.R., Hashimoto A., Pais G., Wang Q., Wang X. Achillion Pharmaceuticals Inc. 2018. *Aryl, heteroaryl, and heterocyclic compounds for treatment of medical disorders*. U.S. Patent Application 2018305375 A1.
152. Wiles J.A., Phadke A.S., Deshpande M., Agarwal A., Chen D., Gadhachanda V. R., Hashimoto A., Pais G., Wang Q., Wang X. Achillion Pharmaceuticals Inc. 2020. *Aryl, heteroaryl, and heterocyclic compounds for treatment of medical disorders*. U.S. Patent 10822352 B2.
153. Kang C. Danicopan: first approval. *Drugs*. 2024. **84**(5): 613–618.
doi:10.1007/s40265-024-02023-6.
154. Verdin P. FDA new drug approvals in Q1 2024. *Nat. Rev. Drug. Discov*. 2024. **23**(5): 331.
doi:10.1038/d41573-024-00063-x.
155. Kulasekararaj A.G., Lazana I. Paroxysmal nocturnal hemoglobinuria: Where are we going. *Am. J. Hematol*. 2023. **98**(S5): 33–43.
doi:10.1002/ajh.26882.
156. Voydeya (danicopan) granted first-ever regulatory approval in Japan for adults with PNH to be used in combination with C5 inhibitor therapy. Available at https://www.astrazeneca.com./media-centre/press-releases/2024/voydeya-danicopan-granted-first-ever-regulatory-approval-in-japan-for-adults-with-pnh-to-be-used-in-combination-with-c5-inhibitor-therapy.html(accessed, December, 2024).
157. First oral treatment against residual haemolyticanaemia in patients with paroxysmal nocturnal haemoglobinuria. Available at https://www.ema.europa.eu/en/news/first-oral-treatment-against-residual-haemolytic-anaemia-patients-paroxysmal-nocturnal-haemoglobinuria(accessed, December, 2024).
158. Wiles J. A., Phadke A.S., Deshpande M., Agarwak A., Chen D., Gadhachanda V.R., Hashimoto A., Pais G., Wang Q., Wang X. Achillion Pharmaceuticals Inc. 2017. *Aryl, heteroaryl, and heterocyclic compounds for treatment of medical disorders*. WO2017035353A1.
159. Phadke A., Hashimoto A., Andres M. Achillion Pharmaceuticals Inc. 2020. *Morphic forms of complement factor D inhibitors*. WO2020069024A1.
160. Phadke A. Achillion Pharmaceuticals Inc. 2020. *Morphic forms of complement factor D inhibitors*. WO2020051538A1.
161. Moore J.L., Taylor S.M., Soloshonok V.A. An efficient and operationally convenient general synthesis of tertiary amines by direct alkylation of secondary amines with alkyl halides in the presence of Huenig'sbase. *Arkivoc*. 2005. **2005**(6): 287–292.
doi: 10.3998/ark.5550190.0006.624.
162. Drug Trials Snapshots: OJEMDA. Available athttps://www.fda.gov/drugs/drug-approvals-and-databases/drug-trials-snapshots-ojemda(accessed, December, 2024).
163. Verdin P. FDA new drug approvals in Q2 2024. *Nat. Rev. Drug Discov*. 2024. **23**(8): 573.
doi:10.1038/d41573-024-00118-z.
164. Dhillon S. Tovorafenib: First Approval. *Drugs*. 2024. **84**(8). 985–993.
doi:10.1007/s40265-024-02069-6.
165. Chen W., Cossrow J., Franklin L. et al. Biogen Idec Inc.; Sunesis Pharmaceuticals Inc. 2010. *Compounds useful as RAF kinase inhibitors*. Chinese Patent CN101784545A.
166. Chen W., Cossrow J., Franklin L. et al. Biogen

Idec Inc.; Sunesis Pharmaceuticals Inc. 2010. *Compounds useful as RAF kinase inhibitors*. Chinese Patent CN101784545B.
167. Zhang T., Xu B., Tang F., He Z., Zhou J. Type II RAF inhibitor tovorafenib for the treatment of pediatric low-grade glioma. *Expert Rev. Clin. Pharmacol*. 2024. **17**(11): 999–1008. doi:10.1080/17512433.2024.2418405.
168. Sun Y., Alberta J.A., Pilarz C. *et al*. A brain-penetrant RAF dimer antagonist for the noncanonical BRAF oncoprotein of pediatric low-grade astrocytomas. *Neuro Oncol*. 2017. **19**(6): 774–785. doi:10.1093/neuonc/now261.
169. FDA grants accelerated approval to tovorafenib for patients with relapsed or refractory BRAF-altered pediatric low-grade glioma. Available athttps://www.fda.gov/drugs/resources-information-approved-drugs/fda-grants-accelerated-approval-tovorafenib-patients-relapsed-or-refractory-braf-altered-pediatric(accessed, December, 2024).
170. Drugs@FDA: FDA-Approved Drugs. Available at https://www.accessdata.fda.gov/scripts/cder/daf/index.cfm?event=overview.process&ApplNo=218033 (accessed, December, 2024).
171. Hirano S., Takeda Y., Nakamoto K., Ikeuchi M., Kitayama M., Yamada M., Kawakami J. Day One Biopharmaceuticals Inc. 2020. *Method for producing optically active compound.* U.S. Patent Application 2020/0317659 A1.
172. Han J., Takeda R., Sato T. Optical Resolution of Rimantadine. *Molecules*. 2019. **24**(9): 1828. doi:10.3390/molecules24091828.
173. Turner N.C., Im S.-A., Saura C. et al. Inavolisib-based therapy in *PIK$_3$CA*-mutated advanced breast cancer. *N. Engl. J. Med*. 2024. **391**(17):1584–1596. doi: 10.1056/NEJMoa2404625.
174. Bartsch R. Next generation of drugs in breast cancer. *Memo - Mag. Eur. Med. Oncol.* 2024. **17**(4): 280–286. doi: 10.1007/s12254-024-00999-1.
175. Singh S., Bradford D., Li X. *et al*. FDA approval summary: Alpelisib for PIK$_3$CA-related overgrowth spectrum. *Clin. Cancer Res*. 2024. **30**(1):23–28. doi: 10.1158/1078-0432.CCR-23-1270.
176. Sirico M., D'Angelo A., Gianni C. *et al*. Current State and Future Challenges for PI3K Inhibitors in Cancer Therapy. *Cancers*. 2023. **15**(3): 703. doi: 10.3390/cancers15030703.
177. Salphati L., Pang J., Plise E.G. *et al*. Preclinical assessment of the PI3Kα selective inhibitor inavolisib and prediction of its pharmacokinetics and efficacious dose in human. *Xenobiotica*. 2024. **54**(10): 808–820. doi: 10.1080/00498254.2024.2415103.
178. Shan K.S., Bonano-Rios A., Theik N.W.Y. *et al*. Molecular targeting of the phosphoinositide-3-protein kinase (PI3K) pathway across various cancers. *Int. J. Mol. Sci.* 2024. **25**(4): 1973. doi: 10.3390/ijms25041973.
179. Belli C., Repetto M., Anand S. *et al*. The emerging role of PI3K inhibitors for solid tumour treatment and beyond. *Br. J. Cancer*. 2023. **128**(12): 2150–2162. doi: 10.1038/s41416-023-02221-1.
180. Yu M., Chen J., Xu Z. *et al*. Development and safety of PI3K inhibitors in cancer. *Arch. Toxicol*. 2023. **97**(3): 635–650. doi: 10.1007/s00204-023-03440-4.
181. Vanhaesebroeck B., Perry M.W.D., Brown J.R. *et al*. PI3K inhibitors are finally coming of age. *Nat. Rev. Drug Discov.* 2021. **20**(10): 741–769. doi: 10.1038/s41573-021-00209-1.
182. Song K.W., Edgar K.A., Hanan E.J. *et al*. RTK-dependent inducible degradation of mutant PI3Kα drives GDC-0077 (Inavolisib) efficacy. *Cancer Discov*. 2022. **12**(1): 204–219. doi: 10.1158/2159-8290.CD-21-0072.
183. Hanan E.J., Braun M.-G., Heald R.A. et al. Discovery of GDC-0077 (Inavolisib), a highly selective inhibitor and degrader of mutant PI3Kα. *J. Med. Chem.* 2022. **65**(24): 16589–16621. doi: 10.1021/acs.jmedchem.2c01422.
184. Ndubaku C.O., Heffron T.P., Staben S.T. *et al*. Discovery of 2-{3-[2-(1-isopropyl-3-methyl-1*H*-1,2–4-triazol-5-yl)-5,6-dihydrobenzo[f]imidazo[1,2-*d*][1,4]oxazepin-9-yl]-1*H*-pyrazol-1-yl}-2-methylpropanamide (GDC-0032): A β-sparing phosphoinositide 3-kinase inhibitor with high unbound exposure and robust

in vivo antitumor activity. *J. Med. Chem*. 2013. **56**(11): 4597–4610. doi:10.1021/jm4003632.
185. Deeks E.D. Asciminib: First Approval. *Drugs*. 2022. **82**(2): 219–226. doi: 10.1007/s40265-021-01662-3.
186. Schoepfer J., Jahnke W., G. Berellini G. et al. Discovery of Asciminib (ABL001), an allosteric inhibitor of the tyrosine kinase activity of BCR-ABL1. *J. Med. Chem*. 2018. **61**(18): 8120–8135. doi: 10.1021/acs.jmedchem.8b01 040.
187. Mulik B.M., Srivastava N., Pendharkar D., Guin M. Design, aynthesis, and anticancer activity of novel methoxycyclohexylnicotinamides. *Russ. J. Org. Chem.* 2024. **60**(1): 173–184. doi: 10.1134/S1070428024010226.
188. Kurzrock R., Gutterman J.U., Talpaz M. The molecular genetics of Philadelphia chromosome-positive leukemias. *N. Engl. J. Med*. 1988. **319**(15): 990–998. doi: 10.1056/NEJM198810133191506.
189. Schuld P., Grzesiek S., Schlotte J. *et al*. Structural and biochemical studies confirming the mechanism of action of Asciminib, an agent specifically targeting the ABL myristoyl pocket (STAMP). *Blood*. 2020. **136** (Supplement 1): 34–35. doi: 10.1182/blood-2020-140968.
190. Wylie A.A., Schoepfer J., Jahnke W. *et al*. The allosteric inhibitor ABL001 enables dual targeting of BCR-ABL1. *Nature*. 2017. **543**(7647): 733–737. doi: 10.1038/nature21702.
191. Milojkovic D., Apperley J. Mechanisms of resistance to Imatinib and second-generation Tyrosine inhibitors in chronic myeloid leukemia. *Clin. Cancer Res*. 2009. **15**(24): 7519–7527. doi: 10.1158/1078-0432.CCR-09-1068.
192. Novartis Scemblix® FDA approved in newly diagnosed CML, offering superior efficacy, and favorable safety and tolerability profile. Available athttps://www.novartis.com/news/media-releases/novartis-scemblix-fda-approved-newly-diagnosed-cml-offering-superior-efficacy-and-favorable-safety-and-tolerability-profile(accessed, December, 2024).
193. Blank J., Koecher C., Pachinger W.H. *et al*. Novartis AG. 2020. *Process for the preparation of N-[4-(chlorodifluoromethoxy)phenyl]-6-[(3R)-3-hydroxypyrrolidin-1-yl]-5-(1H-pyrazol-5-yl) pyridine-3-carboxami de*. WO 2020230100 A1.
194. Dodd S.K., Furet P., Grotzfeld R.M. *et al*. Novartis AG. 2013. *Benzamide derivatives for inhibiting the activity of abl1, abl2 and bcr-abl1*. WO 2013171639 A1.
195. Issa G.C., Aldoss I., Di Persio J. *et al*. The menin inhibitor revumenib in *KMT2A*-rearranged or*NPM1*-mutant leukaemia. *Nature*. 2023. **615**(7954): 920–924. doi: 10.1038/s41586-023-05812-3.
196. Issa G.C., Aldoss I., Di Persio J.F. *et al*. The menininhibitor SNDX-5613 (revumenib) leads to durable responses in patients (Pts) with KMT2A-rearranged or NPM1 mutant AML: Updated results of a phase (Ph) 1 study. *Blood*. 2022. **140** (Supplement 1): 150–152. doi: 10.1182/blood-2022-164849.
197. Fareed A., Inam N., Faraz F. Breakthrough treatment choice for acute myeloid leukemia in pediatric and adult patients: Revumenib, an oral selective inhibitor of KMTA 2Ar. *Rare Tumors*. 2023. **15**: 20363613231183785. doi:10.1177/20363613231183785.
198. Candoni A., Coppola G.A. 2024. update on menininhibitors. A new class of target agents against KMT2A-rearranged and NPM1-mutated acute myeloid leukemia. *Hematol. Rep*. 2024. **16**(2): 244–254. doi: 10.3390/hematolrep16020024.
199. Zhou G., Liu K., Wei Y., Yuan H. Acerand Therapeutics (Hong Kong) Ltd. 2022. *Diazaspirobicylic compounds as protein-protein interaction inhibitors and applications thereof.* WO2022257047 A1.
200. Fleischmann M., Bechwar J., Voigtländer D. *et al*. Synergistic effects of the RAR *alpha* agonist Tamibarotene and the menininhibitor Revumenib in acute myeloid leukemia cells with KMT2A rearrangement or NPM1 mutation. *Cancers*. 2024. **16**(7):1311. doi: 10.3390/cancers16071311.
201. Thomas X. Small molecule menininhibitors:

Novel therapeutic agents targeting acute myeloid leukemia with *KMT2A* rearrangement or*NPM1* mutation. *Oncol. Ther.* 2024. **12**(1): 57–72.
doi: 10.1007/s40487-024-00262-x.

202. Cacatian S., Claremon D.A., Dillard L.W. *et al.* Vitae Pharmaceuticals Inc. 2017. *Inhibitors of the menin-MLL interaction.* WO2017214367 A1.
203. Soloshonok V.A. Remarkable amplification of self-disproportionation of enantiomers on achiral-phase chromatography columns. *Angew. Chem. Int. Ed*. 2006. **45**(5): 766–769. doi: 10.1002/anie.200503373.
204. Soloshonok V.A, Ueki H., Yasumoto M. *et al.* Phenomenon of optical self-purification of chiral non-racemic compounds. *J. Am. Chem. Soc*. 2007. **129**(40): 12112–12113. doi: 10.1021/ja065603a.
205. Soloshonok V.A., Klika K.D. Terminology related to the phenomenon 'self-disproportionation of enantiomers' (SDE). *Helv. Chem Acta*. 2014. **97**(11): 1583–1589. doi: 10.1002/hlca.201400122.
206. Ueki H., Yasumoto M., Soloshonok V.A. Rational application of self-disproportionation of enantiomers via sublimation–a novel methodological dimension for enantiomeric purifications. *Tetrahedron: Asymmetry*. 2010. **21**(11–12): 1396–1400. doi: 10.1016/j.tetasy.2010.04.040.
207. Sorochinsky A.E., Katagiri T., Ono T. *et al.* Optical purifications via self-disproportionation of enantiomers by achiral chromatography; Case study of a series of α-CF_3-containing secondary alcohols. *Chirality*. 2013. **25**(6): 365–368. doi: 10.1002/chir.22180.
208. Sorochinsky A.E., Aceña J.L., Soloshonok V.A. Self-disproportionation of enantiomers of chiral, non-racemic fluoroorganiccompounds: Role of fluorine as enabling element. *Synthesis*. 2013. **45**(2): 141–152. doi: 10.1055/s-0032-1316812.
209. Han J., Wzorek A., Kwiatkowska M. *et al*. The self-disproportionation of enantiomers (SDE) of amino acids and their derivatives. *Amino Acids*. 2019. **5 1**(6): 865–889. doi: 10.1007/s00726-019-02729-y.
210. Wzorek A., Sato A., Drabowicz J. *et al*. Remarkable magnitude of the self-disproportionation of enantiomers (SDE) via achiral chromatography; application to the practical-scale enantiopurification of β-amino acid esters. *Amino Acids*. 2016. **48**(2): 605–613. doi: 10.1007/s00726-015-2152-5.
211. Hosaka T., Imai T., Wzorek A. *et al.* The self-disproportionation of enantiomers (SDE) of α-amino acid derivatives; facets of steric and electronic properties. *Amino Acids*. 2019. **51**(2): 283–294. doi: 10.1007/s00726-018-2664-x.
212. Soloshonok V.A., Wzorek A., Klika K.D. A question of policy: should tests for the self-disproportionation of enantiomers (SDE) be mandatory for reports involving scalemates? *Tetrahedron: Asymmetry*. 2017. **28**(10): 1430–1434. doi: 10.1016/j.tetasy.2017.08.020.
213. Han J., Soloshonok V.A., Klika K.D. *et al*.. Chiral sulfoxides: advances in asymmetric synthesis and problems with the accurate determination of the stereochemical outcome. *Chem. Soc. Rev*. 2018. **47**(4): 1307–1350. doi: 10.1039/c6cs00703a.
214. Soloshonok V.A., Roussel C., Kitagawa O., Sorochinsky A.E. Self-disproportionation of Enantiomers via achiral chromatography: a warning and extra dimension in optical purifications. *Chem. Soc. Rev*. 2012. **41**(11): 4180–4188. doi:10.1039/C2CS35006H.
215. Han J., Kitagawa O., Wzorek A. *et al.* The self-disproportionation of enantiomers (SDE): a menace or an opportunity? *Chem. Sci*. 2018. **9**(7): 1718–1739. doi: 10.1039/C7SC05138G.

Стаття надійшла 10.07.2024.